REVERSAL OF MULTIDRUG RESISTANCE BY SMALL INTERFERING RNAS (SIRNA) IN DOXORUBICIN RESISTANT MCF-7 BREAST CANCER CELLS

A THESIS SUBMITTED TO
THE GRAUDATE SCHOOL OF NATURAL AND APPLIED SCIENCES
OF
MIDDLE EAST TECHNICAL UNIVERSITY

BY

YAPRAK DÖNMEZ

IN PARTIAL FULFILLMENT OF THE REQUIREMENTS
FOR
THE DEGREE OF MASTER OF SCIENCE
IN
BIOLOGY

FEBRUARY 2010

Approval of the thesis:

REVERSAL OF MULTIDRUG RESISTANCE BY SMALL INTERFERING RNAS (SIRNA) IN DOXORUBICIN RESISTANT MCF-7 BREAST CANCER CELLS

submitted by **YAPRAK DÖNMEZ** in partial fulfillment of the requirements for the degree of **Master of Science in Biology Department, Middle East Technical University** by,

Prof. Dr. Canan Özgen   _____
Dean, Graduate School of **Natural and Applied Sciences**

Prof. Dr. Musa Doğan   _____
Head of Department, **Biology**

Prof. Dr. Ufuk Gündüz   _____
Supervisor, **Biology Dept., METU**

Examining Committee Members:

Prof. Dr. Semra Kocabıyık   _____
Biology Dept., METU

Prof. Dr. Ufuk Gündüz   _____
Biology Dept., METU

Prof. Dr. Ali Uğur Ural   _____
Hematology Dept.,
Gülhane Military School of Medicine

Dr. Can Özen   _____
Biotechnology Dept., METU

Dr. Özlem Darcansoy İşeri   _____
Transplantation and Gene Sciences Inst.,
Başkent University

Date: 01.02.2010

I hereby declare that all information in this document has been obtained and presented in accordance with academic rules and ethical conduct. I also declare that, as required by these rules and conduct, I have fully cited and referenced all material and results that are not original to this work.

Name, Last name : YAPRAK DÖNMEZ

Signature :

ABSTRACT

REVERSAL OF MULTIDRUG RESISTANCE BY SMALL INTERFERING RNAS (SIRNA) IN DOXORUBICIN RESISTANT MCF-7 BREAST CANCER CELLS

Dönmez, Yaprak

M.Sc., Department of Biology

Supervisor: Prof. Dr. Ufuk Gündüz

February 2010, 107 pages

Resistance to anticancer drugs is a serious obstacle to cancer chemotherapy. A common form of multidrug resistance (MDR) is caused by the overexpression of transmembrane transporter proteins P-glycoprotein and MRP1, encoded by *MDR1* and *MRP1* genes, respectively. These proteins lead to reduced intracellular drug concentration and decreased cytotoxicity by means of their ability to pump the drugs out of the cells. Breast cancer tumor resistance is mainly associated with overexpression of P-gp/*MDR1*. Although some chemical MDR modulators aim to overcome MDR by impairing the function of P-gp, they exhibit severe toxicities limiting their clinical relevance. Consequently, selective blocking of the expression of P-gp/*MDR1* specific mRNA through RNA interference strategy may be an efficient tool to reverse MDR phenotype and increase the success of chemotherapy.

Aim of this study was re-sensitizing doxorubicin resistant breast cancer cells to anticancer agent doxorubicin by selective downregulation of P-gp/*MDR1* mRNA. The effect of the selected *MDR1* siRNA and *MRP1* expression after *MDR1* silencing was determined by qPCR analysis. XTT cell proliferation assay was performed to

determine the effect of *MDR1* silencing on doxorubicin sensitivity.Intracellular drug accumulation and localization was investigated by confocal laser scanning microscopy after treatment with *MDR1* siRNA or other MDR modulators; verapamil or promethazine. The role of P-gp in migration characteristics of resistant cells was evaluated by wound healing assay.

The results demonstrated that approximately 90% gene silencing occurred by the selected siRNA targeting *MDR1* mRNA. However the level of *MRP1* mRNA did not change after *MDR1* downregulation. Introduction of siRNA resulted in about 70% re-sensitization to doxorubicin. Silencing of P-gp encoding *MDR1* gene resulted in almost complete restoration of the intracellular doxorubicin accumulation and re-localization of the drug to the nuclei. Despite the considerably high concentration of the modulators, verapamil and promethazine were not as effective as siRNA for reversal of the drug efflux. According to wound healing assay, *MDR1* silencing did not have any effect on migration characteristics of resistant cells, that is, P-gp expression does not seem to affect the motility of the cells.

Selected siRNA duplex was shown to effectively inhibit *MDR1* gene expression, restore doxorubicin accumulation and localization, and enhance chemo-sensitivity of resistant cells, which makes it a suitable future candidate for therapeutic applications.

Key words: MDR reversal, P-glycoprotein, siRNA, doxorubicin, breast cancer

ÖZ

DOKSORUBİSİNE DİRENÇLİ MCF-7 MEME KANSERİ HÜCRE HATTINDA ÇOKLU İLAÇ DİRENÇLİLİĞİNİN SİRNA KULLANILARAK GERİ DÖNÜŞTÜRÜLMESİ

Dönmez, Yaprak

Yüksek Lisans, Biyoloji Bölümü

Tez Yöneticisi: Prof. Dr. Ufuk Gündüz

Şubat 2010, 107 sayfa

Kullanılan ilaçlara karşı gelişen dirençlilik kanser kemoterapisinde başarıyı düşüren faktörlerden biridir. Çoklu ilaç dirençliliğinin en etkin nedenleri *MDR1* gen ürünü P-glikoproteininin (P-gp, MDR1) ve *MRP1* ürünü çoklu ilaç direnci ile ilişkili proteinin (MRP1) yüksek düzeyde ifade edilmeleridir. Bu taşıyıcı proteinler, tümör hücrelerinde ilacın dışarı atılmasını sağlayarak, hücre içi ilaç miktarının azalmasına ve bu yolla ilacın toksik etkisinin düşmesine yol açmaktadır. Meme kanseri tümörlerinde ağırlıklı olarak P-glikoproteininin (P-gp, MDR1) fazla ifade edildiği görülmektedir. Çoklu ilaç dirençliliği bazı kimyasallar tarafından engellenebilir. Ancak bu kimyasalların toksik olmaları klinik kullanımlarını kısıtlamaktadır. *MDR1* geninin dizeye özgü engelleyici RNA'lar (siRNA) yoluyla baskılanması çoklu ilaç dirençliliğinin geri çevrilmesi için etkili bir araç olabilir.

Bu çalışmada amaç, doksorubisine dirençli meme kanseri hücrelerinin *MDR1* genini hedefleyen engelleyici küçük RNA (siRNA) molekülleri kullanılarak yeniden ilaca duyarlı hale getirilmesidir. Seçilen siRNA molekülünün *MDR1* genini baskılama

düzeyi ve *MRP1* gen ifadesinin bu durumdan ne şekilde etkilendiği eş zamanlı PZR ile belirlenmiştir. *MDR1* genini hedefleyen siRNA moleküllerinin doksorubisin dirençliliğine olan etkisinin incelenmesi için sitotoksisite analizi yapılmıştır. Hücre içi ilaç birikimi ve yerleşimi, siRNA uygulamasından sonra konfokal lazer tarama mikroskopisi ile saptanmış, diğer çoklu ilaç dirençliliği engelleyici kimyasallardan verapamil veya prometazin uygulanan hücreler ile karşılaştırılmıştır. Dirençli hücrelerin hareketlilik özellikleri ile P-glikoprotein ifadesi arasındaki ilişki "yara iyileşme testi" ile belirlenmiştir.

Sonuçlar, siRNA molekülünün *MDR1* geninin ifadesini yaklaşık %90 oranında baskıladığını, *MRP1* gen ifadesini ise etkilemediğini göstermiştir. *MDR1* geninin baskılanması, dirençli hücreleri doksorubisine karşı yaklaşık %70 daha duyarlı hale getirmiştir. siRNA uygulaması, hücre içi ilaç birikiminde, ilaca duyarlı hücrelerdeki düzeyde artışa ve ilacın çekirdekte toplanmasına yol açmıştır. Yüksek derişimde verapamil veya prometazin ilacın dışarı atılmasını siRNA kadar etkili bir şekilde engelleyememişlerdir. Ayrıca, *MDR1* genini hedefleyen siRNA uygulamasının dirençli hücrelerin hareketlilik özelliklerinde herhangi bir etkisinin olmayabileceği gösterilmiştir.

MDR1 gen ifadesinin etkili bir şekilde engellenmesi, hücre içi ilaç birikimi ve yerleşimini, ilaca duyarlı hücrelerdeki durumuna getirmiş ve dirençli hücrelerin doksorubisin duyarlılığını arttırmıştır. Kullanılan siRNA'nın tedavi amaçlı uygulamalar için uygun bir aday olabileceği düşünülmektedir.

Anahtar Kelimeler: MDR geri çevrilmesi, P-glikoproteini, siRNA, doksorubisin, meme kanseri

To my family

ACKNOWLEDGMENTS

My deepest thanks are extended to Semih Çakıl, who made life worth and easier with his endless trust, encouragement, understanding, moral support, care and patience at every stage of this thesis.

METU Central Laboratory Molecular Biology and Biotechnology R&D Center Light Microscopy Facility and Spectroscopy Unit are also greatly acknowledged.

TABLE OF CONTENTS

xii

LIST OF TABLES

TABLES

LIST OF FIGURES

FIGURES

LIST OF ABBREVIATIONS

ABC   ATP-Binding Cassette

BCRP   Breast Cancer Resistance Protein

bp   Base pair

Cmoat   Cannalicular Multispecific Organic Anion Transporter

DEPC   Diethylpyrocarbonate

dH_2O Distilled water

DMSO   Dimethly Sulfoxide

dNTP   Deoxy Nucleotide Triphosphate

DOX   Doxorubicin

dsRNA   Double stranded RNA

EtBr   Ethidium Bromide

FR   Fold reversal

GSH   Glutathione

IC_{50} Inhibitory concentration 50

LRP   Lung Resistance Protein

MCF-7/Dox   Doxorubicin resistant MCF-7 subline

MCF-7/S   Sensitive MCF-7

MDR   Multidrug Resistance

MRP1   Multidrug Resistance Protein 1

PBS   Phosphate buffered saline

Pgp/MDR1   P-glycoprotein

Prm   Promethazine

qPCR	Quantitative Real-Time Polymerase Chain Reaction
R	Relative resistance index
RISC	RNA-inducing silencing complex
RNAi	RNA Interference
rpm	Revolution per minute
RT	Reverse Transcription
SEM	Standard Error of the Means
siRNA	Small Interfering RNA
TAE	Tris-acetate-EDTA
TM	Transmembrane
V	Volt
Vp	Verapamil
w/v	Weight per volume

CHAPTER 1

INTRODUCTION

1.1 Biology of Cancer

Cancer accounted worldwide to about 7.6 million deaths in 2007 (American Cancer Society, 2007). In 2005, approximately 52,000 people in Turkey died of cancer and 37,000 of those people were under the age of 70. Cancer is the third most common cause of death in Turkey, exceeded by heart and other chronic diseases. According to World Health Organization, in 2030, about 84,100 Turkish people are expected to die of cancer, which accounts for nearly 1 of every 7 deaths (World Health Organization, 2006).

The development of cancer is the end result of a series of inherited and/or acquired mutations that leads to a remarkable change in the behavior of a single cell and its offspring (Rieger, 2004). The causes of cancer are both external factors (tobacco, infectious organisms, chemicals, and radiation) and internal factors (inherited mutations, hormones, immune conditions, and mutations that occur from metabolism). These causal factors may act together or in sequence to initiate or promote carcinogenesis (American Cancer Society, 2009). The evolution of the normal cell to a malignant one consists of processes by which genes involved in normal homeostatic mechanisms controlling proliferation and cell death suffer various damages which cause the activation of genes stimulating proliferation or protection against cell death, the oncogenes, and the inactivation of genes which would normally inhibit proliferation, the tumor suppressor genes (Bertram, 2001). The mechanisms of gene activation/inactivation have been found including mutations, chromosomal alterations, and epigenetic events (Wodarz, 2005). Hanahan and Weinberg (Hanahan and Weinberg, 2000) proposed six essential

1

alterations in cell physiology that collectively dictate malignant growth: self-sufficiency in growth signals, insensitivity to growth-inhibitory (antigrowth) signals, evasion of programmed cell death (apoptosis), limitless replicative potential, sustained angiogenesis, and tissue invasion and metastasis. Each of these changes is shared by most if not all cancer cells during tumor development. Even after they become malignant, cancer cells continue to accumulate mutations and gain new properties which make them even more dangerous (Karp, 2002).

1.2 Breast Cancer

More than 100 distinct diseases are collectively termed as cancer, and each cancer type has different biological and clinical features (Fearon, 1999). In 2005, breast cancer was the most common cancer found in women in Turkey (World Health Organization, 2006). Likewise, in US, breast cancer is the most frequently diagnosed cancer in women; an estimated 192,370 new cases of invasive breast cancer are expected to occur among women during 2009 (American Cancer Society, 2009). Usually, breast cancer either begins in the cells of the lobules, which are the milk-producing glands, or the ducts, the passages that drain milk from the lobules to the nipple. Less commonly, breast cancer may begin in the stromal tissues, which include the fatty and fibrous connective tissues of the breast. Over time, cancer cells may invade nearby healthy breast tissue and make their way into the underarm lymph nodes, so that they can metastasize into other parts of the body (http://www.breastcancer.org/symptoms/understand_bc/what_is_bc.jsp). The risk factors for breast cancer include being overweight or obese after menopause, use of menopausal hormone therapy (especially combined estrogen and progestin therapy), physical inactivity, consumption of one or more alcoholic beverages per day, high breast tissue density, radiation therapy to the chest and family history of breast cancer (American Cancer Society, 2009).

1.3 Treatment of Breast Cancer

Treatment of breast cancer involve surgery, radiation therapy, chemotherapy (before or after surgery), hormonal therapy (tamoxifen, raloxifene, aromatase inhibitors), or targeted therapy taking into account tumor size, stage, nodal status, menopausal status of the patient, hormone receptor status of the tumor and other tumor characteristics as well as patient preference (Skeel, 2005).

1.3.1 Surgery

Surgery is usually the first treatment strategy against breast cancer. Lumpectomy (breast-conserving surgery) is the removal of only the tumor and a small amount of surrounding tissue, whereas mastectomy is the removal of all of the breast tissue. The results and long term follow-up of large national and international clinical trials have firmly established that breast conserving surgery is equivalent to mastectomy for women whose tumors are 5cm or less and localized to the breast (Fisher *et al.*, 2002; Veronesi *et al*., 2002). Lymph node removal (axillary lymph node dissection) can take place during lumpectomy and mastectomy if the biopsy indicates that breast cancer has spread outside the milk duct (http://www.breastcancer.org /treatment/surgery/).

Breast cancer treatment uses surgery and/or radiation therapy to provide a local control, protect the breast tissue developing cancer and systemic treatment which is achieved by using chemotherapy to treat any cancer cells that have escaped to other parts of the body (http://cancer.stanford.edu/patient_care/services/surgery/ breast.html).

1.3.2 Hormonal Therapy

Women with early-stage or metastatic estrogen receptor positive breast cancers benefit from treatment with hormone therapy which lowers the amount of the

3

hormone estrogen in the body and/or blocks the action of estrogen on breast cancer cells. Prospective randomized trials of adjuvant tamoxifen, a nonsteroidal estrogen antagonist, were shown to improve both relapse-free survival and overall survival (Sledge, 1996). Cummings and co-workers (Cummings *e. al.,* 1999) demonstrated that raloxifene, a selective estrogen receptor modulator, led to a 76% decrease in the risk of invasive breast cancer after 3 years of treatment. Recent studies recommended that risk of breast cancer recurrence is further reduced when hormone therapy is followed by treatment with an aromatase inhibitor, such as anastrozole and exemestane (American Cancer Society, 2009).

1.3.3 Targeted Therapy

Targeted therapy uses drugs or other agents to identify and attack specific cancer cells without harming normal cells. Monoclonal antibodies and tyrosine kinase inhibitors are two types of targeted therapies being studied in the treatment of breast cancer. For women who have HER2/neu positive tumors, approved targeted therapies include trastuzumab (Herceptin) and lapatinib (Tykerb) (American Cancer Society, 2009). About one-fourth of patients with breast cancer have tumors that may be treated with trastuzumab combined with chemotherapy (http://www.cancer.gov /cancertopics/pdq/treatment/breast/Patient/page5).

1.3.4 Radiation Therapy

The basis of radiation therapy is the fact that ionizing radiation destroys tumor cells. X rays and gamma rays have the ability to penetrate the tissue depth, destroying tumor cells even from deep layers. Radiotherapy induces direct lesions in DNA or molecules of cell, which eventually affect DNA. These changes deregulate cell division, leading the death of the daughter cells (Baba and Cătoi, 2007).

Radiotherapy is mostly given to the breast after lumpectomy to destroy any remaining cancer cells that may have been left after the removal of the tumor. Also,

it may be recommended after mastectomy to damage any breast cells that may remain at the mastectomy site (http://www.breastcancer.org/treatment/radiation/ when_appropriate.jsp).

1.3.5 Chemotherapy

Chemotherapy is presently used in three main clinical settings: (a) chemotherapy alone; (b) adjuvant chemotherapy to local methods of treatment including surgery and/or radiation therapy; and (c) neoadjuvant chemotherapy for patients who present the localized disease, for whom local forms of therapy, such as surgery or radiation, are not adequate by themselves (Chu and DeVita, 2009).

Chemotherapy has been used in anti-cancer treatment for about seventy years and the results have been remarkably successful. In this sense, the following can be mentioned:

- the perspective of a normal life for some patients with different types of metastasized tumors;
- increased recovery rates, in the case of the use of an adjuvant in surgical therapy or radiotherapy;
- total remission in more than 25% of the treated patients;
- an increased rate of response, with a significant prolongation of life duration;
- objective regression in 30–50% of patients treated for the first time with a chemical product (Baba and Cătoi, 2007).

Randomized trials of adjuvant chemotherapy for breast cancer show significant differences in favor of chemotherapy in long-term disease free and overall survival. Although breast cancer responds to several types of cytotoxic agents, it responds preferentially to doxorubicin (Adriamycin®). Also cyclophosphamide, methotrexate and 5-fluorouracil treatments result in substantial response (Paul and Cowan, 1999). Cyclophosphamide is an alkylating agent, which prevents cell division primarily by crosslinking DNA strands after its transformation into active alkylating metabolites, acrolein and phosphoramide mustard. Methotrexate is a cell cycle phase-specific (S

phase) antimetabolic agent, which inhibits DNA, RNA and protein synthesis by causing the depletion of nucleotide precursors. 5-fluorouracil is also an antimetabolic agent and its active form inhibits DNA synthesis by inhibiting normal production of thymidine (Kumar, 2006). Further, microtubule-stabilizing taxenes have been to found to produce an impressive response rate in breast cancer patients (Paul and Cowan, 1999). The taxenes, paclitaxel and docetaxel are two well studied plant alkaloids, which bind to microtubules and inhibit their depolymerization into tubulin, leading to block in cell cycle progression in the G_2-M phase. Paclitaxel is more effective in advanced breast carcinomas (Olofsson, 2006).

The principle hindrance to the clinical efficiency of chemotherapy has been toxicity to the normal tissues and the development of cellular drug resistance. Intense research continues to improve the clinical outcome of cancer patients undergoing treatment, especially in those with cancers that have been resistant to conventional chemotherapy (Chu and DeVita, 2009).

1.3.5.1 Doxorubicin (Adriamycin®)

Doxorubicin (Adriamycin®) (Figure 1.1), an anthracyclinic antibiotic, is one of the most commonly used chemotherapeutic drugs and exhibits a wide spectrum of activity against solid tumors, lymphomas, and leukemias (Swift *et al.,* 2006).
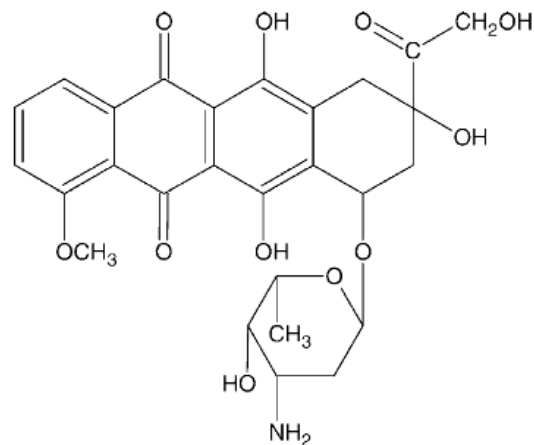
Doxorubicin

Figure 1. 1 Doxorubicin (Adriamycin®) (Pajeva *et al.*, 2004).

The interaction of doxorubicin with DNA- and DNA-associated enzymes is well recognized. A number of studies have shown that doxorubicin intercalates into DNA molecules: detailed studies of doxorubicin affinity for DNA have identified a preference for 5'TCA (Chabner and Longo, 2005). The binding of doxorubicin to DNA inhibits DNA polymerase and nucleic acid synthesis (Shen *et al.*, 2008). DNA-doxorubicin complex significantly alters the ability of helicases to dissociate duplex DNA into DNA single strands, thus limiting replication (Guano *et al.,* 1999). Further, doxorubicin is classified as a classic topoisomerase IIα poison (Burden and Osheroff 1998; DeVita *et al.*, 2001). It stabilizes the cleavable complex between DNA and topoisomerase II enzyme subunits, resulting in DNA double-strand breaks, which eventually lead to an apoptotic response (Swift *et al.,* 2006). It has been demonstrated that doxorubicin exerts a cytotoxic effect also through interaction with the cell membrane, especially with negatively charged phospholipids (Goormaghtigh *et al.*, 1980; Triton *et al.*, 1982; Nicloay *et al.*, 1988; Pajeva *et al.*, 2003). Binding of the drug and insertion into the membrane is shown to affect the intrinsic transport characteristics of the membrane (Speelmans *et al.*, 1994; Pajeva *et al.*, 2003). Doxorubicin can undergo cycles of reduction and oxidation in almost all intracellular compartments, including nucleus and mitochondrion, mediating the

7

formation of reactive oxygen species. Redox cycling has been shown to oxidize DNA bases in human chromatin and in intact tumor cells. Additionally, reactive oxygen metabolism of doxorubicin results in the iron dependent production of formaldehyde from a variety of carbon sources, leading to the production of formaldehyde-drug conjugates. Such conjugates have the ability to form covalent DNA cross-links enhancing the cytotoxic activity of doxorubicin. Doxorubicin, being able to undergo one or two electron reduction to reactive compounds, leads to a widespread damage to intracellular macromolecules, including lipid membranes, DNA bases and thiol containing transport proteins. The electron reduction capability of doxorubicin leads to the cumulative and dose-dependent cardiac toxicity of the drug. In addition, it has been reported that doxorubicin can directly inhibit nitric oxide synthase activity, which may result in significant alterations in vascular tone both in the heart and in tumors (Chabner and Longo, 2005). Figure 1.2 summarizes the action mechanisms of doxorubicin on the cells.

The mechanisms of action cause the nucleus to be one of the targets of doxorubicin. Recently, its entry to the nucleus has been described. Once doxorubicin diffuses through the plasma membrane, a substantial portion of the drug is bound to the 20S fraction of the proteosome. Afterwards, the drug is actively transported to the nucleus in an ATP requiring, nuclear pore dependent process by means of nuclear localization signals found in 20S proteosomal subunits. Due to its higher affinity to DNA, doxorubicin dissociates from the proteosome in the nucleus (Chabner and Longo, 2005).
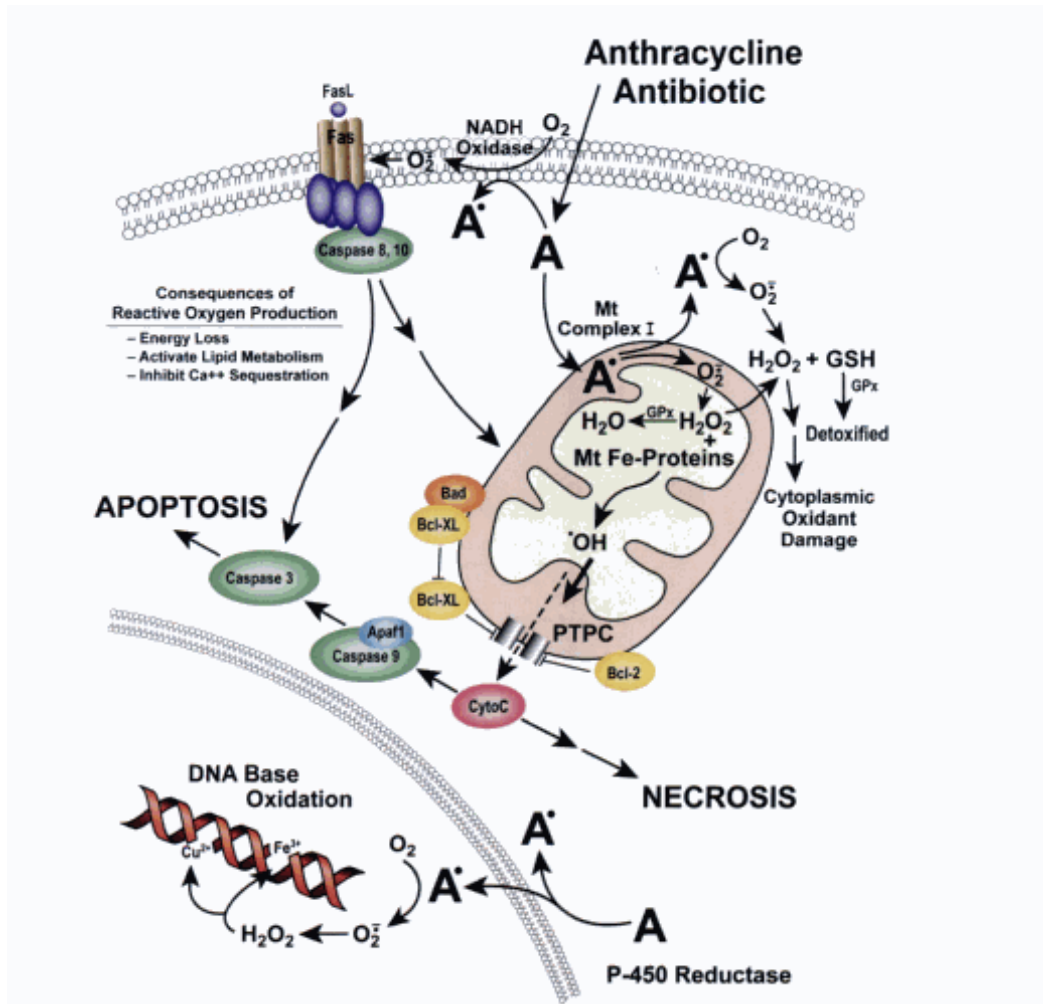
Figure 1. 2 Anthracycline cell death mechanisms (Chabner and Longo, 2005).

1.4 Multidrug Resistance (MDR)

Breast cancer is a disease that responds to a wide variety of chemotherapeutic drugs as well as to hormonal therapy. However, although patients with metastatic breast cancer may initially respond to chemotherapy or hormonal therapy, disease recurrence may occur within a few months to a few years. Moreover, response rates and the duration of the response to the second therapy is generally less than that of initial therapy (Paul and Cowan, 1999).

Drug resistance is a significant factor that limits the effectiveness of chemotherapeutic drugs. Tumors may be intrinsically resistant to chemotherapy prior to treatment, or drug resistance can be induced by chemotherapeutic drug during treatment, so that tumors that are initially sensitive become resistant to chemotherapy (Longley and Johnston, 2005). Currently, drug resistance to chemotherapy is believed to cause failure in over 90% of patients with metastatic cancers (Battisti, 2007). In 1973, it was discovered that, daunomycin was transported outward by drug resistant cells, which were cross-resistant to other chemotherapeutic drugs, such as vinca alkoloids and other anthracyclins (Dano, 1973; Leonard *et al.,* 2003). Multidrug resistance is the term to define the phenomenon characterized by the ability of drug resistant tumors to exhibit simultaneous resistance to a number of structurally and functionally unrelated chemotherapeutic agents (Krishna and Mayer, 2000). Simon and Schindler (Simon and Schindler, 1994) suggested the following models, which account for multidrug resistance: *(i)* an ATP driven transporter that pumps drugs out of the cells *(ii)* an increased trapping of drugs in intracellular organelles away from the cytosol and nucleoplasm *(iii)* an increased rate of exocytosis that results in drug efflux from the intracellular organells *(iv)* an alkaline shift of cellular pH that reduces the accumulation of the drugs (most of which are weak bases) inside of cells *(v)* nuclear mechanisms including modifications of DNA binding, DNA repair, altered expression and/or activity of topoisomerase II, altered apoptosis regulation and the permeability of nuclear envelope *(vi)* alternative cytoplasmic mechanisms including detoxification pathways and *(vii)* changes in plasma membrane structure which affect drug permeability.

Doxorubicin resistance in the cells is generally associated with MDR1/MRP overexpression, altered levels of topoisomerase II expression, expression of mutated forms of topoisomerase II, increased glutathione or glutathione peroxidase levels, DNA mismatch repair deficits, cellular resistance to apoptosis and finally changes in the membrane lipid composition (Paul and Cowan, 1999; Pajeva *et al*., 2003).

1.4.1 Transport Based MDR

Transport based MDR is generally characterized by over-expression of one or several members of the ATP-Binding Cassette (ABC) transporter family. To date, 48 human ABC transporter genes have been identified and organized into seven subfamilies (ABCA-ABCG), that are expressed both in normal and malignant cells (Table 1.1) (Leonard *et al*., 2003). Many of the ABC transporters are constitutively expressed in various normal tissues, like epithelial cells of the colon, kidney, adrenal, pancreas or liver to drive the active transport of endo- and xeno-biotics, including detoxification. Consequently, tumors derived from these tissues exhibit intrinsic multidrug resistance to cytostatic agents even before chemotherapy is initiated (Borowski *et al*., 2005).

Table 1. 1 Tissue localization and possible functions of ABC transporters (Gottesman *et al*., 2002).

Common name	Systematic name	Tissue	Non-chemotherapy substrates	Chemotherapy substrates (known and suspected)
P-GP/ MDR1	ABCB1	Intestine, liver, kidney, placenta, blood-brain barrier	Neutral and cationic organic compounds, many commonly used drugs	Doxorubicin, daunorubicin, vincristine, vinblastine, actinomycin-D, paclitaxel, docetaxel, etoposide, teniposide, bisantrene, homoharringtonine
MDR2	ABCB4	Liver	Phosphatidylcholine, some hydrophobic drugs	Paclitaxel, vinblastine
MRP1	ABCC1	All tissues	Glutathione and other conjugates, organic anions, leukotriene C4	Doxorubicin, epirubicin, etoposide, vincristine, methotrexate
MRP2, cMOAT	ABCC2	Liver, kidney, intestine	Similar to MRP1, non-bile salt organic anions	Methotrexate, etoposide, doxorubicin, cisplatin, vincristine, mitoxantrone
MRP3	ABCC3	Pancreas, kidney, intestine, liver, adrenalglands	Glucuronate and glutathione conjugates, bile acids	Etoposide, teniposide, methotrexate, cisplatin, vincristine, doxorubicin

Table 1. 1 (continued).

MRP4	ABCC4	Prostate, testis, ovary, intestine, pancreas, lung	Nucleotide analogues, organic anions	Methotrexate, thiopurines
MRP5	ABCC5	Most tissues	Nucleotide analogs, cyclic nucleotides, organic anions	6-Mercaptopurine, 6-Thioguanine
MRP6	ABCC6	Liver, kidney	Anionic cyclic pentapeptide	Unknown
MXR,BCRP, ABC-P	ABCG2	Placenta, intestine, breast, liver	Prazosin	Doxorubicin, daunorubicin, mitoxantrone, topotecan, SN-38
BSEP, SPGP	ABCB11	Liver	Bile salts	Paclitaxel
ABCA2	ABCA2	Brain, monocytes	Steroid derivatives, lipids	Estramustine

1997 metaanalysis of 31 reports from 1989–1996 demonstrated overexpression of P-gp in 41% of breast tumors (Gottesman *et al*., 2002). Moreover, increased MDR1 expression was reported in breast tumors of patients following treatment with neoadjuvant chemotherapy and in breast tumors following relapse. Another study showed overexpression of P-gp in a majority of breast cancer patients with locally advanced or metastatic breast cancer, associating with a lack of response to chemotherapy and shorter progression-free survival (Paul and Cowan, 1999). Due to constitutive MRP1 expression, it is not surprising that MRP1 mRNA can be detected in all breast cancer samples at levels comparable to that in normal tissues. A correlation has been noticed between relapse-free survival and MRP1 in invasive primary breast carcinomas (Gottesman *et al.,* 2002). Overexpression of MRP1 and its role in chemotherapy resistance has been reported in early- stage breast cancer (Filipits *et al*., 2005).

The breast cancer resistance protein (BCRP, MXR, ABC-P) is 95-kDa phosphoglycoprotein drug transporter with only one transmembrane and one ATP binding domain unlike P-gp and MRP. Fewer studies have reported the expression of BCRP in breast cancer (Borowski *et al*., 2005). Kanzaki and co-workers (Kanzaki

et al., 2001) reported uniformly low levels of BCRP expression in breast cancer tumors. According to Fanayte and co-workers (Fanayte *et al*., 2002), there is no indication that elevated BCRP expression in breast carcinomas confers resistance to anthracyclines.

Lung resistance protein (LRP) is a major vault protein found in the cytoplasm and on the nuclear membrane. Due to its high expression levels in drug-resistant cell lines and some tumors, it is frequently included in discussions of drug resistance, although it is not an ABC transporter (Gottesman *et al.*, 2002). However, high LRP expression was mainly evaluated in lung cancer (from which it derives its name) leukemias and ovarian cancer (Schneider *et al.*, 2001).

1.4.1.1 P-glycoprotein (P-gp/MDR1)

P-gp is a large transmembrane glycoprotein with molecular weight approximately 170 kD and is composed of two homologous halves each consisting of six predicted transmembrane (TM) domains and an intracellular loop with consensus ATP binding motif (Figure 1.3) (Paul and Cowan, 1999). When a substrate binds to the high affinity binding site, following ATP hydrolysis, a conformational change shifts the substrate to a lower affinity binding site and then releases it into the extracellular space or outer leaflet of the membrane. Binding of another drug is achieved by return to the conformation via hydrolysis of ATP at the second binding site (Leonard *et al.,* 2003).
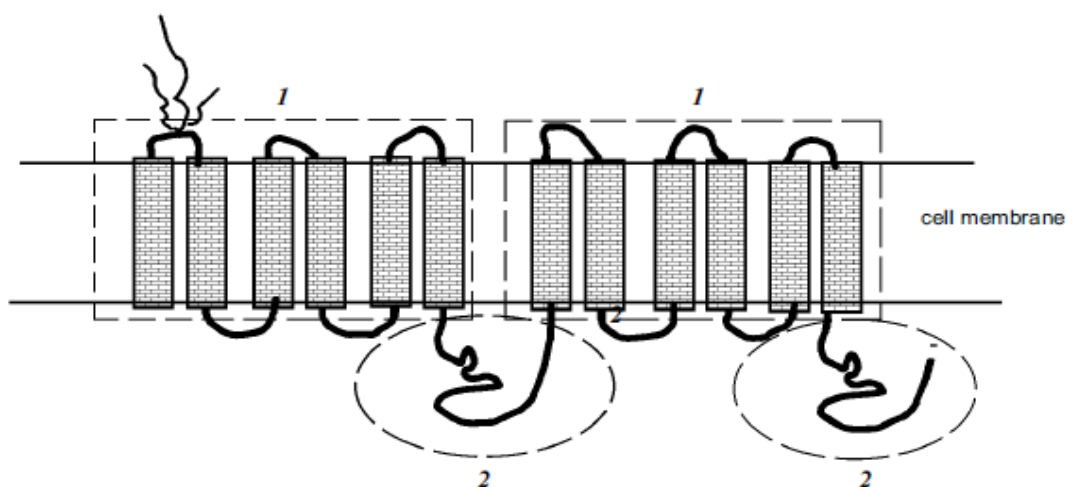
Figure 1. 3 Proposed structure of P-glycoprotein (Pgp): 1) transmembrane domains (indicated by rectangles); 2) ATP-binding domains (framed by oval) (Stavrovskaya, 1999).

The broad substrate spectrum of Pgp comprises preferably neutral or cationic amphiphilic organic compounds (Table 1.2). The recognition of multiple substrates is based on mainly the number, strength and spacial location of electron-donoring groups for hydrogen bonding with hydrogen donors from defined amino-acid sequence in P-glycoprotein (Seelig, 1998; Borowski *et al*., 2005).

Table 1. 2 Cytotoxic substrates of P-gp (Paul and Cowan, 1999).

Anthracyclines	**Taxenes**
Doxorubicin	Paclitaxel
Daunorubicin	Docetaxel
Epirubicin	
Vinca alkaloids	**Camptothecins**
Vincristine	Topotecan
Vinblastine	Irinotecan (CPT-11)
Vinorelbine	
Epipodophyllotoxins	**Antitumor antibiotic**
Etoposide	Actinomycin D
Teniposide	

In humans, two members of the P-gp gene family (*MDR1* and *MDR3*) exist, while three members of this family (*mdr1a*, *mdr1b* and *mdr2*) are found in mice. The P-gp encoded by human *MDR*1 and mouse *mdr*1*a*/1*b* genes function as a drug efflux transporter by extruding drugs out of cells, while human MDR3 P-gp and mouse mdr2 P-gp are suggested to be functional in phospholipid transport (Lin, 2003). P-gp is expressed in a variety of tumors as well as normal tissues such as transporting epithelia of the liver, kidney, colon, small intestine, pancreas, placenta, uterus and in specialized capillary endothelial cells in the brain and testis. P-gp expression in the brain suggests a role in the blood–brain barrier, thus preventing the permeation and persistence of hydrophobic agents in the central nervous system (Krishna and Mayer, 2000).

1.4.1.2 Multidrug Resistance Protein 1 (MRP1)

The amino-acid sequence of MRP1 resembles P-gp to only a modest extent (~15%), and its structure is distinct as well (Kruh and Belinsky, 2003). MRP1, a 190-kDa protein, has an additional five transmembrane (TM) segments located at the amino terminus and connected to a P-gp like core by a linker region (Figure 1.4). This transmembrane domain zero (TMD_0) is believed to be responsible for the organic anion affinity of MRP1 (Leonard *et al.*, 2003).
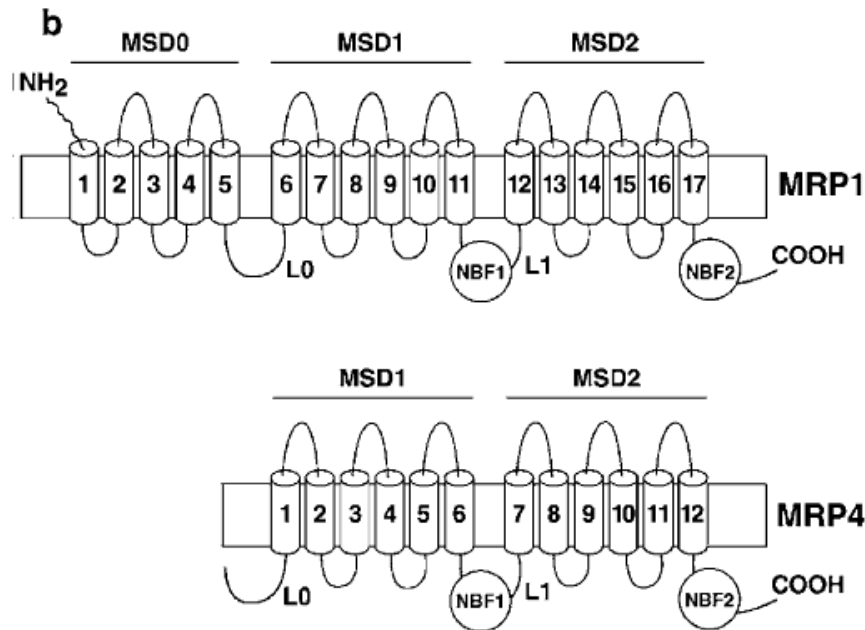
Figure 1. 4 Schematic representation of MRP1 (which resembles MRP2, MRP3, MRP6 and MRP7) and MRP4 (which resembles MRP5, MRP8 and MRP9). NBF, nucleotide binding fold MSD, membrane spanning domain. (Kruh and Belinsky, 2003).

Substrates of MRP1 include organic anions such as methotrexate. Non-anionic compounds may be transported as glutathione, glucuronide or sulfate conjugates, or may be co-transported with glutathione without conjugation (Leonard *et al*., 2003). The ability of MRP1 to transport glutathione conjugates as well as its widespread presence in normal tissues indicates that it is a ubiquitous GS-X pump and acts as a cellular detoxifying factor (Kruh and Belinsky, 2003). The chemotherapeutic drugs demonstrating MRP1 mediated drug resistance are listed in Table 1.3.

Table 1. 3 Cytotoxic substrates of MRP1 (Paul and Cowan, 1999).

Anthracyclines	**Camptothecins**
Doxorubicin	Topotecan
Daunorubicin	
Epirubicin	
Vinca alkaloids	**Epipodophyllotoxins**
Vincristine	Etoposide
Vinblastine	Teniposide
Vinorelbine	
Antitumor antibiotic	
Actinomycin D	
Methotrexate	

Several isoforms of MRP other than MRP1 have been identified: MRP2 (or cannalicular multispecific organic anion transporter or cMOAT), and MRP3-8 (Figure 1.4). MRP2 it is also a GS-X pump, associated with bilirubin glucuronide transport, with defects causing Dubin-Johnson syndrome. It is also a transporter for MRP1 substrates and cisplatin, with the potential to confer resistance to these agents. The properties of MRP family are summarized in Table 1.4. To date, the only convincing evidence for clinical drug resistance for MRP family is associated with MRP1 (Leonard *et al*., 2003).

Table 1. 4 MRP family members. (Kruh and Belinsky, 2003).

Protein	Transport: Conjugates	Transport: Glutathione	Resistance Profile	Substrates
MRP1	+	+	Anthracyclines, Vincristine, Etoposide, Camptothecins, Methotrexate	leukotriene C4
MRP2	+	+	Anthracyclines, Vincristine, Etoposide, Camptothecins, Methotrexate, Cisplatin	Bilirubin glucuronide
MRP3	+	-	Etoposide, Methotrexate	Glycocholic acid
MRP4	+	+	6-Mercaptopurine, Methotrexate, Paramethoxyethylamphetamine	Cyclic nucleotides
MRP5	-	+	6-Mercaptopurine, Paramethoxyethylamphetamine	Cyclic nucleotides
MRP6	+	?	Anthracyclines, Etoposide, Cisplatin	?
MRP7	+	?	?	?
MRP8	?	?	5-Fluorouracil, Paramethoxyethylamphetamine	Cyclic nucleotides

1.5 Strategies to Overcome MDR in Cancer Cells

Cancer chemotherapeutics can exert their cytotoxic effects only if optimal pharmacokinetics, tumor penetration, and intracellular concentration are maintained in the malignant cancerous cell (Tiwari *et al.*, 2009). Unfortunately, as stated earlier, overexpression of ABC transporters results in MDR, whose presence has been widely demonstrated in various types of cancer (Modok *et al.,* 2006). Breast cancer tumor resistance is mainly associated with overexpression of P-gp (Gottesman *et al.*, 2002). Therefore, in order to achieve better clinical outcome and increase the success of chemotherapy in breast cancer tumors, several strategies to overcome P-gp transporter mediated MDR have been proposed (Figure 1.5). These strategies aim to restore the cytotoxicity of available antitumor drugs against resistant cells by interfering with either the expression of P-gp transporters or their functioning (Borowski *et al.*, 2005).
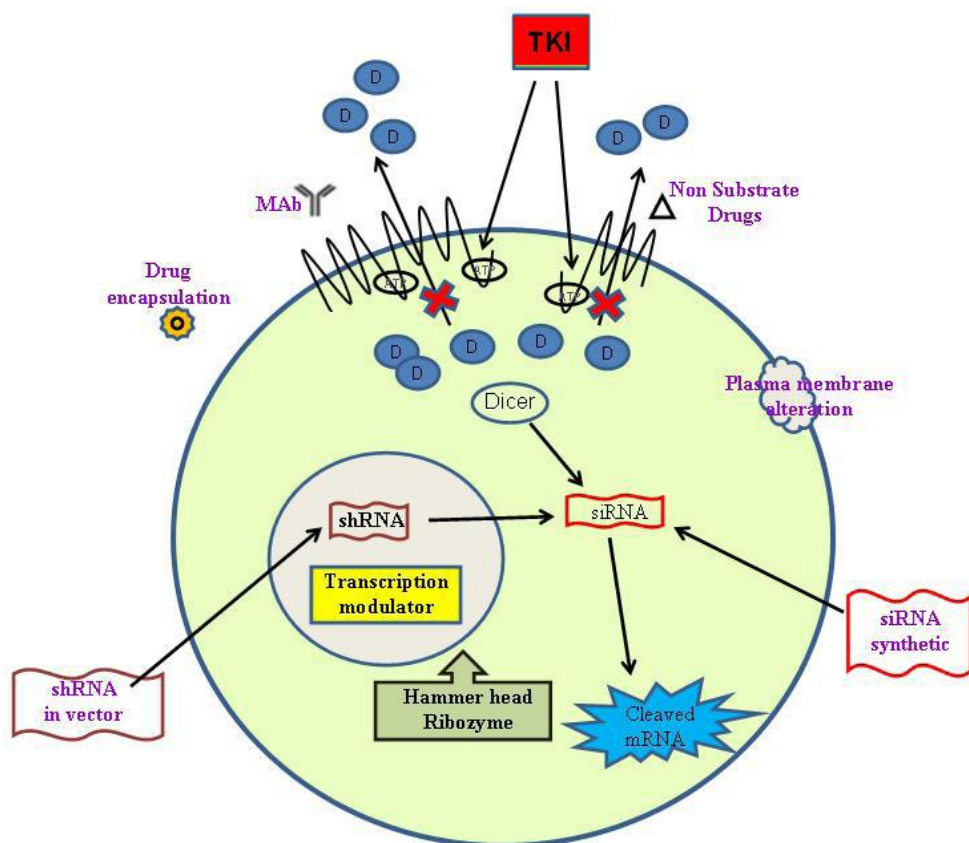
Figure 1. 5 Schematic representation of different approaches to avoid P-gp mediated MDR. TKI represents Tyrosine kinase inhibitors. (Tiwari *et al*., 2009).

1.5.1 Control of Expression of P-gp

Considerable attention has been paid to the gene-silencing methods of molecular biology to selectively block the expression of P-glycoprotein in human cancers. Relevant studies include:

- Ecteinascidin 743 (ET-743), a marine-based antitumor agent presently in phase II clinical trials, has been shown to abolish transcriptional activation of *MDR1* (Jin *et al*., 2000).
- Modification of *MDR1* promoter region and consequently inhibition of the transcriptional activity was achieved by 5-azacytidine (Efferth *et al*., 2001).
- HMN-176, an active metabolite of the antitumor agent HMN-214, has been reported to restore the chemosensitivity of MDR cells by targeting a *MDR1*-specific transcription factor (Tanaka *et al*., 2003; Borowski *et al*., 2005).

19

- Histone deacetylase inhibitor trichostatin A (TSA) has been demonstrated to downregulate *MDR1* expression through a transcriptional mechanism, independently of promoter methylation (El-Khoury *et al*., 2007).

- Antisense oligodeoxyribonucleotides (ODNs), which form duplexes with the target mRNA and cause interruption of translation, have been noted to suppress *MDR1* expression in drug-resistant tumor cells (Cucco and Calabretta, 1996; Motomura *et al*., 1998).

- Hammerhead ribozymes, which hybridize to a complementary sequence of mRNA and catalyze site-specific cleavage of the substrate, has been proposed to reverse P-glycoprotein-mediated MDR phenotype back to a drug-sensitive one (Kobayashi *et al*., 1994; Matsushita *et al*., 1998; Nagata *et al*., 2002).

- RNA Interference has been proposed as an alternative and more efficient strategy to prevent the biosynthesis of P-gp by selectively blocking the expression of P-gp/*MDR1* specific mRNA (Wu *et al*., 2003; Peng *et al*., 2004; Lage, 2005; Stierlè *et al*., 2005).

- Inhibition of signal transduction has been suggested as another potential approach to reverse P-gp mediated MDR, since expression of MDR1 is governed by appropriate signals (Yang *et al*., 2001; Borowski *et al*., 2005).

- The postranslational modifications comprising N-glycosylation and phosphorylation have been recommended as an alternative group of potential targets for MDR reversal (Borowski *et al*., 2005).

1.5.1.1 RNA Interference Strategy

Although successful in some applications, antisense ODNs and ribozyme based gene silencing technologies have been difficult to apply universally (Lage, 2005). These methodologies are still pursued, but adapting them as broadly applicable functional genomic and therapeutic tools has proven difficult (Takeshita and Ochiya, 2006). RNA interference (RNAi) is a more powerful and specific gene-silencing process that holds great promises in the field of cancer therapy.

RNAi was first described in animal cells by Fire and colleagues in the nematode *Caenorhabditis elegans* as a naturally occurring cellular mechanism that induces post-transcriptional gene silencing, in which double-stranded RNA (dsRNA) triggers specific degradation of the complementary mRNA sequence and eventually suppresses the expression of a target gene (Fire *et al*., 1998; Takeshita and Ochiya, 2006). RNAi, a highly conserved mechanism found in almost all eukaryotes, is believed to serve as an antiviral defense mechanism against viruses and transposable genetic elements. On entry into the cell, the dsRNA is cleaved by an RNase III like enzyme, Dicer, into small interfering (21- to 23- nt) RNAs (siRNAs), which have symmetric 2–3 nucleotide 3' overhangs and 5' phosphate and 3' hydroxyl groups (Figure 1.6) (Dillin, 2003). These RNA duplexes associate with a multiprotein RNA-inducing silencing complex (RISC), guiding RISC to a complementary target mRNA and triggering its endonucleolytic cleavage by Slicer (Argonaute-2), an enzyme residing within the RISC complex (Pai *et al*., 2006). For incorporation of siRNAs into RISC, siRNAs should be phosphorylated at the 5' end (Nykanen *et al*., 2001). The cleavage of target mRNA occurs at a single site, which is 10 nucleotides away from the 5' phosphate of the antisense strand of siRNA molecule. Due to the loss of either 5' 7-methylguanine cap or 3' poly(A) tail structures, the cleaved target mRNA is no longer protected against endogenous RNases and degraded (Lage, 2005). Mismatches more than 1–2 bp within the 21- to 23-nt siRNA effectively disrupt proper degradation of the target mRNA (Dillin, 2003).
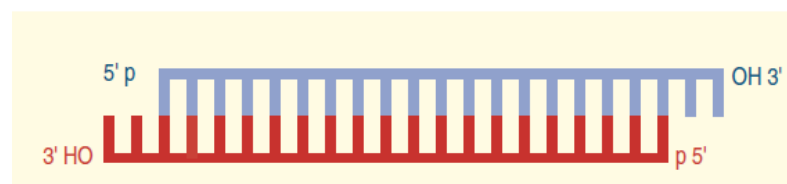
Figure 1. 6 Schematic overview of siRNA molecule (Lage, 2005).

RNA interference can be induced in mammalian cells either by introducing synthetic small interfering RNA (siRNA) or by plasmid and viral vector systems that express short hairpin RNAs (shRNA) that are processed to siRNA by Dicer (Takeshita and Ochiya, 2006).

Introduction of dsRNA into mammalian cells does not result in efficient Dicer-mediated generation of siRNA, but this problem can be bypassed by introducing synthetic 21-nt siRNA duplexes (Nieth *et al*., 2003). Although easier to administrate than shRNAs, the major disadvantage associated with chemically synthesized siRNAs is their transient gene expression inhibition effect. Whereas the duration of gene silencing in differentiated or slowly dividing cells is relatively long (on the order of several weeks), in more rapidly dividing cells, there is a short lived RNAi effect, peaking at around 3 days and lasting for approximately 1 week. The underlying reasons may include the increasing dilution of the siRNA with repeated cell division, as well as ongoing cellular enzymatic degradation (Pai *et al*., 2006).

The transient nature of siRNAs may be partly overcome by some chemical modifications to make them more resistant to serum RNases without disturbing biological activity. siRNAs can be coupled with fusogenic peptides, linked to antibodies to cell surface receptor ligands for cell-specific delivery, or encased in lipid complexes, cationic liposomes or other types of particles (Shankar *et al*., 2005; Pai *et al*.,2006), which would increase their effectiveness in potential therapeutic applications.

Expression vectors have been developed for stable long termed RNAi effects, which use plasmid or viral expression vectors containing an expression cassette for the production of siRNA-like transcripts; that are, synthesis of small hairpin RNAs (shRNA). Alternatively, expression cassettes driving the production of sense and antisense strands separately are utilized, whereby the two strands hybridize inside the cell to form functional active siRNA (Lage, 2005). The siRNAs derived from vector-based shRNAs, like synthetic siRNAs, are incorporated into the RISC and are able to induce the sequence specific and effective silencing of genes by following the RNAi pathway (Figure 1.7) (Takeshita and Ochiya, 2006).

22
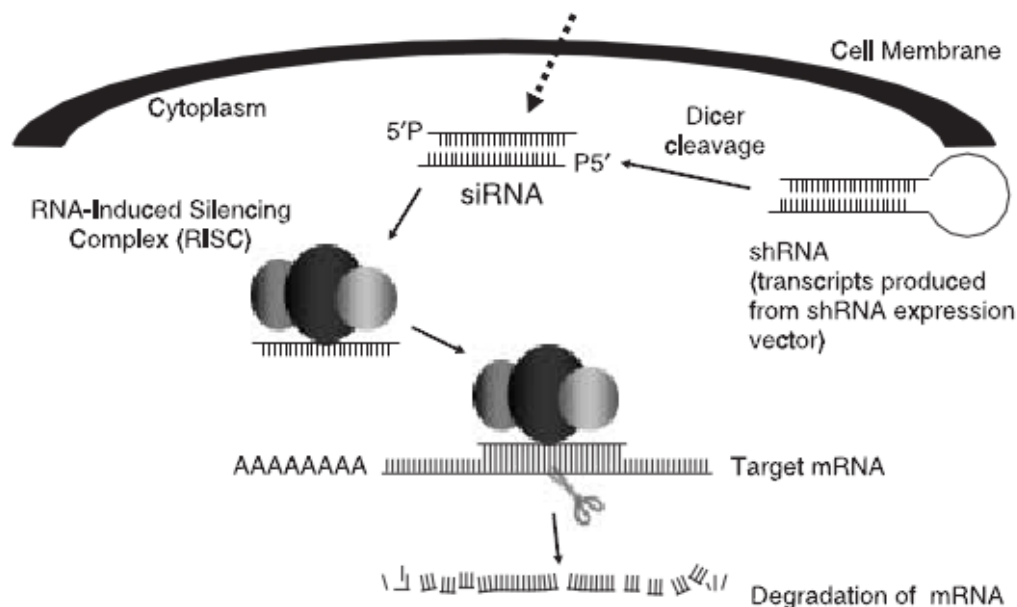
Figure 1. 7 Mechanisms of RNA interference. (Takeshita and Ochiya, 2006).

Although stable, long term supression of gene expression is the desired effect, the uptake and long-term stability of shRNAs serve one of the significant obstacles in establishing RNAi as a therapeutic approach (Pai *et al*., 2006). Expression of P-gp in a variety of normal tissues such as transporting epithelia of the liver, kidney, colon, small intestine, pancreas, placenta, uterus and in specialized capillary endothelial cells in the brain and testis makes transient transfection more advantageous for reversal of clinical MDR. Furthermore, it was demonstrated that, the specifity of siRNAs as well as shRNAs is sequence as well as concentration dependent. At ~100 nM, they nonspecifically induce a significant number of genes, many of which are known to be involved in apoptosis and the stres response (Semizarov *et al*., 2003; Persengiev et al., 2004). These non specific responses can be avoided by reduction of the siRNA concentration to 20nM (Semizarov *et al*., 2003; Persengiev et al., 2004). However, the levels of gene silencing can not be adjusted with shRNAs due to their stable supression effects. Moreover, technical and ethical problems due to the use of expression vectors, especially potential retrovirusor adenovirus-based shRNA delivery systems are needed to be addressed (Nieth *et al*., 2003). Finally, synthetic siRNAs are more suitable for combination therapies. Chemically

synthesized siRNAs in combination against the transcripts of various MDR-associated genes or genes encoding apoptosis and cell cycle regulating factors would be easier to use than stable systems (Nieth *et al*., 2003). In fact, in clinics MDR reversal strategies may demonstrate the highest efficiency in combination therapies, e.g., imatinib combined with anti-*Bcr Abl* tyrosine kinase and anti-*MDR1* RNAi mediating siRNAs for treatment of chronic myelogenous leukemia (Lage, 2005).

1.5.2 Modulation of P-gp Function

There are many studies conducted to overcome MDR by impairing the function of P-gp, to suppress or circumvent MDR mechanisms. The use of anticancer drugs which are not the substrates of P-gp including alkylating drugs (cyclophosphamide), antimetabolites (5-fluorouracil), and the anthracycline modified drugs (annamycin and doxorubicin-peptide) might be a solution to avoid drug resistance (Ozben, 2006).

The development of pharmacological agents that reverse drug resistance is another way to re-sensitize MDR cells to the chemotherapeutic agents. The process of chemo-sensitization comprises co-administration of a P-gp inhibitor (MDR modulator) with an anticancer drug in order to cause enhanced intracellular anticancer drug accumulation via distrupting the P-gp function (Krishna and Mayer, 2000). Among the many MDR modulators are the following compounds: calcium channel blockers (e.g. verapamil), cyclosporine A, phenothiazines, steroid hormones and non-ionic detergents, which are in general classified as those belonging to first, second and third generations (Michalak *et al.,* 2001).

- First generation MDR modulators include calcium channel blockers (e.g., verapamil), calmodulin antagonists, steroidal agents, protein kinase C inhibitors, immunosuppressive drugs (e.g., cyclosporine A), antibiotics (e.g., erythromycin), antimalarials (e.g., quinine), psychotropic phenothiazines and indole alkaloids (e.g., fluphenazine and reserpine), steroid hormones and anti-steroids (e.g., progesterone and tamoxifen), detergents (e.g.,

cremophorEL) and surfactants, many of which were themselves substrates for ABC transporters and competed with the cytotoxic drugs for efflux by the MDR pumps. Consequntly, requirement of high serum concentrations of the chemosensitizers resulted in unacceptable high toxicity, limiting their clinical applications (Ozben, 2006).

- Second generation MDR modulators, such as valspodar (PSC833), biricodar (VX-710), demonstrated more positive outcomes with less toxicity, more bioavailability at the tumor site, and re-sensitization of MDR cells when re-treated with initial chemotherapy in resistant cancer (Goldman, 2003; Tiwari *et al*., 2009). However, since most of them were also substrates for cytochrome P450 3A4 and metabolized by this enzyme, unpredictable pharmacokinetic interactions occured and clinical trials failed (Ozben, 2006).

- Third generation MDR modulators has been developed by combinatorial chemistry and from studying structure–activity relationships (Modok *et al.,* 2006). They comprise the P-gp specific cyclopropyldibenzosuberane LY 335979, the acridonecarboxamide GF 120918, the diketopiperazine XR9051, the diarylimidazole OC144-093, as well as both P-gp and MRP specific VX-710 and VX-853 (Krishna and Mayer*,* 2000). Their advantages include high in vitro potency and improved selectivity (Modok *et al.,* 2006). Clinical trials with these new third-generation agents are in process aiming a longer survival in cancer patients (Ozben, 2006).

1.5.2.1 Verapamil (Isoptin®)

Verapamil (Figure 1.8) is a currently available FDA-approved calcium channel blocker drug traditionally used to treat irregular heartbeats (arrhythmias) and high blood pressure by relaxing blood vessels. Tsuruo and colleagues first demonstrated that verapamil could also reverse Pgp-mediated MDR (Tsuruo *et al*., 1981; Ling, 1997). They reported that verapamil has the ability to inhibit the binding of photoactivatable drug analogs to P-glycoprotein, restoring drug accumulation and enhancing drug sensitivity of cultured cells that overexpress this protein (Tsuruo *et al.,* 1981; Sharom, 1997; Loe *et al*., 2000). In numerous cell lines verapamil

treatment resulted in enhanced accumulation of many anticancer drugs, including doxorubicin (Roepe, 1992; Coley *et al*., 1993; Consoli *et al*., 1997; Krishna and Mayer*,* 2000; Stierlè *et al*., 2005; Shen *et al.*, 2008). The reversal mechanism of verapamil has been proposed as the direct binding of verapamil to P-gp through competitive inhibition of drug transport (Yusa and Tsuruo, 1989). Moreover, verapamil has been suggested to interact with phosphatidylserine leading to an alteration of lipid phase properties, which may also affect the activation of protein kinase C that is basically for P-gp phosphorylation (Chaudhary and Roninson, 1992; Pajeva *et al*., 2004). Further, verapamil, a substrate for P-gp, is proposed to potentially stimulate ATPase activity (Shapiro and Ling, 1995; Sharom, 1997; Loe *et al*., 2000). However, this property of verapamil is the reason of its high toxicity, limiting its clinical applications, due to the competition between anticancer drugs and verapamil for P-gp.

Verapamil has been demonstrated to significantly chemo-sensitize the P-gp, as well as MRP1 overexpressing cells. Reversal of MRP1 mediated MDR may be more related to the ability of verapamil to stimulate GSH efflux and reduce intracellular GSH levels than direct inhibition of the transporter itself (Loe *et al*., 2000; Cullen *et al*., 2001; Leslie *et al*., 2003; Perrotton *et al*., 2007).
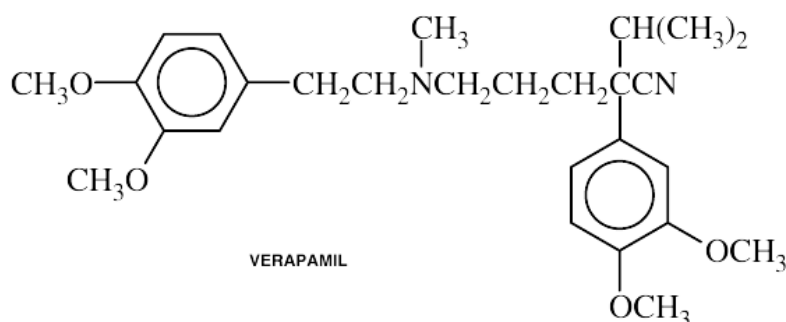
Figure 1. 8 Verapamil (Isoptin®) (http://home.caregroup.org/clinical/altmed/ interactions /Images/Drugs/verapami.gif).

1.5.2.2 Promethazine (Phenergan®)

Promethazine (Figure 1.9) is in a group of drugs called phenothiazines and is used to treat allergy symptoms and also prevents motion sickness, treats nausea and vomiting or pain after surgery.

Phenothiazines, apart from their wide biological activity, have also been described as effective multidrug resistance modifiers (Engi *et al*., 2006). Phenothiazine derivatives share a highly hydrophobic multiring system in the core of their molecules and more or less hydrophilic substitutions located around this lipophilic moiety that make them well suited for interaction either with the lipid phase of membranes or with membrane proteins (Michalak *et al*., 2007). This ability of phenothiazine derivatives is thought to drive the reversal of MDR (Pajeva *et al*., 1996; Pajeva *et al*., 1998). According to the "vacuum cleaner" hypothesis, P-gp substrates are recognized within the lipid phase during their diffusion across the cell membrane. An alteration of lipid phase properties in the presence of modulators may affect substrate binding to transporter molecules or enhance the passive diffusion of drugs across the lipid bilayer, leading to their increased intracellular accumulation (Sharom, 1997; Michalak *et al*., 2007). Moreover, it has been suggested that the altered biophysical properties of the membrane lipid phase influence P-gp conformation and its ATPase activity (Fertè, 2000; Michalak *et al*., 2007). Promethazine has been reported to modulate MDR in various cell lines (Michalak *et al*., 2007; Kars *et al*, 2008). However its additional cytotoxic effects may limit its usage in clinics (Engi *et al*., 2006).
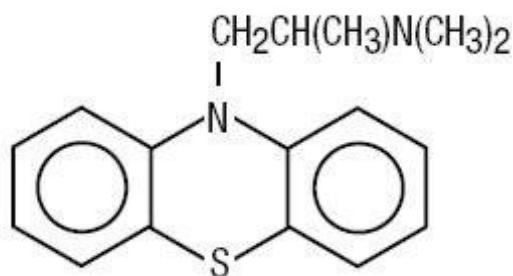
Figure 1. 9 Promethazine (Phenergan®) (http://dailymed.nlm.nih.gov/dailymed/fda /fdaDrugXsl.cfm?id=702&type=display).

1.6 Aim of the Study

The aim of this study is reversal of P-gp/MDR1 mediated multidrug resistance with newly selected and applied siRNA. Selective down-regulation of *MDR1* expression can re-sensitize doxorubicin resistant cells to anticancer agent doxorubicin, a substrate of P-gp/MDR1, and increase the success of chemotherapy. The objectives of this study may be listed as:

- Downregulation of *MDR1* expression in a specific manner using a siRNA targeting *MDR1* mRNA in doxorubicin resistant MCF-7 cells.
- Determination of *MRP1* expression levels after *MDR1* silencing.
- Investigation of doxorubicin accumulation and localization, and reversal of the efflux in doxorubicin resistant cells after applying *MDR1* siRNA or other MDR modulators verapamil and promethazine, than comparison of siRNA, verapamil and promethazine efficacy for MDR reversal.
- Determination of inhibitory concentration 50 (IC_{50}) values for doxorubicin and evaluation of chemo-sensitivity in doxorubicin resistant cells in response to *MDR1* silencing.
- Investigation of migratory behavior of doxorubicin resistant cells after *MDR1* silencing in order to assess the relationship of P-gp expression and motility.
- Comparison of the MDR modulatory efficacy of the newly applied siRNA duplex in this study with previous studies.

CHAPTER 2

MATERIALS AND METHODS

2.1 MATERIALS

2.1.1 Cell Lines

MCF-7 human breast adenocarcinoma cell line was denoted by Şap Institute, Ankara, Turkey. Doxorubicin resistant cell line, MCF-7/Dox was developed from the parental MCF-7 cell line (MCF-7/S) previously in our laboratory by continuous drug application in dose increments (final dose: 1μM) and shown to express high levels of P-gp (Kars *et al.,* 2006).

2.1.2 Chemicals and Reagents

Doxorubicin (DOX) and Verapamil (Isoptin®) were kindly provided by Prof. Dr. Fikret Arpacı (Gülhane Military Medical Academy, School of Medicine, Department of Oncology). The stock solution of doxorubicin was prepared as 3.4mM with sterile distilled water and stored at 4ºC. Promethazine was kindly denoted by Prof. Dr. Jozsef Molnár (University of Szeged, Faculty of Medicine, 6720, Szeged, Hungary).

RPMI 1640 medium and fetal bovine serum (FBS) were obtained from Biochrom AG, Germany. Gentamycin, trypsin-EDTA, trypan blue and XTT Cell Proliferation Kit were purchased from Biological Industries, Israel. Phosphate buffered saline (PBS) and dimethyl sulfoxide (DMSO) were obtained from Sigma-Aldrich, USA. Lipofectamine RNAi-MAX siRNA transfection reagent and OPTI-MEM I reduced

serum medium were obtained from Invitrogen, USA. DEPC, isopropanol, ß-mercaptoethanol and agarose were purchased from Applichem, Germany. RNeasy Mini RNA isolation kit was purchased from Qiagen, USA. High Range RNA ladder, 50 bp DNA ladder, 6X loading buffer, Moloney-Murine Leukemia Virus Reverse Transcriptase, dNTP set, $MgCl_2$ and *Taq* DNA polymerase were obtained from Fermentas, Lithuania. Light- Cycler-FastStart DNA Master SYBR Green I kit was obtained from Roche Diagnostics, Switzerland.

2.1.3 siRNA

Alexa Fluor® red fluorescent oligo, *MDR1* siRNA and mock siRNA were obtained from Invitrogen, USA.

2.1.4 Primers

MDR1, MRP1 and *ß-actin* primers were purchased from Alpha DNA, Canada. Primer sequences and amplicon sizes are represented in Table 2.1.

Table 2. 1 Primers used in quantitative real-time polymerase chain reaction (qPCR) and the amplicon sizes.

Primer	Sequence	Location	Amplicon Size
MDR1 Sense	5'ACAGAAAGCGAAGCAGTGGT3'	Exon 15	62 bp
MDR1 Antisense	5'ATGGTGGTCCGACCTTTTC3'	Exon 16	
MRP1 Sense	5'TGTGGGAAAACACATCTTTGA3'	Exon 18	80 bp
MRP1 Antisense	5'CTGTGCGTGACCAAGATCC3'	Exon 19	
ß-actin Sense	5'CCAACCGCGAGAAGATGA3'	Exon 3	97 bp
ß-actin Antisense	5'CCAGAGGCGTACAGGGATAG3'	Exon 4	

2.2 METHODS

2.2.1 Cell Culture

2.2.1.1 Cell Line and Culture Conditions

Parental MCF-7 cells (MCF-7/S) and doxorubicin resistant cells (MCF-7/Dox) were maintained in 15 mL of RPMI 1640 medium (Appendix A) with 10% (v/v) fetal bovine serum (FBS) and 1% (v/v) gentamycin in T-75 filter cap tissue culture flasks (Greiner Bio-One, Germany). They were incubated at 37 °C in a humidified atmosphere with 5% (v/v) CO_2 in a Heraeus incubator (Hanau, Germany).

2.2.1.2 Subculturing (Passaging)

Passaging cells involves detaching the cells from their substrate and transferring them to new culture flasks. When cells have covered the available surface area or have reached a population density which suppresses their growth (Kaplan *et al.*, 1979), cells were passaged by trypsinization under sterile conditions. Medium was discarded and cells were washed with 1-2 ml of PBS to remove the traces of serum, since trypsin is inactivated in the presence of serum. Trpsin-EDTA (2 mL) was added and cells were incubated at 37 °C for 4-6 minutes until the cells detached and the media became cloudy. Detached cells were resuspended in medium containing serum and required number of cells were transferred to a new flask. Doxorubicin (1μM) was added to the resistant cells after every passage for the maintainance of the resistance.

2.2.1.3 Freezing Cells

Detached cells were resuspended in 5 mL of medium containing serum and centrifuged at 1,000 rpm for 5 min. After discarding supernatant, the cell pellet was homogenized in 5 mL of PBS and centrifuged at 1,000 rpm for another 5 min. The

supernatant was removed and cells were resuspended in the freezing medium (10% (v/v) DMSO + 90% (v/v) FBS) to have a final concentration of approximately 2 x 10^6 cells / mL. The cell suspension was taken into cryovials (Greiner) and the cells were incubated at 4 °C for 30 min and at -20 °C for 3-4 hours before the overnight incubation at –80 °C. Finally cryovials were transferred to liquid nitrogen for long term storage.

2.2.1.4 Thawing Frozen Cells

Cryovials were taken from liquid nitrogen. Since above 4 °C DMSO is toxic to the cells, it is very important to thaw them quickly at 37 °C. The cells were transferred into 15 mL Falcon tubes (Greiner) and centrifuged at 1,000 rpm for 5 min. Then the cells were seeded into culture flasks in previously defined culture medium.

2.2.1.5 Viable Cell Count Using Trypan Blue Exclusion Method

The reactivity of Trypan Blue dye is based on the fact that the chromopore is negatively charged and does not interact with the cell unless the membrane is damaged (Freshney, 1987). Therefore, viable cells exclude the dye and the dead cells are stained into blue.

The cell suspension was mixed with trypan blue solution (0.5 %) with a ratio of 9 : 1 and counted in a Neubauer hemacytometer (Bright-line, Hausser Scientic, USA) under phase contrast microscopy (Olympus, USA).

The hemacytometer consists of 16 large squares and each of them is divided into 16 small squares. One small square represents a volume of $0.00025mm^3$. The number of cell in 1mL was determined using the following formula (Equation 2.1):

Cell number/mL = Average count per square x Dilution factor x 4 x 10^6 (2.1)

2.2.2 siRNAs and Transfection

2.2.2.1 siRNA Design

MDR1 siRNA and mock siRNA (21 nucleotides) were designed using BLOCK-iT™ RNAi Designer Software (Invitrogen). Among 10 designed oligos, the most efficient *MDR1* siRNA was choosen according to the criteria described previously (Elbashir *et al*., 2001; Sioud and Leirdal, 2004; Stierle´ *et al.,* 2007). The siRNA sequence targeted *MDR1* mRNA at nucleotides 2815-2835 in the coding region relative to the start codon. Mock siRNA was a scrambled control siRNA without any known target in the human genome. The sequences of siRNAs are represented in Table 2.2.

Table 2. 2 The sequences of *MDR1* siRNA and mock siRNA.

siRNA	Sequence
MDR1 Sense	5'GGAUGUGAGUUGGUUUGAUdTdT3'
MDR1 Antisense	5'AUCAAACCAACUCACAUCC dTdT3'
Mock Sense	5'GGAAGUUUGUGGUUUGGAUdTdT3'
Mock Antisense	5'AUCCAAACCACAAACUUCC dTdT3'

2.2.2.2 BLOCK-IT™ Alexa Fluor® Red Fluorescent Oligo

Alexa Fluor® Red Fluorescent Oligo is a red-labeled dsRNA oligomer. It has the same length, charge, and configuration as the standard siRNA and is not homologous to any known gene in the human genome (Invitrogen, 2006). It was used to assess and optimize the uptake of siRNA molecules into doxorubicin resistant MCF-7 cells.

2.2.2.3 Transfection

Transfection was carried out using Lipofectamine RNAi-MAX transfection reagent and OPTI-MEM I reduced serum medium according to the manufacturer's protocol. In a 6-well format transfection, 60 pmol siRNA duplex was diluted in 500µL of OPTI-MEM I reduced serum medium in a well of 6-well tissue culture plate (Greiner). 5 µL of the transfection reagent was added to each well and after gentle mixing, the plate was incubated at room temperature for 15-20 minutes. During the incubation period, MCF-7/Dox cells were trypsinized and diluted in complete growth medium without antibiotics, so that 2.5 mL of medium contains 250,000 cells. Diluted cell suspension was added to each well containing siRNA and transfection reagent, and they were mixed by rocking the plate back and forth gently. The final concentration of siRNA was 20 nM and gene silencing was assayed 48 or 72 hours after transfection.

In a 96-well format transfection, 1.2 pmol siRNA duplex was diluted in 20 µL of OPTI-MEM I and mixed with 0.2 µL of Lipofectamine RNAi-MAX. Finally, 10,000 cells per well were seeded.

2.2.3 Reverse Transcription-Quantitative Polymerase Chain Reaction (RT-qPCR)

2.2.3.1 Isolation of Total RNA

All the glassware and other utensils were treated with diethyl carbonate (DEPC) treated dH_2O (Appendix B) prior to RNA isolation in order to inactivate RNases.

Total RNA isolation was performed using RNeasy Mini Kit according to the manufacturer's instructions. All the steps of the protocol, including centrifugation, were carried out at room temperature.

Total RNA was extracted after 48 and 72 hours of transfection in 6-well format. Briefly, cells were discarded, trypsinized and centrifuged at 1,000 rpm for 5 min. Supernatant was poured off and the cell pellet was homogenized in 350 µL of Buffer RLT (containing 10 µL β-Mercaptoethanol per 1 mL) by pipetting. Equal volume of 70% (v/v) Ethanol (350 µL) was added to the homogenized lysate and mixed well by pipetting. The sample was then transferred to an RNeasy Column in a 2 mL collection tube and centrifuged for 15 sec at 12,000 rpm. Afterwards, the flow-through was discarded and 700 µL of Buffer RW1 was added to the RNeasy Column. After centrifugation for 15 sec at 12,000 rpm, the flow-through was poured off and 500 µL of Buffer RPE was added to the RNeasy Column. The column was centrifuged for 15 sec at 12,000 rpm, the flow-through was discarded and another 500 µL of Buffer RPE was added. Then, after centrifugation for 2 min at 12,000 rpm, the RNeasy Column was placed in a new 1.5 mL collection tube and 40 µL of RNase-free dH2O was directly applied to the column membrane. The column was centrifuged for 1 min at 12,000 rpm for the elution of RNA.

2.2.3.2 Quantitation of the Isolated RNA

The concentration and purity of RNA sample was determined by measuring optical density at 260 and 280 nanometers. Absorbance measurements at 260nm permit the calculation of RNA concentration in a sample (Equation 2.2), where absorbance ratio of 260 nm to 280 nm enables the assessment of purity.

[RNA] µg/ml = A260 x DF x 40.0

where

A260 = absorbance (in optical densities) at 260 nm

DF = dilution factor (200)

40.0 = average extinction coefficient of RNA   (2.2)

A pure sample of RNA has an A260/A280 ratio of 2.0±0.1.

2.2.3.3 Agarose Gel Electrophoresis of RNA

The intactness of the RNA samples and the presence of DNA contamination were examined by horizontal agarose gel electrophoresis.

Agarose (0.6 g) was weighted and dissolved in 50 mL of 1X TAE buffer (Appendix B). The mixture was boiled in the microwave oven until the agarose melted completely. The gel solution was cooled and 2 μL ethidium bromide solution (Appendix B) was added. Gel solution was poured into electrophoresis apparatus and the comb was placed. After solidification, 5 μL of RNA sample was mixed with 1 μL of 6X loading dye (Appendix B) and loaded. The samples were run on 1.2 % agarose gel at 70 V for 65 min and visualized by UV gel acquisition system.

2.2.3.4 Reverse Transcription (cDNA Synthesis)

cDNA synthesis was performed with 5 μg total RNA and 20 pmol either of *MDR1*, *MRP1* and *ß-actin* gene specific primer.

The reaction was performed in DEPC treated, sterile 0.5 mL eppendorf tube (Greiner). 5 μg total RNA, 20 pmol of the primer and RNase-free dH_2O (Fermentas) were put into the tube with a total volume of 11 μL. The tube was incubated at 70°C for 5 min to disrupt the secondary structure of RNA. Afterwards, 4 μL of 5X reaction buffer (Fermentas), 2 μL of 10mM dNTP mix and 2.7 μL of RNase-free dH_2O were added and the reaction mixture was incubated at 37 °C for 5 min for primer annealing. Finally, 0.3 μL Moloney-Murine Leukemia Virus Reverse Transcriptase added and the mixture was incubated at 42 °C for 60 min for synthesis. The reaction was terminated by incubation at 70 °C for 10 min and cDNA were stored at -20 °C until use.

2.2.3.5 Quantitative Real-Time Polymerase Chain Reaction (qPCR)

Real-time PCR (qPCR) was carried out in Rotor-Gene 6000 (Corbett Research, Australia). Amplification products were detected via intercalation of the fluorescent dye SYBR green (Light- Cycler-FastStart DNA Master SYBR Green I kit, Roche Diagnostics) according to the manufacturer's instructions.

The mixture was prepared in the sterile 0.2 mL PCR-eppendorf tubes. Briefly, 10 µL reaction mix contained 2X master mix, 2.8 µL cDNA and 0.3 µL from each sense and antisense primers. Amplification conditions of *MDR1*, *MRP1* and *ß-actin* genes are represented in Table 2.3. Each sample run were performed in triplicates. A non template control containing dH_2O instead of cDNA was also included to identify any background signal. Amplification plots were displayed by plotting fluorescence versus treshold cycle number.

The melting peaks of all PCR products were determined by melting-curve analysis in order to ensure that only the expected products had been generated. After real time PCR amplification, the machine was programmed to do a melt curve, in which the temperature ramped from 50 °C to 99 °C raising one degree at each step and the change in fluorescence was measured. All PCR products for a particular primer pair should have the same melting temperature, unless there is a contamination, mispriming or primer dimer.

Table 2. 3 Amplification conditions of *MDR1*, *MRP1* and *ß-actin* genes.

	MDR1	*MRP1*	*ß-actin*
Pre-incubation	95 °C, 10 min	95 °C, 10 min	95 °C, 10 min
Denaturation	94 °C, 30 sec	94 °C, 15 sec	94 °C, 15 sec
Annealing	57 °C, 30 sec	55 °C, 45 sec	55 °C, 45 sec
Extension	72 °C, 30 sec	72 °C, 45 sec	72 °C, 45 sec
Melting	50-99 °C	50-99 °C	50-99 °C
Cycle number	45	40	40

2.2.3.6 Quantitation of qPCR Products

Delta delta Ct ($2^{-\Delta\Delta C_T}$) relative quantitation method was used for quantitation of qPCR products. This method presents the data as fold change in gene expression normalized to an internal control and relative to some reference group such as untreated control or a sample at time zero in a time-course study (Livak and Schmittgen, 2001). The changes in expression of the *MDR1* or *MRP1* genes were analyzed according to the following equation (Equation 2.3):

Fold change= $2^{-\Delta\Delta C_T}$

$$\Delta\Delta C_T = (C_{T\ Target} - C_{T\ Internal\ Control})_{Treatment} - (C_{T\ Target} - C_{T\ Internal\ Control})_{No\ Treatment} \quad (2.3)$$

The fold change in the *MDR1* and *MRP1* genes was normalized to the internal control gene *ß-actin* and determined for each sample using Eq. 2.3 relative to the untreated control. The treshold cycle values for *MDR1*, *MRP1* and *ß-actin* genes are demonstrated in Appendix C.

2.2.3.7 Statistical Analysis

All data are representative of three independent experiments, each run in triplicates and expressed as mean ± standard error of the means (SEM). They were statistically evaluated by one way ANOVA test using SPSS 13.0 Software (SPSS Inc, USA) and the mean difference was significant at the 0.05 level. In order to find groups whose mean differences were significant, Post hoc Tukey analyses were carried out.

2.2.4 Confocal Laser Scanning Microscopy and Image Analysis

2.2.4.1 Microscopy after Alexa Fluor® Red Fluorescent Oligo Treatment

MCF-7/Dox cells were transfected in 6-well format. Transfection complexes were prepared as directed by the manufacturer and the final concentrations of Alexa Fluor® oligo were 10nM, 20nM, 30nM, 40nM or 50nM with one negative control.

The excitation peak of Alexa Fluor® is 555 nm and the emission peak is 565 nm. 15 hours after transfection, cells were washed with PBS for three times and the culture medium was replaced with PBS for improved fluorescence detection. Images were collected using a Zeiss LSM 510 confocal laser scanning microscope (Jena, Germany) with LD A-Plan 20X/0.30 Ph1 lens. All images were scanned at 1024 X 1024 pixels as 12 bit images with pinhole size set to 1 airy unit and with the same laser power and detector sensitivity settings. High quality digital images were required for quantitation analysis, therefore frame size was set to 1024 X 1024 and bit depth was set to 12.

2.2.4.2 Microscopy after *MDR1* siRNA Treatment

Autoclaved coverslips (Marienfeld, Germany) were placed into the wells of a 6-well plate. MCF-7/Dox cells were seeded onto the coverslips and transfected in 6-well format. 48 or 72 hours after transfection, cells were washed three times with PBS. After treatment with 1 or 4 µM of doxorubicin for 1 hour, they were fixed with 2% (w/v) paraformaldehyde in PBS (Appendix B). The coverslips were wet-mounted on microscope slides and observed under the Zeiss LSM 510 confocal laser scanning microscope with Plan-Neofluar 40X/1.3 Oil DIC lens to determine the intracellular doxorubicin accumulation and localization. All images were scanned at 1024 X 1024 pixels as 12 bit images with pinhole size set to 1 airy unit and with the same laser power and detector sensitivity settings. The excitation and emission wavelengths of doxorubicin were 488 and 530 nm, respectively.

2.2.4.3 Microscopy after Verapamil or Promethazine Treatment

Cells were trypsinized and pelleted. Viable cells were counted using trypan blue dye exclusion method under phase contrast microscopy. MCF-7/S and MCF-7/Dox cells were seeded onto autoclaved cover slips as 600,000 cells/slip and they were allowed to grow overnight. On the following day, cells were washed with PBS for three times and incubated with or without verapamil (60µM) or promethazine (9.6µM) for

30 min prior to one hour 4μM doxorubicin treatment. After incubation, medium was discarded, cells were fixed with 2% (w/v) paraformaldehyde in PBS and the coverslips were wet-mounted on microscope slides. The images were collected using the Zeiss LSM 510 confocal laser scanning microscope with Plan-Neofluar 40X/1.3 Oil DIC lens with the same parameters and same settings as the transfected MCF-7/Dox cells.

2.2.4.4 Image Analysis

For quantitation of Alexa Fluor® oligo uptake and intracellular drug accumulation, at least 40 cells were randomly picked from 3 cell images for each particular treatment or subline and analyzed using Image J I.41 software (National Institutes of Health, USA) as mean fluorescence intensity per pixel.

2.2.4.5 Statistical Analysis

The results of image analysis are expressed as mean ± SEM and were subjected to one way ANOVA test using SPSS Software to determine the significant mean difference at the 0.05 level. In order to find groups whose mean differences were significant, Post hoc Tukey analyses were carried out.

2.2.5 Determination of Cell Proliferation

2.2.5.1 Cell Proliferation Assay with XTT Reagent

XTT Cell Proliferation Kit was used to measure cell proliferation. The assay is based on the ability of metabolic active cells to reduce the tetrazolium salt XTT to orange colored compounds of formazan. The reduced formazan compounds are water soluble and the compound intensity can be spectrophotometrically measured

at a given wavelength. The intensity is proportional to the number of metabolicly active cells (Biological Industries, 2002).

In brief, MCF-7/Dox cells were seeded to 96-well plates starting from the second column (Figure 2.1) and transfected with *MDR1* or mock siRNA in 96-well format. 48 hours after transfection, medium was discarded and cells were washed with PBS for three times. Afterwards, 150 µL of medium was added into the first and second columns, third column was empty and 50 µL of medium was added in to the rest of the columns. First column was the medium control column (only medium) and second column was the cell control column (only untreated cells and medium). The top and bottom horizontal rows were left as medium control of doxorubicin (only medium and drug) in order to eliminate the interference of doxorubicin absorbance with that of formazan at 500 nm. The columns 3 to 12 contained serial dilutions of the drug: 200 µL of concentrated doxorubicin was applied into the third column and it was serially diluted by taking 150 µL portion of doxorubicin solution from the third column and putting into the next column. Finally, all volumes were completed to 150 µL by adding 100 µL of medium and cells were incubated at 37 °C for 48 hours.

To assay the cell proliferation of MCF-7/S and MCF-7/Dox cells, cells were seeded in to 96-well plates (10,000 cells), incubated overnight and subjected to the same serial dilutions as transfected cells.

Column Number:

1 2 3 4 5 6 7 8 9 10 11 12

Top row

Bottom row

Figure 2. 1 XTT cell proliferation assay design in a 96-well plate.

XTT and activator reagents were applied to the plates at the end of the incubation and the optical density of soluble product was measured at 500 nm with a Spectromax 340 96-well plate reader (Molecular Devices, USA).

In order to obtain cell proliferation curve for a plate, the intensity of the dye in each well was converted to percent viability. For each column, the average intensity of the dye (except top and bottom wells) was calculated. The average of intensity of top and bottom wells was substracted from the calculated value. The same procedure was carried out for the second column with untreated cells, which were assumed as 100% viable. IC_{50} values, resistance indices and fold reversal values were determined for each particular treatment and subline. Inhibitory concentration 50 (IC_{50}) for a particular drug was defined as the concentration of the drug which reduces cell proliferation to 50% of untreated control cells. Relative resistance index (R) was expressed as the ratio of the IC_{50} of the resistant cells to the IC_{50} of the sensitive cells (Dalton *et al.,*1986). Fold reversal (FR) was defined as the ratio of the IC_{50} of the resistant cells to the IC_{50} of the modulator treated resistant cells (Wu *et al.*, 2003). IC_{50} values were calculated from the logarithmic trend line of the %cell

proliferation versus concentration plots. Logarithmic equations of the viability graphs and IC_{50} calculations are given in detail in Appendix D.

Resistance indices (R) were determined using the following formula (Equation 2.4):

R= IC_{50} of the resistant cells / IC_{50} of the sensitive cells   (2.4)

Fold reversal (FR) was calculated by the formula given below (Equation 2.5):

FR= IC_{50} of resistant cells / IC_{50} of *MDR1* siRNA treated cells   (2.5)

2.2.5.2 Statistical Analysis

All experiments were performed in triplicates and expressed as mean ± SEM. They were statistically evaluated by one way ANOVA test using SPSS Software and the mean difference was significant at the 0.05 level. In order to find groups whose mean differences were significant, Post hoc Tukey analyses were carried out.

2.2.6 Cell Migration Assay and Image Analysis

2.2.6.1 Wound Healing Assay

Wound healing assay was used for determination of directional cell migration (Todaro *et al*., 1965). MCF-7/Dox cells were transfected in 6-well format. 72 hours after transfection, cells were grown to 100% confluency and they were washed with PBS for three times. A sterile pipette tip was used to make a straight line wound on the cell culture. After washing the cells with PBS to remove the detached cells, they were exposed to 4 μM of doxorubicin. An untreated control group was also included. The wound was photographed after 24 hours using phase contrast microscopy with 4 X objective (overall magnification: 40 X).

2.2.6.2 Image Analysis

For quantitation of the wound closure, the distances between the wound edges were measured at 10 different points from the images of the wound using the ImageJ 1.41 program. The mean distances were determined for each treatment and the images, which were taken at 0. and 24. hours, were compared and expressed as wound healing percent using the following formula (Equation 2.6):

% Wound Healing = [(Distance between the edges of original wound − Distance between the edges of wound during healing) / Distance between the edges of original wound] x 100   (2.6).

2.2.6.3 Statistical Analysis

All experiments were performed in triplicates and expressed as mean ± SEM. They were statistically evaluated by one way ANOVA test using SPSS Software and the mean difference was significant at the 0.05 level. In order to find groups whose mean differences were significant, Post hoc Tukey analyses were carried out.

CHAPTER 3

RESULTS AND DISCUSSION

3.1. Isolation of Total RNA

Isolated total RNA was examined on 1.2 % agarose gel before proceeding to cDNA synthesis (Figure 3.1). The most abundant component of a purified sample of total RNA is rRNA, which constitutes 80 to 85% of the sample. mRNA is usually no more than 2 to 3% of the total RNA, so mRNA cannot be visualized by agarose gel electrophoresis. Figure 3.1 represents agarose gel electrophoresis of isolated RNA samples. Accordingly, bands correspond to 28S and 18S rRNA. Since distinct bands are well separated without smear, RNA samples are assumed to be intact. In addition, there is no contamination of genomic DNA. Therefore, isolated RNA were suitable for cDNA synthesis.
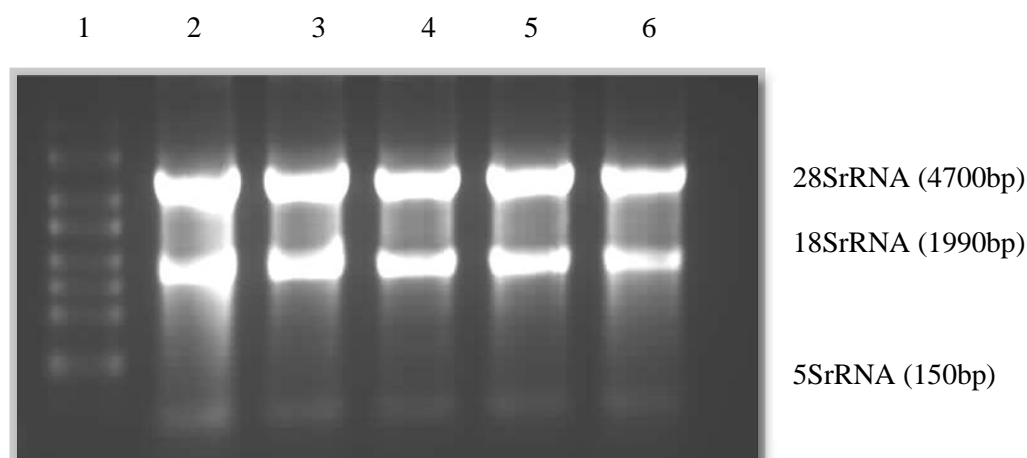
Figure 3.1 RNA ladder (lane 1) and total RNAs isolated from transfected MCF-7/Dox cells (lane 2 to 6) on 1.2 % agarose gel.

3.2 Quantitative Real-Time Polymerase Chain Reaction (qPCR): Expression analysis of *MDR1* and *MRP1* genes

MCF-7/Dox cells, which express high levels of P-gp, were treated with *MDR1* or mock siRNA for 48 or 72 hours and qPCR was performed for *MDR1*, *MRP1* and *ß-actin* genes. Amplification plots were displayed by plotting fluorescence versus treshold cycle number (Figure 3.2).
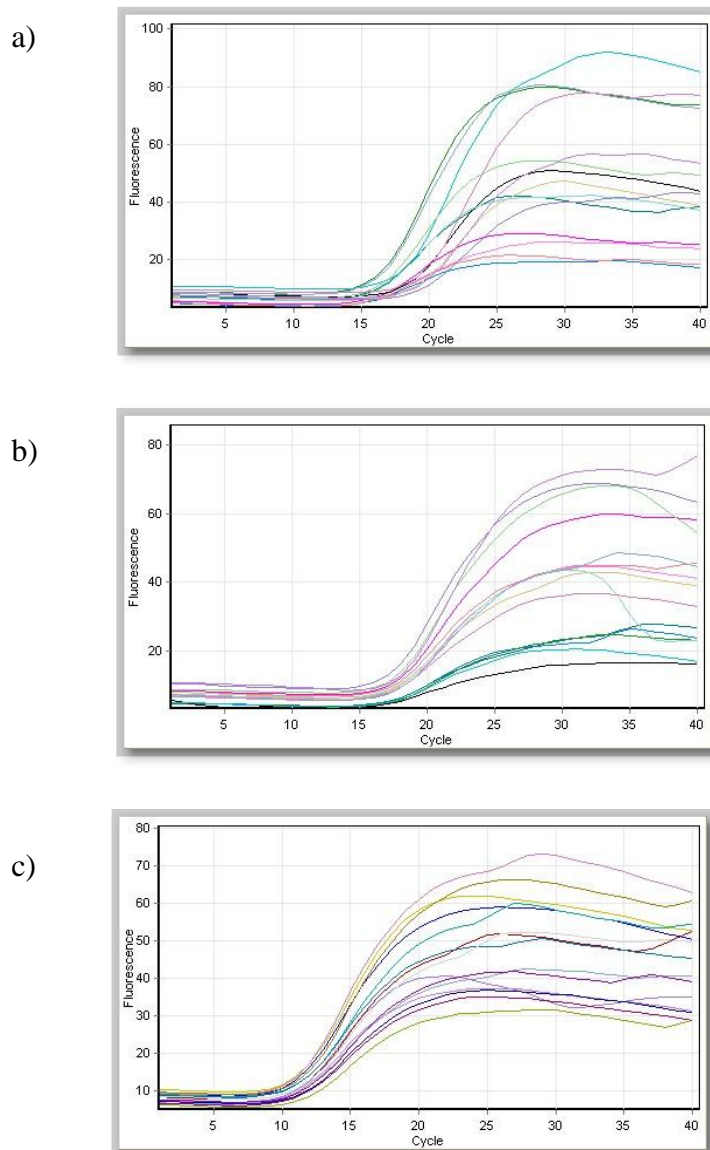
Figure 3. 2 qPCR Amplification plots for a) *MDR1* b) *MRP1* and c) *ß-actin* genes.

After cycling runs have been finished, a melt step was added for each gene to visualize the dissociation kinetics of the amplified products (Figure 3.3)

a)

Tm=79.2^{0}C

b)

Tm=79.3^{0}C

c)

Tm=80.8^{0}C
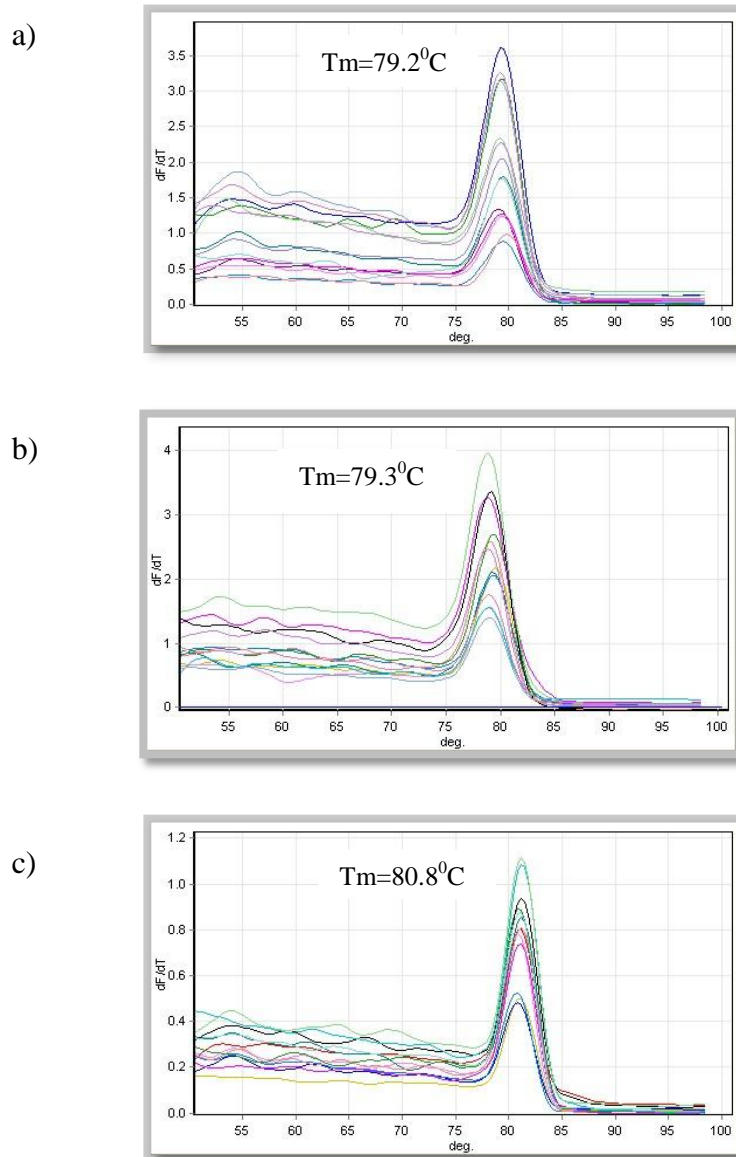
Figure 3.3 qPCR Melting-curve analysis for a) *MDR1* b) *MRP1* and c) *ß-actin* genes.

As shown in Figure 3.3, PCR products of a particular primer pair had the same melting temperature demonstrating that only the expected products had been generated.

The amplification data of *MDR1* and *MRP1* were normalized to *ß-actin* gene and subjected to $2^{-\Delta\Delta C_T}$ quantitation method (Livak and Schmittgen, 2001). The results are represented as bar graphs in Figure 3.4 and Figure 3.5, respectively.
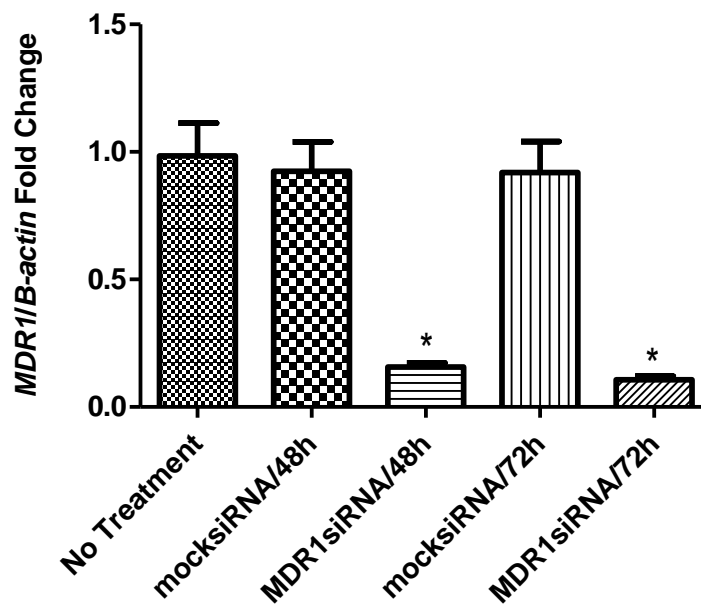
Figure 3.4 *MDR1* gene expression levels after treatment with *MDR1* or mock siRNA for 48 or 72 hours. *p < 0.0001 compared to no treatment control.

According to Figure 3.4, a statistically significant downregulation in *MDR1* gene expression was evaluated with qPCR after 48 or 72 hours treatment with *MDR1* siRNA. 48 hours after transfection, treatment with *MDR1* siRNA decreased the *MDR1* mRNA level to 16% of the original value. 72 hours after transfection, *MDR1* mRNA level decreased to 11% of the initial *MDR1* mRNA level. The mock siRNA

had no significant effect on *MDR1* mRNA expression. The ß-actin encoding mRNA was not affected from any of the treatments.

MCF-7/Dox cells were developed from the parental MCF-7 cell line previously in our laboratory. Whereas no *MDR1* gene expression was seen in original MCF-7/S cells, MCF-7/Dox cells were shown to express high levels of *MDR1* (Kars *et al.,* 2006). As a result, selective down-regulation of *MDR1* expression can re-sensitize MCF-7/Dox cells to anticancer agent doxorubicin, a substrate of P-gp, by preventing the biosynthesis of P-gp.

RNA interference can be induced in mammalian cells by introducing synthetic small interfering RNA (siRNA) or by plasmid and viral vector systems that express short hairpin RNAs (shRNA) that are processed to siRNA by an RNase III like enzyme, Dicer (Takeshita and Ochiya, 2006). Introduction of dsRNA into mammalian cells does not result in efficient Dicer-mediated generation of siRNA, but this problem can be bypassed by introducing synthetic 21-nt siRNA duplexes (Nieth *et al.*, 2003). Peng and co-workers (Peng *et al.*, 2004) reported 60% inhibition at *MDR1* mRNA level by *MDR1* siRNA in resistant human leukemia cell line K562/A02. Also about 60% *MDR1* mRNA reduction was obtained in multidrug resistant MCF-7 cells (Stierlè *et al.*, 2005). Maximum 65% inhibition of *MDR1* expression was evaluated by Wu and co-workers (Wu *et al.*, 2003) in MDR breast cancer cell line MCF-7/BC-19 despite of the high siRNA concentration (200nM). They stated that the incomplete inhibition may be due to the high content of P-gp, the relatively long half-life of the protein and transfection efficiency. MDR phenotype could be reversed 58% in MDR gastric carcinoma cell line EPG85-257RDB and 89% in the resistant pancreatic carcinoma MDR cell line EPP85-181RDB (Nieth *et al.*, 2003). The level of *MDR1* mRNA in transfected multidrug-resistant hepatocellular carcinoma cell line Bel7402/5-Fu reduced to 22.5% of the initial value (Ren, 2006). Furthermore, 86% downregulation of *MDR1* mRNA level was reported for multidrug resistant K562/Adr cells (Lim *et al.*, 2007).

In this study, the siRNA sequence targeting *MDR1* mRNA was selected following the stringent design rules for efficient uptake into RISC and efficient target mRNA

cleavage (Elbashir *et al.*, 2001; Sioud and Leirdal, 2004; Stierle´ *et al.,* 2007). Selected siRNA corresponded to the nucleotides 2815-2835 in the coding region relative to the start codon of *MDR1* mRNA. AUG start and the termination codons were avoided, since these regions are believed to be sites for intracellular proteins (Sioud and Leirdal, 2004). The GC content was about 41%, which should be between 30% and 52% for efficient siRNAs (Stierle´ *et al.,* 2007). Each strand had 2-nt 3′-TT overhangs for the synthetic siRNA to mimic physiological RNAi pathway, and also to safeguard them from exonuclease activity (Mittal, 2004). Moreover, siRNA did not display any secondary structure and did not have more than three repetitive nucleotides. Particularly long stretches of G's were avoided, since they form G-quartet structures (Sioud and Leirdal, 2004). Reynolds and co-workers (Reynolds et al., 2004) stated that siRNA functionality has a correlation with low internal stability of the duplex and the sense strand at 3' end, contributing to the strand selection and RISC incorporation. The relative amount of A/U residues at the 5' end of the antisense strand and G/C residues at the 5' end of the sense strand determines which strand behaves as guide strand for target mRNA degradation (Reynolds *et al.*, 2004; Hutvagner, 2005; Jagla *et al.*, 2005; Stierle´ *et al.,* 2007). Effective siRNA duplexes can be generated by modifying the sense strand of the siRNA duplex, so that the antisense strand preferentially enters the RNAi pathway (Mittal, 2004). Selected siRNA had low internal stability at the 5' end of the antisense strand: U at the 5' end of the antisense strand, G at the 5'end of the sense strand and AU-richness in the 5' end of the antisense strand.

According to Figure 3.4, 84% and 89% reduction in *MDR1* expression was obtained after 48 and 72 hours of transfection, respectively. Accordingly, transfection for 72 hours was more effective in decreasing *MDR1* mRNA levels in comparison to 48 hours. Stierlè and co-workers (Stierlè *et al.*, 2005) reported P-gp half-life to alter from 16 h (Cohen *et al.*, 1990) to about 72 h (Richert *et al.*, 1988) depending on the cell line and factors such as serum deprivation or high cell density (Muller *et al.*, 1995). The long half life of P-gp seems to be the main reason for increased inhibition of *MDR1* mRNA after 72 hours of transfection. It could be asked how transient transfection would be still effective after 72 hours. The reason is the long doubling time of MCF-7/Dox cells (51.5 hours), that minimizes the dilution of

siRNA duplexes and enables them to effectively inhibit MDR for a longer duration when compared to faster dividing cells.

For potential therapeutic applications, the more biologically effective siRNA should be chosen. In comparison to the literature, 84% and 89% gene-silencing activity of the selected *MDR1* siRNA duplex in doxorubicin resistant MCF-7 cells demonstrates its high efficiency for *MDR1* inhibition, although the concentration was kept as low as 20nM.
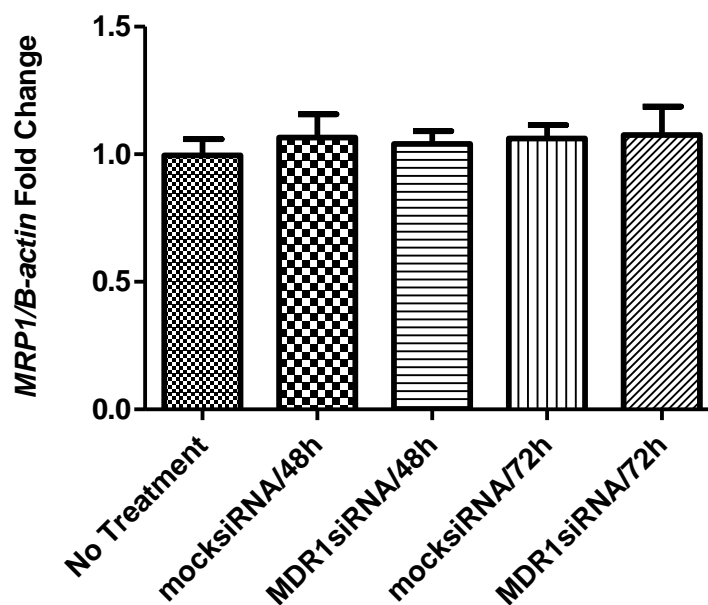
Figure 3.5 *MRP1* gene expression levels after treatment with *MDR1* or mock siRNA for 48 or 72 hours.

qPCR results for *MRP1* gene did not demonstrate significant change in expression levels after 48 or 72 hours treatment with *MDR1* siRNA. In addition, mock siRNA had no effect on *MRP1* mRNA level.

Approximately 3 fold decrease in expression level of the *MRP1* gene in MCF-7/Dox cells in comparison to parental MCF-7/S cells was reported previously. Moreover, it was noted that the other transporter proteins BCRP and LRP were not expressed neither in MCF-7/S nor MCF-7/Dox cells (İşeri, 2009). The downregulation of *MRP1* and overexpression of *MDR1* genes may indicate that P-gp mediated drug extrusion is the major transport based resistance mechanism in MCF-7/Dox cells, although doxorubicin is a substrate for both of the proteins. The same *MRP1* mRNA level even after *MDR1* silencing demonstrates that some other transporter protein like BCRP or other resistance mechanisms may become activated. Altered apoptosis regulation, altered expression levels or activities of drug targets and increased detoxification and cellular repair are other possible mechanisms of multidrug resistance (Krishna and Mayer, 2000).

Results of *MRP1* gene expression analysis are consistent with the literature. Celius and co-workers (Celius *et al*., 2004) also demonstrated no significant change in the expression level of *MRP1* gene after *MDR1* gene silencing in MDR human colon adenocarcinoma Caco-2 cell line. Moreover, Watanabe and co-workers (Watanabe *et al*., 2005) constructed *MDR1* inhibited Caco-2 cells and they noted no significant change in *MRP1* expression levels. Furthermore, downregulation of *MDR1* gene and P-gp expression had no effect on *MRP1* gene in MDR chronic myelogenous leukemia cell line K562/A02 (Miao *et al,* 2003).

3.3 Assessment of Transfection Efficiency

MCF-7/Dox cells were treated with Alexa Fluor® oligo to assess the uptake of siRNA molecules, since it has the same length, charge, and configuration as *MDR1* siRNA. The fluorescence signal was detected 15 hours after transfection.
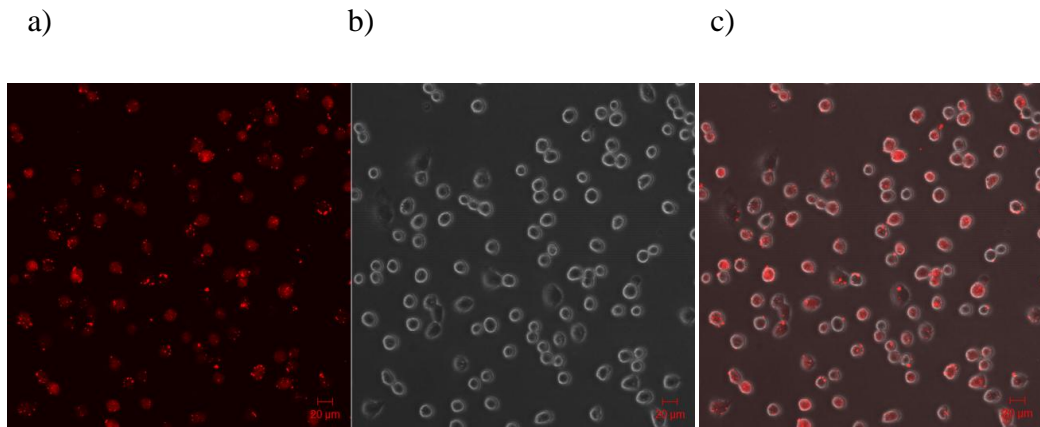
Figure 3.6 MCF-7/Dox cells treated with Alexa Fluor® oligo a) Fluorescence image b) transmission image c) overlay of fluorescence and transmission images with LD A-Plan 20X/0.30 Ph1 objective.

The red labeled oligo was successfully uptaken in to the transfected cells (Figure 3.6). Ideally, the siRNA should not cause any effects other than sequence-specific degradation of target mRNAs. However, in literature it was stated that, there is a widespread nonspecific effect that siRNA could potentially display. These nonspecific effects include degradation of mRNA other than the target due to cross-hybridization followed by downstream effects, binding to cellular proteins in a sequence-specific manner (aptamer effect) and inducing all of the downstream transcriptional effects, translational silencing through miRNA effect, and induction of ''dsRNA response'' nonspecific with respect to the siRNA sequence (Semizarov *et al*., 2003, Doench *et al*., 2003). These off-target effects can interfere with experimental results and may limit the use of siRNAs for effective mRNA silencing. This problem may be partly overcome by following the stringent design rules, which were also obeyed during the selection of *MDR1* siRNA in this study (Elbashir *et al*., 2001; Stierle´ *et al.,* 2007). However, it was demonstrated that, the specifity of siRNAs is also concentration dependent. At ~100 nM, siRNAs nonspecifically induce a significant number of genes, many of which are known to be involved in apoptosis and the stress response (Semizarov *et al*., 2003; Persengiev et al., 2004). It was reported that siRNAs as well as shRNAs can activate one of the cell's antiviral defense mechanisms, which is a dsRNA-dependent protein kinase (PKR) (Sledz *et*

53

al., 2003; Lage, 2005). Once activated, PKR has the ability to phosphorylate translation initiation factor, eIF2, resulting in a general downregulation of the translation and sequence-independent mRNA degradation (Williams, 1997; Lage, 2005). However, reduction of the siRNA concentration to 20nM eliminates these nonspecific responses (Semizarov *et al*., 2003; Persengiev et al., 2004). Accordingly, transfection was performed with different concentrations of the Alexa Fluor® oligo to test whether 20nM oligo is efficiently uptaken by the cells and gives a sufficient fluorescence in comparison to other concentrations (Figure 3.7).

According to Figure 3.7, even 10nM Alexa Fluor® oligo was successfully introduced in to the MCF-7/Dox cells. It was observed that, when the oligo concentration is increased, more oligo is accumulated inside the cells.
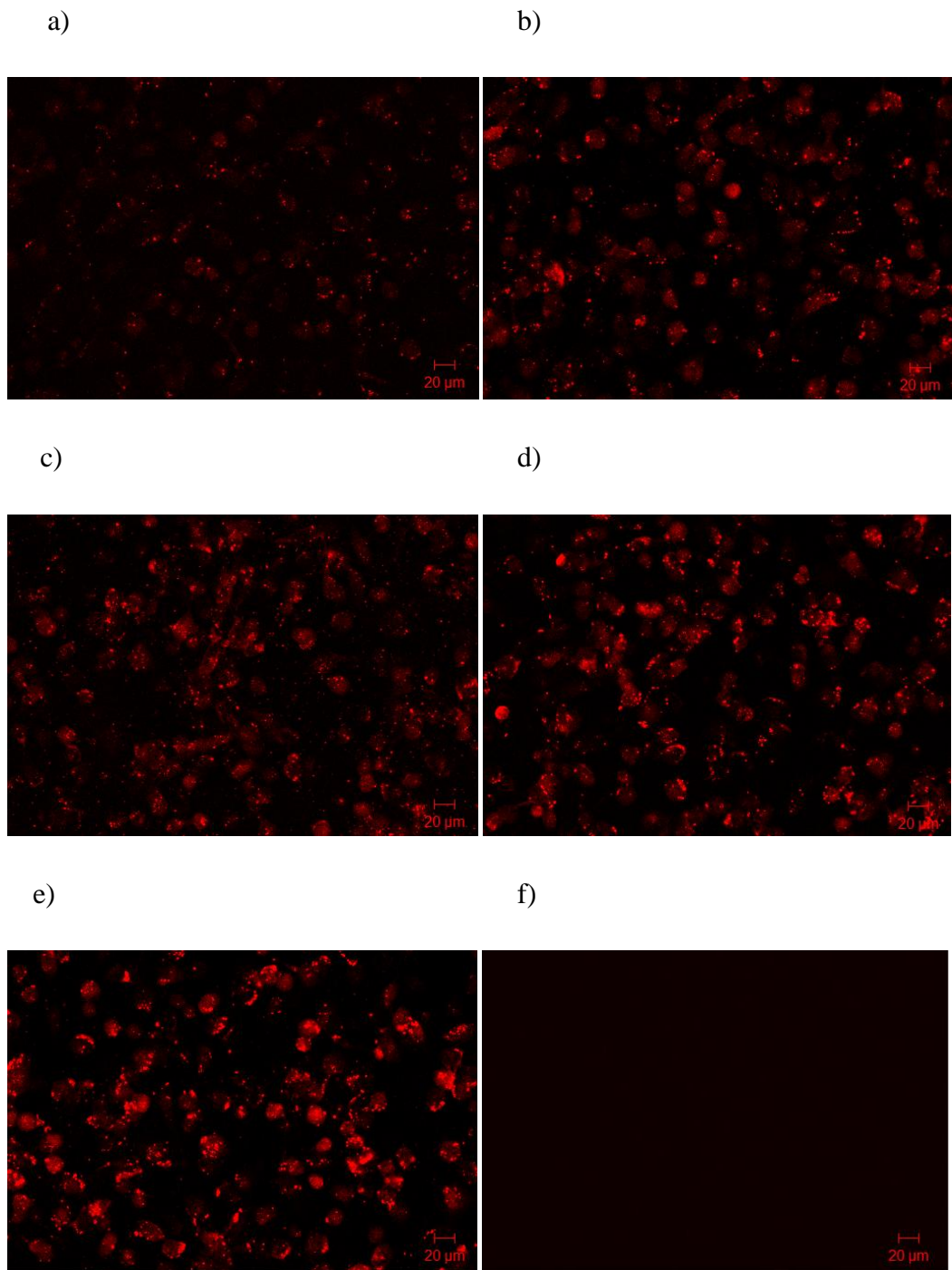
Figure 3.7 Fluorescence images of MCF-7/Dox cells with LD A-Plan 20X/0.30 Ph1 objective at different concentrations of Alexa Fluor® oligo a)10nM, b)20nM, c)30nM, d)40nM or e)50nM f) Negative control.
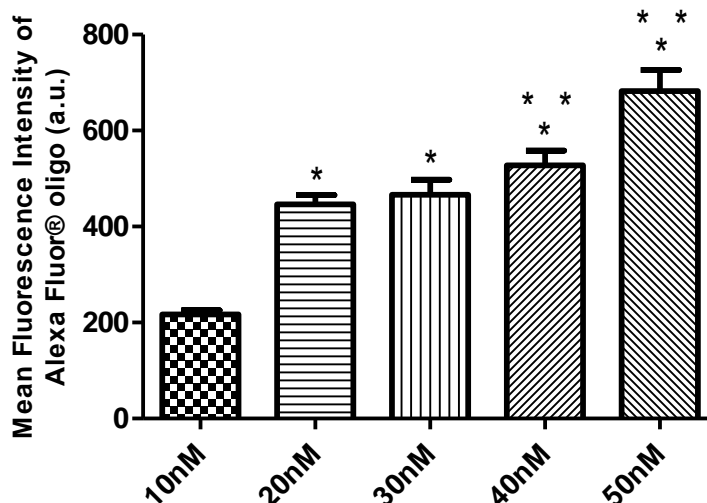
Figure 3.8 Fluorescence intensity bar graph of Alexa Fluor® oligo per pixel for different concentrations. *$p < 0.0001$ compared to 10nM oligo treated cells, **$p < 0.05$ compared to 20nM oligo treated cells.

The fluorescence signal was quantified and represented as bar graph (Figure 3.8). The bar graph demonstrated a gradual increase in the signal with increasing oligo concentration. The fluorescence intensity per pixel with 10nM oligo was significantly lower than the intensity with 20nM oligo. Further, the fluorescence intensities with 40 or 50 nM oligo were significantly higher than that with 20 nM oligo. Despite the significantly higher fluorescence intensities with 40 or 50 nM oligo, 20 nM was the selected siRNA concentration for this study, since it is probably safer in terms of the non-specific interactions, mentioned above. In conclusion, studies with Alexa Fluor® oligo ensured that 20 nM siRNA would be efficiently taken by the cells, so transfection of the cells with higher concentrations was not required, which would possibly induce nonspecific responses in the cells.

3.4 Evaluation of Intracellular Doxorubicin Accumulation and Localization

Reversal of drug resistance was also demonstrated by confocal laser scanning microscopy. The images were used to compare the intracellular doxorubicin accumulation and localization in MCF-7/S and MDR reversal agents treated or untreated MCF-7/Dox cells.

Transfection with *MDR1* or mock siRNA was carried out, and after 72 hours MCF-7/Dox cells were subjected to 1 µM doxorubicin. Since MCF-7/Dox cells were resistant to 1 µM doxorubicin, this dose of the drug was selected. The same dose of the drug was also applied to MCF-7/S and untreated MCF-7/Dox cells. According to Figure 3.9, fluorescence mode images demonstrated a stronger doxorubicin related fluorescence signal in MCF-7/S cells indicating more intracellular doxorubicin accumulation. The fluorescence signal was quantified and represented as bar graph (Figure 3.10). The bar graph demonstrates 4 fold higher doxorubicin fluorescence intensity in MCF-7/S cells in comparison to untreated MCF-7/Dox cells. However, *MDR1* silencing with siRNA resulted in approximately 2.5 fold increase in fluorescence intensity when compared to untreated MCF-7/Dox cells. Scrambled mock siRNA had no effect on intracellular doxorubicin accumulation.
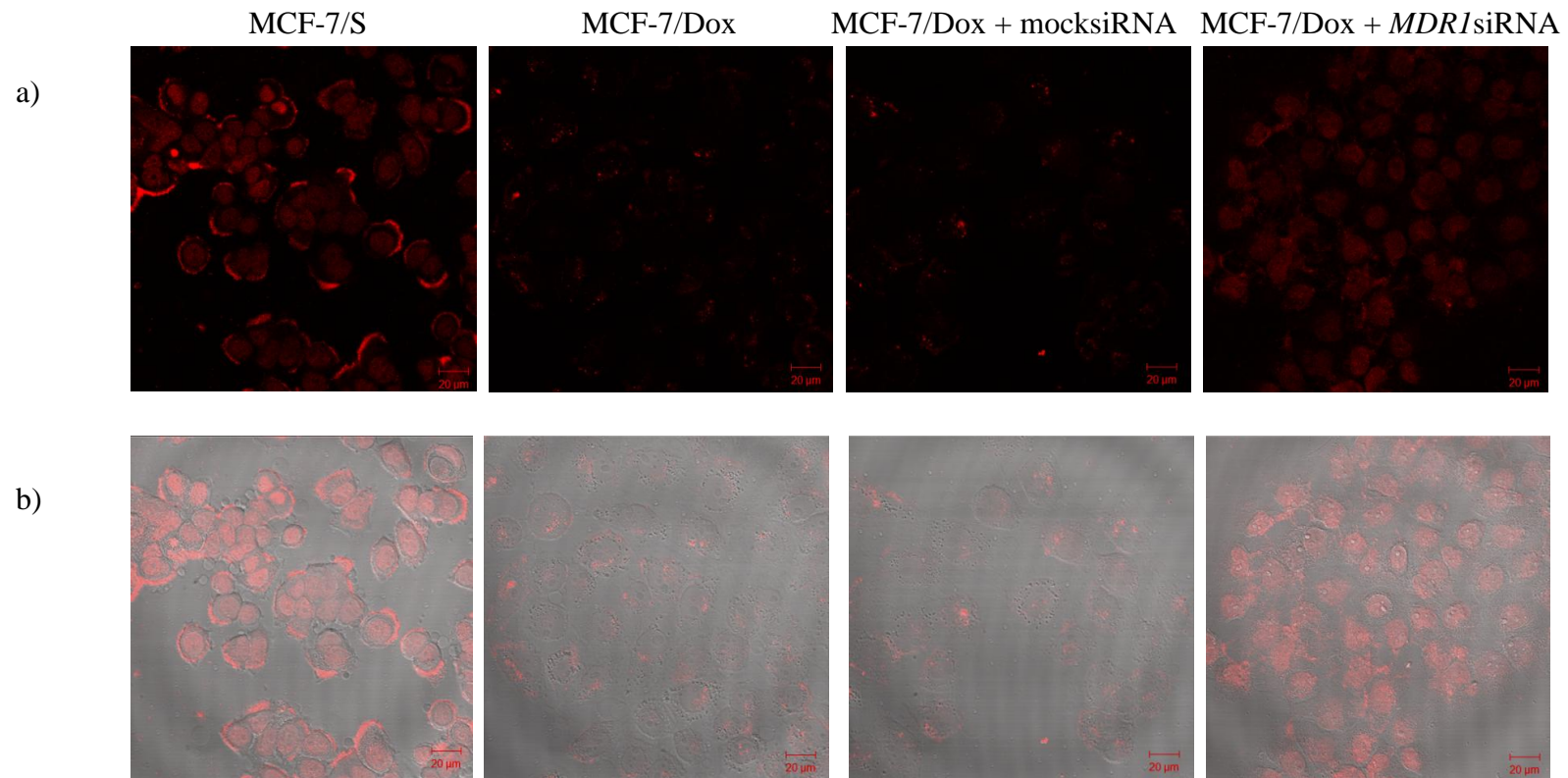
Figure 3. 9 Confocal laser scanning microscopy images of 1 µM doxorubicin treated MCF-7/S, MCF-7/Dox, MCF-7/Dox + mocksiRNA (72h) and MCF-7/Dox + *MDR1*siRNA (72h) cells, a) fluorescence b) overlays of fluorescence and transmission images with Plan-Neofluar 40X/1.3 Oil DIC objective.
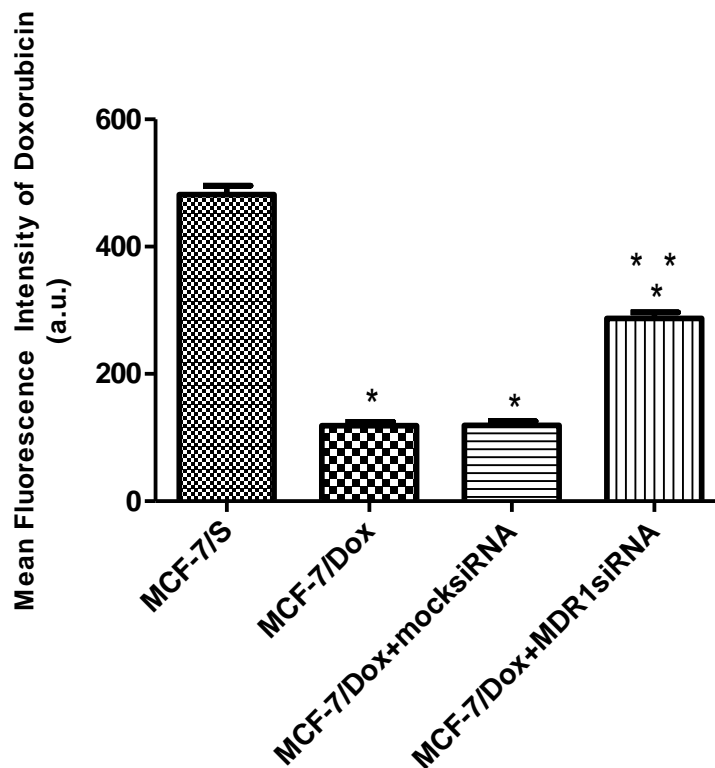
Figure 3.10 Bar graph demonstrating intracellular doxorubicin accumulation in 1 μM doxorubicin treated MCF-7/S and MCF-7/Dox cells. *p < 0.0001 compared to MCF-7/S cells, ** p < 0.0001 compared to untreated MCF-7/Dox cells.

Additionally, MCF-7/Dox cells were incubated in the presence of MDR modulators verapamil or promethazine, or they were transfected for 48 or 72 hours prior to treatment with 4 μM of doxorubicin. Untreated MCF-7/S and MCF-7/Dox cells were also subjected to the same dose of the drug. Figure 3.11 and 3.12 demonstrate the fluorescence mode and overlays of fluorescence and transmission mode images of MCF-7/S and MCF-7/Dox cells after treatments. The bar graph represents the intracellular doxorubicin accumulation as mean doxorubicin fluorescence intensity per pixel (Figure 3.13). Accordingly, MCF-7/S cells demonstrated high doxorubicin accumulation inside the cells. MCF-7/Dox cells accumulated approximately 5.6 fold less drug compared to MCF-7/S cells. However, transfection with *MDR1* siRNA for 48 and 72 hours led to approximately 2.8 and 5.4 fold increase in intracellular drug accumulation, respectively. Introduction of mock siRNA resulted in no significant difference in fluorescence intensity in comparison to untreated MCF-7/Dox cells.

| | MCF-7/S | MCF-7/Dox | MCF-7/Dox + mocksiRNA | MCF-7/Dox + *MDR1*siRNA |

a)

b)
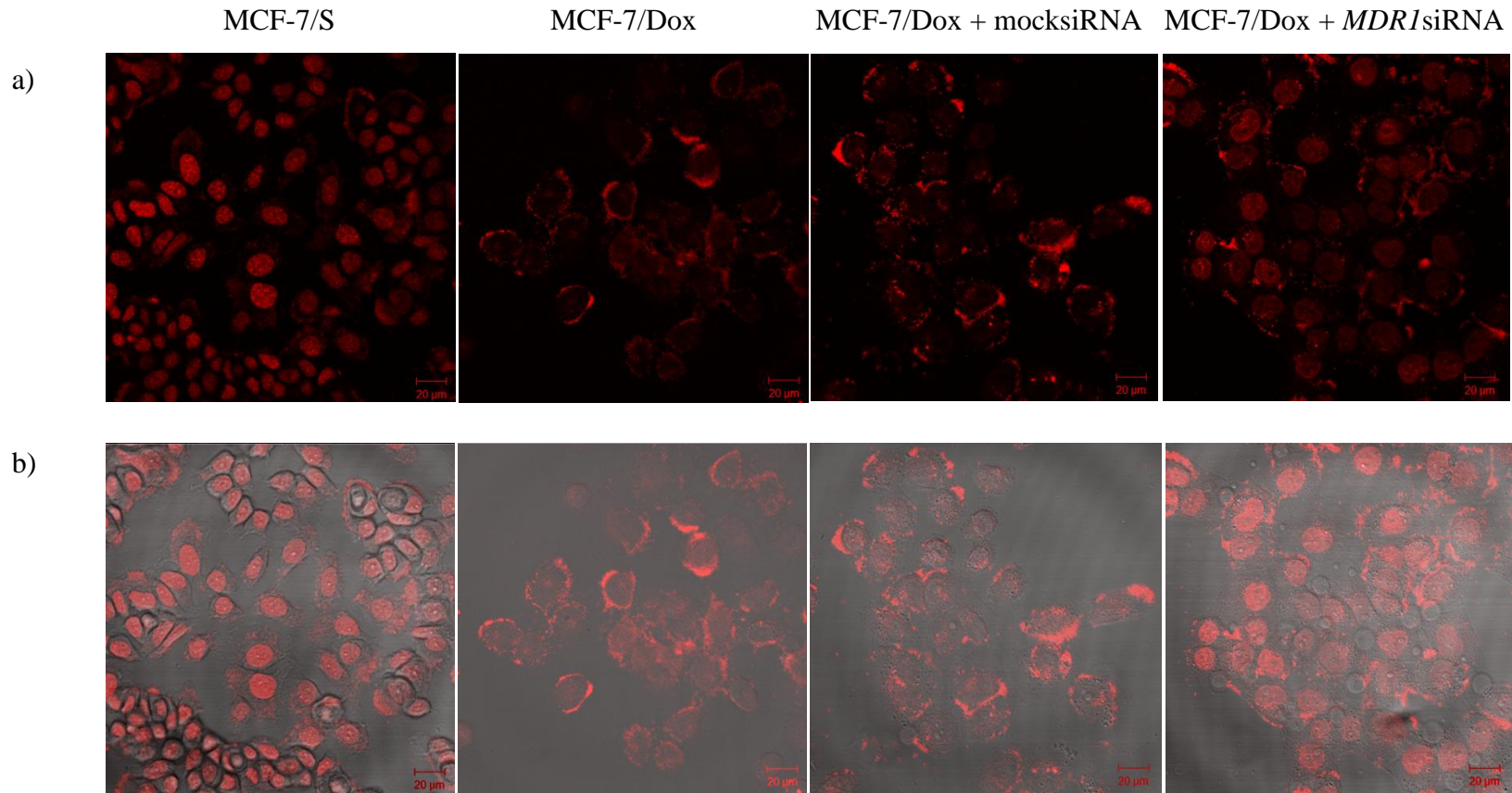
Figure 3.11 Confocal laser scanning microscopy images of 4 µM doxorubicin treated MCF-7/S, MCF-7/Dox, MCF-7/Dox + mocksiRNA (48h) and MCF-7/Dox + *MDR1*siRNA (48h) cells, a) fluorescence b) overlays of fluorescence and transmission images with Plan-Neofluar 40X/1.3 Oil DIC objective.
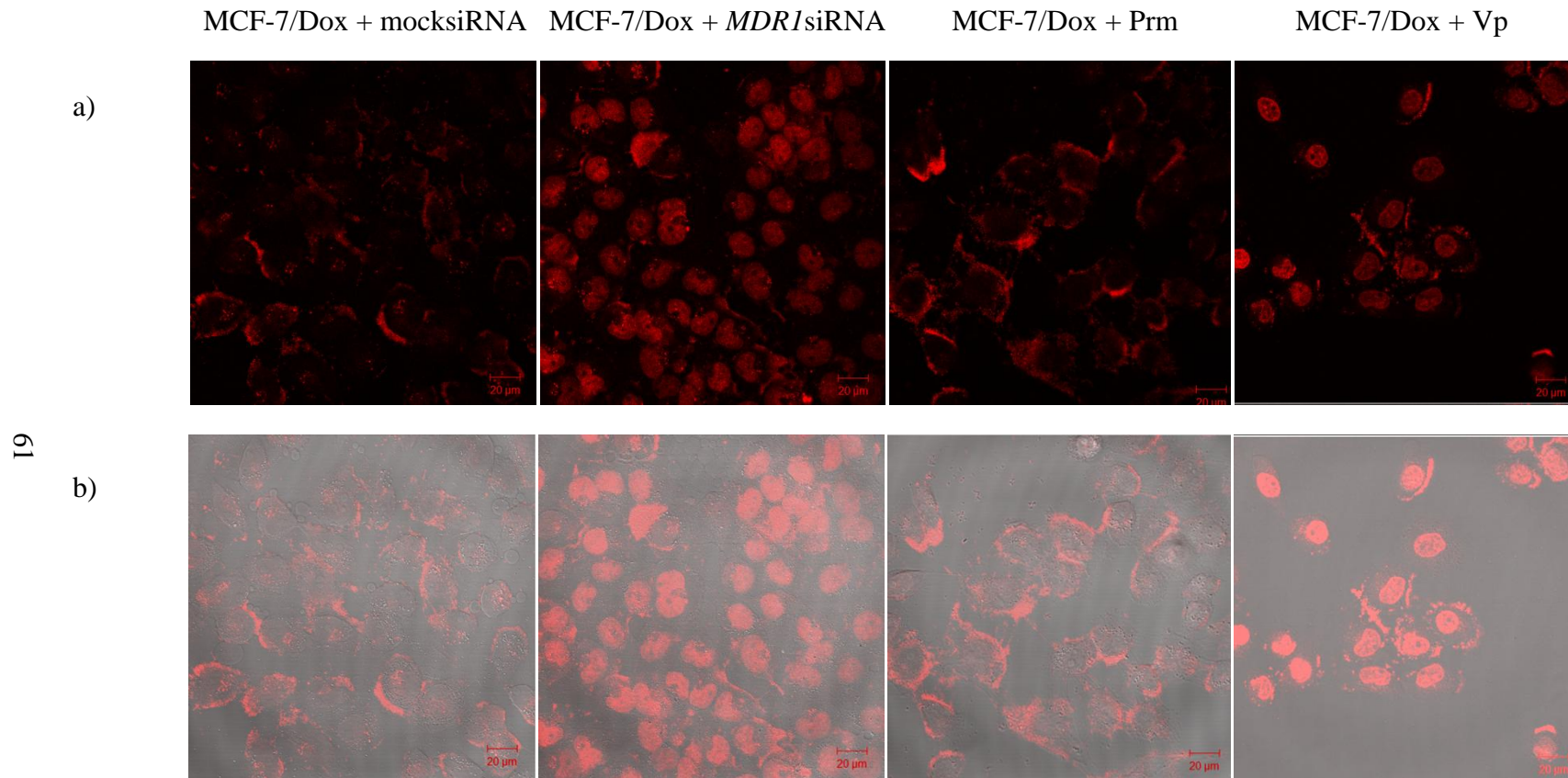
Figure 3.12 Confocal laser scanning microscopy images of 4 µM doxorubicin treated MCF-7/Dox + mock siRNA (72h), MCF-7/Dox + *MDR1* siRNA (72h), MCF-7/Dox + Prm and MCF-7/Dox + Vp cells (30 min prior to one hour doxorubicin treatment), a) fluorescence b) overlays of fluorescence and transmission images with Plan-Neofluar 40X/1.3 Oil DIC objective. Prm: Promethazine, Vp: Verapamil.
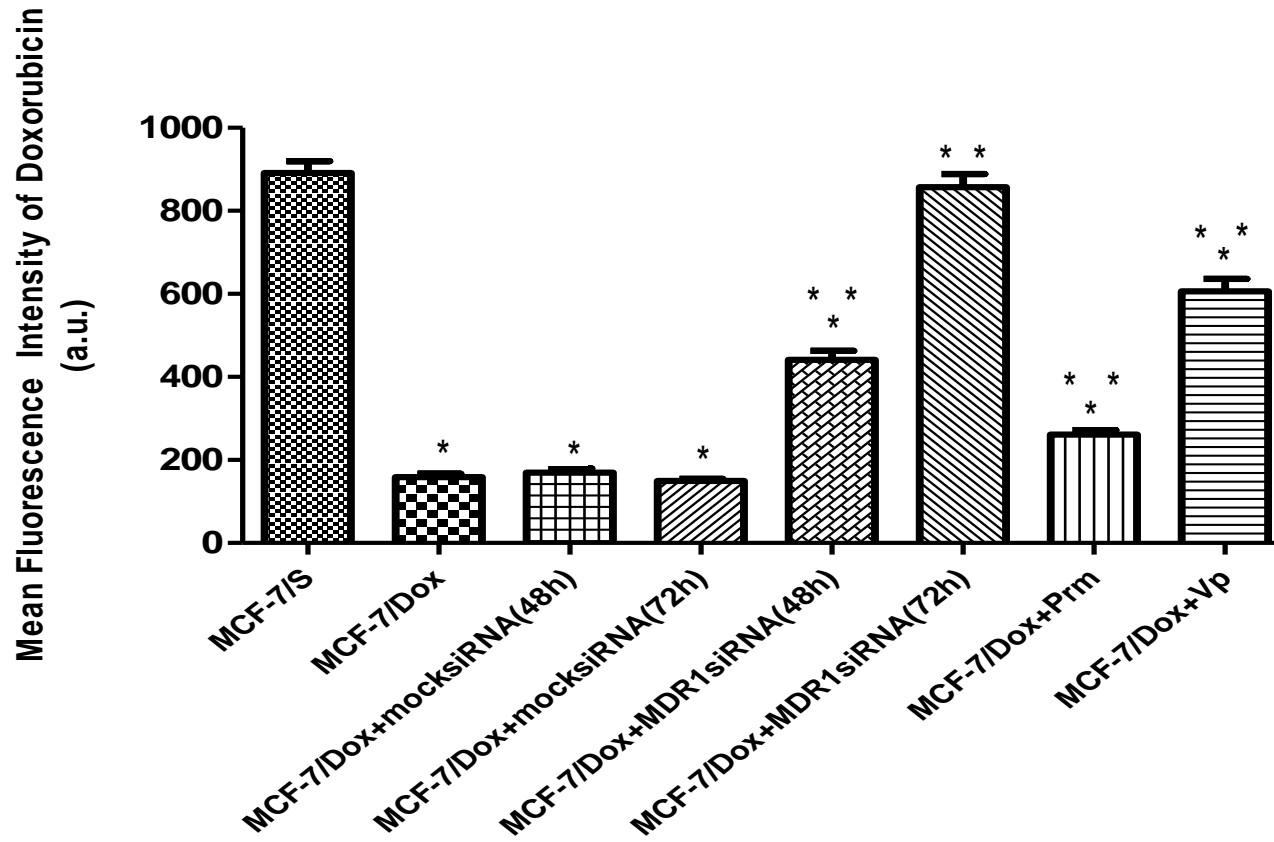
Figure 3. 13 Bar graph demonstrating intracellular doxorubicin accumulation in 4 μM doxorubicin treated MCF-7/S and MCF-7/Dox cells. *p < 0.0001 compared to MCF-7/S cells, ** p < 0.0001 compared to untreated MCF-7/Dox cells. Prm: Promethazine, Vp: Verapamil.

MDR modulators verapamil and promethazine caused significantly higher doxorubicin accumulation inside the cells. Whereas verapamil treated cells demonstrated approximately 3.8 fold increase in doxorubicin fluorescence intensity, promethazine resulted in approximately 1.6 fold increase in fluorescence intensity when compared to untreated MCF-7/Dox cells.

MCF-7/S cells collected doxorubicin specifically in their nuclei. However, MCF-7/Dox cells accumulated doxorubicin in their cytoplasm with most of the drug concentrated at the cell periphery. Figure 3.14 demonstrates higher magnification images (2X digital acquition zoom) making easier to discriminate the localization of the drug.
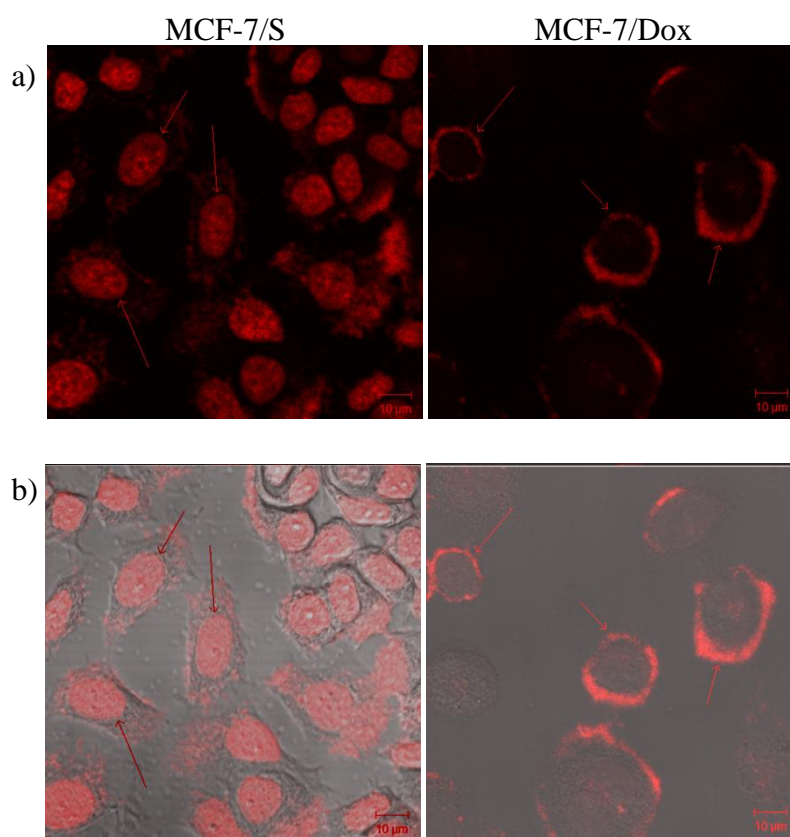
Figure 3.14 Higher magnification images of 4 µM Dox treated MCF-7/S and MCF-7/Dox cells with Plan-Neofluar 40X/1.3 Oil DIC objective using 2X digital acquisition zoom. a) Fluorescence b) overlays of fluorescence and transmission images.

Doxorubicin is classified as a topoisomerase II poison, which stabilizes the cleavable complex between DNA and topoisomerase II enzyme subunits, resulting in DNA double-strand breaks (Swift *et al.,* 2006). Additionally, the binding of doxorubicin to DNA inhibits DNA polymerase and nucleic acid synthesis (Shen *et al.*, 2008). Furthermore, doxorubicin can undergo cycles of reduction and oxidation in almost all intracellular compartments, including nucleus, mediating the formation of reactive oxygen species (Bachur *et al*., 1982). Concordantly, mainly nucleus is the target of doxorubicin. Doxorubicin is taken to the cells by free diffusion of the un-ionized drug. Once it diffuses through the plasma membrane, the drug is actively transported to the nucleus in an ATP requiring, nuclear pore dependent process (Chabner and Longo, 2005). In MCF-7/S cells, which lack P-gp, doxorubicin successfully accessed in to the cells and mainly concentrated in the nuclei (Figure 3.14). However, some of the drug was accumulated also in the cytoplasm and at the cell periphery. The reason may be that, doxorubicin is reported to exert a cytotoxic effect also through interaction with the cell membrane, especially with negatively charged phospholipids (Goormaghtigh *et al*., 1980; Triton *et al*., 1982; Nicloay *et al.*, 1988; Pajeva *et al*., 2003). Binding of the drug and insertion into the membrane is shown to affect the intrinsic transport characteristics of the membrane (Speelmans *et al*., 1994; Pajeva *et al*., 2003). Moreover, fluorescence signal on the membrane may indicate doxorubicin efflux from MRP1 pumps. In MCF-7/Dox cells, which overexpress P-gp, doxorubicin was concentrated mainly on the cell membrane and it had little access to the nuclei. According to Pajeva and co-workers (Pajeva *et al*., 2004), concentration of doxorubicin mainly in the cytoplasmic-face of the membrane due to interaction of the drug with negatively charged phosphatidylserine enables the drug to be captured and pumped out by P-gp easyly. Moreover, they stated that the drug may adopt the right conformation in the membrane that is necessary for its binding to the protein. As a result, after free diffusion in to the cell, doxorubicin efflux was carried out by the action of ATP-dependent membrane transporter proteins, resulting in decreased intracellular fluorescence intensity in untreated MCF-7/Dox cells. It should be noted that, the efflux of the drug was mainly driven by P-gp considering its overexpression and MRP1downregulation in these cells in comparison to MCF-7/S cells. The absence of the other transporter

proteins such as BCRP and LRP in both MCF-7/S and MCF-7/Dox cells was also demonstrated previously (İşeri, 2009).

According to the Figures 3.9, 3.11 and 3.12; *MDR1* siRNA and verapamil led to changes in doxorubicin localization besides the intracellular accumulation of the drug. As expected, the negative control mock siRNA did not have any effect on neither doxorubicin localization nor accumulation. MCF-7/Dox cells tranfected with mock siRNA for both 48 and 72 hours displayed the same localization pattern with the untreated MCF-7/Dox cells. Also, promethazine treated cells accumulated doxorubicin mostly at the cell periphery. However, *MDR1* siRNA and verapamil treatments enabled doxorubicin to access to the nuclei of the cells.

It has long been known that, calcium channel blocker verapamil has the ability to inhibit the binding of photoactivatable drug analogs to P-glycoprotein, restoring drug accumulation and enhancing drug sensitivity of cultured cells that overexpress this protein (Tsuruo *et al.,* 1981; Sharom, 1997; Loe *et al*., 2000). Yusa and Tsuruo (Yusa and Tsuruo, 1989) demonstrated the direct binding of verapamil to P-gp, suggesting a reversal mechanism through competitive inhibition of drug transport. Additionally, Pajeva and co-workers (Pajeva *et al*., 2004) reported stronger interactions of verapamil with phosphatidylserine than doxorubicin. Accordingly, an alteration of lipid phase properties increases membrane fluidity facilitating the passive diffusion of doxorubicin through the membrane. They also stated that, this indicates a competition between doxorubicin and verapamil for interaction with the phospholipid. Furthermore, they suggested that interactions of verapamil and phosphatidylserine may also affect the activation of protein kinase C which phosphorylates P-gp (Chaudhary and Roninson, 1992; Pajeva *et al*., 2004). Finally, verapamil, a substrate of P-gp, was proposed to potentially stimulate ATPase activity (Shapiro and Ling, 1995; Sharom, 1997; Loe *et al*., 2000). In addition to its several mechanisms to modulate P-gp mediated drug efflux, verapamil has been demonstrated to strongly stimulate MRP1-mediated reduced glutathione (GSH) transport (Loe *et al*., 2000; Cullen *et al*., 2001; Leslie *et al*., 2003; Perrotton *et al*., 2007). Since GSH has been suggested as an important component of the MRP-1 mediated drug efflux (Olsen *et al*., 1998; Krishna and Mayer, 2000), verapamil may

modulate MRP-1 dependent MDR by reducing intracellular GSH levels rather than directly inhibiting the transporter (Loe *et al.*, 2000). Thus, by its ability to strongly inhibit both pumps, verapamil causes high doxorubicin accumulation in the nuclei of the MCF-7/Dox cells (Figures 3.12 and 3.13) allowing drug to reach its corresponding intracellular targets. Similarly, Coley and co-workers (Coley *et al.*, 1993) demonstrated that the presence of verapamil during anthracycline treatment resulted in an increase in the intensity of fluorescence in the resistant cell lines, particularly in the nucleus. Additionally, Consoli and co-workers (Consoli *et al.*, 1997), showed reversal of reduced nuclear mitoxantrone uptake after incubation with verapamil. In another study, Shen and co-workers (Shen *et al.*, 2008) reported relocalization of doxorubicin to the nuclei and significant increase in the drug accumulation of these cells after verapamil treatment.

Promethazine, a phenothiazine derivative, is thought to reverse MDR through its ability to interact with the membrane phospholipids (Pajeva *et al.*, 1996; Pajeva *et al.*, 1998). Sharom (Sharom, 1997) proposed that alterations in the membrane fluidity may influence substrate binding to transporter proteins or enhance passive diffusion of drugs through the lipid bilayer. Additionally, Fertè (Fertè, 2000) and Michalak and co-workers (Michalak *et al.*, 2007) stated that biophysical properties of the membrane lipid phase influence substrate recognition and conformation of P-gp as well as its ATPase activity. Modulation of MDR by promethazine was demonstrated in MDR mouse lymphoma and COLO 320 cells (Michalak *et al.*, 2007), and in drug resistant MCF-7 cells (Kars *et al*, 2008). However, Wesolowska and co-workers (Wesolowska *et al.*, 2005) reported stimulatory effect of phenothiazine derivative compounds, phenothiazine maleates, on MRP1 transporter activity, in addition to P-gp inhibition. According to Figures 3.12 and 3.13, promethazine treatment significantly increased doxorubicin accumulation in MCF-7/Dox cells in comparison to untreated controls. However, verapamil caused approximately 2.5 fold higher intracellular fluorescence intensity than promethazine. Though verapamil treatment caused doxorubicin to concentrate in the nucleus, promethazine treatment did not result in relocalization of the drug in comparison to untreated MCF-7/Dox cells. Previously it was reported that, flow cytometric measurements demonstrated about 5 fold higher P-gp modulatory activity of

verapamil than that of promethazine in doxorubicin resistant MCF-7 cells (Kars *et al.*, 2008).

A considerably higher modulatory activity of verapamil in comparison to promethazine may be due to combined mechanisms of verapamil. Unlike promethazine, verapamil has the ability to competitively inhibit drug transport and affect the activation of protein kinase C, as previously explained. Additionally, whereas verapamil has been shown to inhibit both P-gp and MRP1 mediated drug efflux, promethazine might stimulate MRP1 activity while inhibiting P-gp activity.

MCF-7/Dox cells transfected with *MDR1* siRNA for 72 hours demonstrated the highest intracellular doxorubicin fluorescence intensity among the other treatments (Figure 3.13). *MDR1* siRNA provided the most efficient inhibition of P-gp mediated drug efflux. According to the graph, there is no significant difference in fluorescence intensity between *MDR1* siRNA transfected MCF-7/Dox cells and MCF-7/S cells. Since MCF-7/S cell do not express P-gp, it could be concluded that almost complete reversal of P-gp mediated drug efflux was achieved after transfection with *MDR1* siRNA for 72 hours. Moreover, *MDR1* siRNA exposure for both 48 and 72 hours led to relocalization of doxorubicin by setting the drug free to be transported to the nucleus. However, transfection for 48 hours was less effective than transfection for 72 hours in modulating intracellular drug accumulation. Whereas transfection for 48 hours resulted in approximately 2.8 fold increased drug accumulation, transfection for 72 hours led to 5.4 fold more drug accumulation in comparison to untreated MCF-7/Dox cells. Wu and co-workers (Wu *et al.*, 2003), who obtain a similar result in their study, stated that the incomplete inhibition may be due to the high content of P-gp, the relatively long half-life of the protein and transfection efficiency. In this case, approximately 2 fold difference in transfection for 48 or 72 hours may correlate to long half-life of P-gp. P-gp half-life was reported from 16 h (Cohen *et al.*, 1990) to about 72 h (Richert *et al.*, 1988) depending on cell line and factors as such serum deprivation or high cell density (Muller *et al.*, 1995).

In literature, there are a limited number of studies allowing direct visualization of the MDR reversal after siRNA treatment, since only some groups of P-gp substrates

like anthracyclines have innate fluorescence. Wu and co-workers (Wu *et al*., 2003) demonstrated an increase in the accumulation of doxorubicin in the *MDR1* siRNA treated MDR MCF-7 cells when compared to the mock transfected controls. Moreover, Gan and co-workers (Gan *et al.,* 2005) reported significantly enhanced cellular daunorubicin accumulation due to shRNA vectors targeting *MDR1* gene, though any further analysis for quantitation was not performed. Other investigators carried out flow cytometric measurements to evaluate intracellular drug accumulation quantitatively in response to *MDR1* siRNA. Peng and co-workers (Peng *et al*., 2004) quantified the accumulation of daunorubicin by flow cytometric method and found out approximately 2 fold increased intracellular drug accumulation in the *MDR1* siRNA treated (48 hours) multidrug resistant human acute myelogenous leukemia cell line K562/A02. Moreover, Stierlè and co-workers (Stierlè *et al*., 2005) observed a significant increase in daunorubicin accumulation in MDR MCF-7 cells after 72 hours treatment with *MDR1* siRNA resulting in approximately 49% P-gp reversal. Approximately 30% increase in doxorubicin accumulation was demonstrated after *MDR1* silencing with siRNA (48 hours) in doxorubicin resistant MCF-7 cells (Li *et al*., 2005). Furthermore, treatment of drug resistant KB-8-5 cells with *MDR1* targeting siRNAs resulted in nearly 2.5 fold increased accumulation of the Pgp substrate rhodamine 123 in comparison to untreated cells (Logashenko et al., 2004).

In this study, the innate fluorescence of doxorubicin was taken as an advantage to directly visualize its intracellular accumulation and localization. Moreover, this data was further processed and represented quantitatively. To our knowledge, this is the first report demonstrating re-localization of doxorubicin to the nucleus in response to *MDR1* siRNA transfection and expressing the images quantitatively to enable comparison of drug accumulation between siRNA treated and untreated MDR cells. With the selected siRNA duplex, nearly 5.4 fold increase in intracellular doxorubicin accumulation was demonstrated. Resistant cells treated with verapamil and promethazine accumulated nearly 3.8 and 1.6 more doxorubicin inside the cells in comparison to untreatment control, despite the considerably high concentration of the modulators (60μM and 9.6 μM, respectively). In addition, verapamil and promethazine have a number of side effects. Side effects of verapamil include chest

pain, arrhythmia, heart attacks or strokes, significant water retention, dizziness, lightheadedness, or fainting (Monson and Schoenstadt, 2009). Also promethazine may lead to slow or irregular breathing, tachycardia, hypertension, hallucinations and involuntary muscle movements (American Cancer Society, 2008). However, 20nM of *MDR1* siRNA was enough for almost complete restoration of doxorubicin accumulation and reversal of the resistance in MCF-7/Dox cells, which makes the selected siRNA a suitable candidate for potential therapeutic applications.

3.5 Cell Proliferation Assay with XTT Reagent: Chemo-sensitivity to Doxorubicin

XTT cell proliferation assay was performed to determine the effect of *MDR1* silencing on doxorubicin sensitivity in siRNA treated MCF-7/Dox cells. Chemo-sensitivity of these cells was evaluated in comparison to MCF-7/S and non- or mock treated MCF-7/Dox cells.

MCF-7/Dox cells were transfected for 48 hours in 96-well plates and they were subjected to increasing doses of doxorubicin. After 48 hours of incubation, cell viability profiles, IC_{50} values, resistance indices and fold reversal values were determined for each particular treatment and cell type.

Figure 3.15 and Figure 3.16 demonstrates the antiproliferative effects of increasing concentrations of doxorubicin on MCF-7/S and siRNA or untreated MCF-7/Dox cells, respectively. The graphs show a gradual decrease in cell proliferation with increasing concentrations of doxorubicin. As demonstrated in Figure 3.16, approximately 45% proliferation was obtained in mock or untreated MCF-7/Dox cells after 250 μM doxorubicin exposure. However, *MDR1* siRNA treated cells did not survive at all in the presence of the same drug concentration.
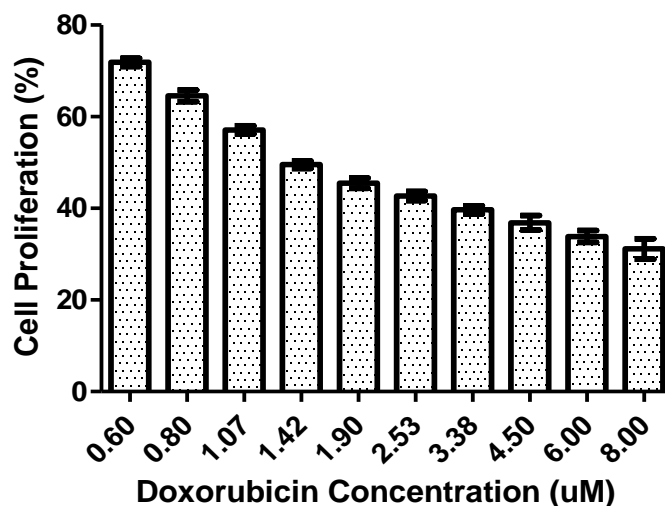
Figure 3. 15 Cell proliferation profiles of MCF-7/S cells after exposure to increasing concentrations of doxorubicin.

IC_{50} values for doxorubicin were calculated for each sample from the logarithmic trend line of the % cell proliferation versus concentration plots. Resistance indices (R) were expressed as the ratio of the IC_{50} of the resistant cells to the IC_{50} of the sensitive cells. Both IC_{50} values and resistance indices for the MCF-7/S and non-, mock or *MDR1* siRNA treated MCF-7/Dox cells are represented in Table 3.1. Accordingly, approximately 1.8 μM doxorubicin induced 50% reduction in cell proliferation in MCF-7/S cells. However, in MCF-7/Dox cells, the necessary concentration for 50% inhibition of cell proliferation is approximately 202.5 μM, with a relative resistance index of nearly 110. This indicates that resistant MCF-7/Dox cells are 110 fold more resistant to doxorubicin than sensitive MCF-7/S cells. Cancer cell resistance to chemotherapotic agents can occur at many levels, including increased drug efflux and decreased drug influx; drug inactivation; alterations in drug target; processing of drug-induced damage; and evasion of apoptosis (Longley and Johnston, 2005). In order to assess whether increased drug efflux and decreased drug accumulation was the main resistance mechanism in MCF-7/Dox cells, which express high levels of P-gp, *MDR1* silencing was performed. As shown in Table 3.1, IC_{50} value for doxorubicin decreased to nearly 56.8 μM in *MDR1* siRNA treated MCF-7/Dox cells with a resistance index of nearly 30.9. As expected, mock siRNA had no effect on either IC_{50} value or resistance index.

70
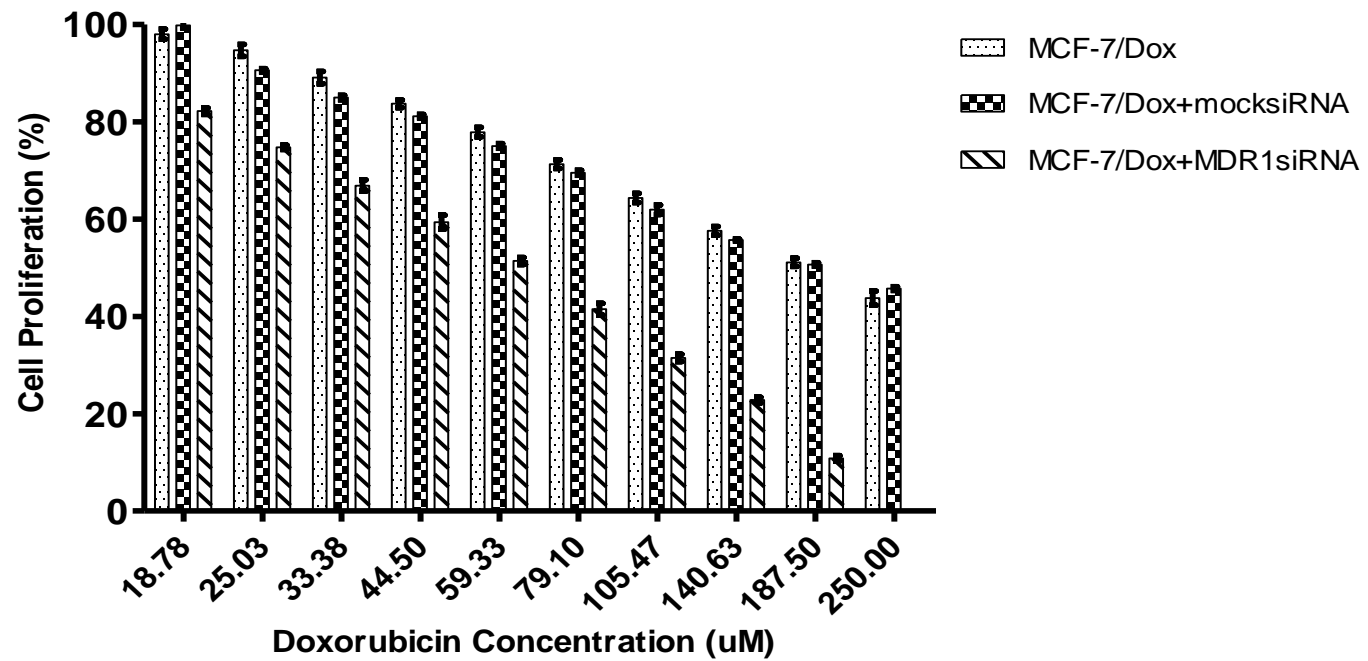
Figure 3. 16 Cell proliferation profiles of non-, mock or *MDR1* siRNA treated MCF-7/Dox cells after exposure to increasing concentrations of doxorubicin.

Table 3. 1 IC_{50} profiles for doxorubicin in MCF-7/S and non-, mock or *MDR1* siRNA treated MCF-7/Dox cells. *p < 0.0001 compared to MCF-7/Dox cells.

	Mean IC50 (μM) ±SEM	**R**
MCF-7/S	1.84 ± 0.07	-
MCF7/DOX	202.57 ± 6.78	110.21
MCF-7/DOX/mock siRNA	195.01 ± 1.03	106.10
MCF-7/DOX/*MDR1* siRNA	56.78 ± 0.39	30.89 *

IC_{50} values for MCF-7/S and MCF-7/Dox cells were graphically represented in Figure 3.17. Accordingly, significantly higher doxorubicin concentration was required for 50% inhibition of cell proliferation in MCF-7/Dox cells in comparison to MCF-7/S cells. Treatment with mock siRNA did not result in any significant difference. However, introduction of *MDR1* siRNA in to the resistant cells led to a significant decrease in IC_{50} value. According to the fold reversal (FR) calculations of resistant cells, *MDR1* siRNA caused about 70% reversal of cellular resistance to doxorubicin, which means about 4 fold re-sensitization (Table 3.2).
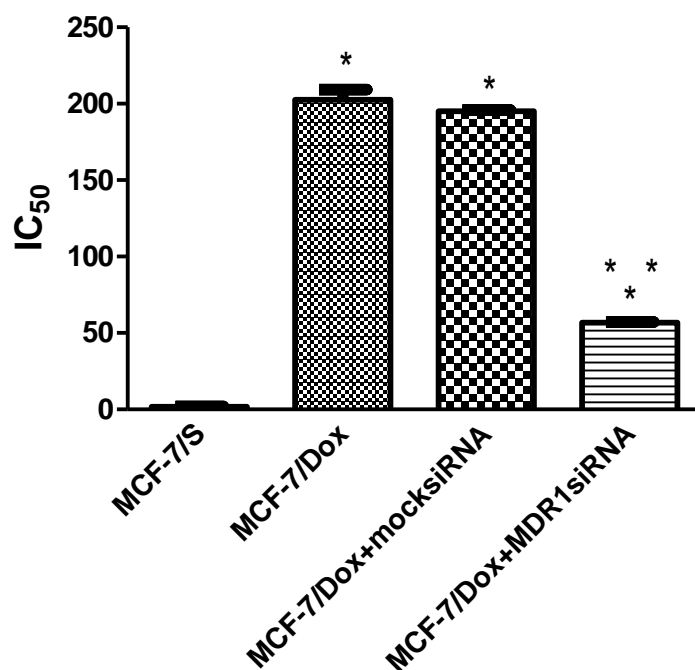
Figure 3. 17 IC_{50} values for doxorubicin in MCF-7/S and non-, mock or *MDR1* siRNA treated MCF-7/Dox cells. *p < 0.0001 compared to MCF-7/S cells, ** p < 0.0001 compared to untreated MCF-7/Dox cells.

Table 3. 2 Fold reversal values for siRNA treated MCF-7/Dox cells.

	FR
MCF7/DOX	-
MCF-7/DOX/mock siRNA	1.04
MCF-7/DOX/*MDR1* siRNA	3.57

The overproduction of P-gp results in an increase in drug efflux from cells, thereby reducing the intracellular drug concentrations (Peng *et al*., 2004). The ultimate aim of targeting P-gp mRNA is re-sensitization of MDR cells to the chemotherapeutic agents and as well as reducing their toxicity and side effects to achieve successful chemotherapy. The major limitation to doxorubicin mediated therapy is its cardiac toxicity (Zhang *et al.*, 2009).

Stierlè and co-workers (Stierlè *et al*., 2005) exposed MDR MCF-7 cells to daunorubicin for 24 hours after a 72 hour-period transfection with *MDR1* siRNA and reported an increase of chemo-sensitivity of about 40%. Moreover, in MDR leukemia cell line K562/A02 cells, *MDR1* silencing for 72 hours caused about 4 fold reversal of resistance to doxorubicin, 11 fold to vincristine and 17 fold to etoposide (Peng *et al*., 2004). Nieth and co-workers (Nieth et al., 2003) noted that the resistance index for daunorubicin was reduced from 595 fold to 310 fold and 595 fold to 250 fold in MDR EPG85-257RDB gastric carcinoma cells with 2 different *MDR1* siRNA constructs after transfection for 48 hours. Furhermore, in MDR EPP85-181RDB pancreatic carcinoma cell line, reversal from 538 fold to 68fold and from 538 fold to 57 fold were also achieved. In another study, Ludwig and co-workers (Kudwig *et al*., 2006) demonstrated that NCI/ADR-RES cells treated with *MDR1* siRNA were 7 fold more sensitive to doxorubicin than cells exposed to negative control siRNA.

As mentioned in part *3.2* (*Expression analysis of MDR1 and MRP1 genes*), selected siRNA duplex had 84% and 89% *MDR1* silencing activity after 48 and 72 hours of transfection, respectively. Whereas intracellular doxorubicin accumulation was increased 2.8 fold after 48 hours of transfection, 72 hours transfection with *MDR1* siRNA duplex resulted in almost complete reversal of P-gp mediated drug efflux with most of the drug being concentrated in the nucleus (see *3.4 Evaluation of Intracellular Doxorubicin Accumulation and Localization*). As a result, complete restoration of the chemotherapeutic sensitivity of MCF-7/Dox cells similar to MCF-7/S cells may be expected. However, introduction of siRNA resulted in about 70% reversal of cellular resistance to doxorubicin. The reasons may be the transient nature of siRNA transfection, incomplete inhibition of P-gp expression, drug efflux by MRP1 pump to some extent and other resistance mechanisms acquired by the cells.

MCF-7/Dox cells were transfected with *MDR1* siRNA for 48 hours and they were subjected to doxorubicin for another 48 hours. This may caused dilution of siRNAs despite the long cell cycle duration of MCF-7/Dox cells. The remaining P-gp mRNA may be responsible for some doxorubicin extrusion from the cells. Although MRP1

is not the main transport based resistance mechanism in resistant cells (see *3.2 Expression analysis of MDR1 and MRP1 genes*), MRP1 mediated efflux may have also contributed to incomplete reversal. In addition to the transport based resistance mechanisms, there are non-transport based mechanisms. For example, altered activity of specific enzyme systems like glutathione *S*-transferase (GST) and topoisomerase II may result in enhanced detoxification and decrease in the cytotoxic activity of drugs (Krishna and Mayer, 2000). Especially, reduction of the activity or decrease in expression levels of topoisomerase II may be one of the important resistance mechanisms in MCF-7/Dox cells, considering inhibitory action of doxorubicin on topoisomerase II. Futscher and co-workers (Futscher *et al.*, 1996) demonstrated that selection of 8226 MM cells with doxorubicin alone resulted in increased P-gp expression. However, concomitant selection with doxorubicin and P-gp modulator verapamil led to decreased levels of topo II protein and activity, with no increase in P-gp expression. Enhanced capacity of cells to repair DNA damage is another drug resistance mechanism. Response of cells to DNA damage is either damage repair or cell death. Therefore it has a determinant effect on tumor chemo-sensitivity (Longley and Johnston, 2005). Since doxorubicin is a DNA intercalating agent, enhanced DNA repair may also be a resistance mechanism in MCF-7/Dox cells. Furthermore, a shift in the proapoptotic / anti-apoptotic balance may affect chemo-sensitivity, since apoptosis plays a critical role in chemotherapy-induced tumor cells killing (Borowski *et al.*, 2005). However, it was demonstrated that alterations in apoptotic gene expression levels did not significantly correlate to development of doxorubicin resistance in MCF-7 cells (İşeri, 2009). In conclusion, incomplete restoration of chemo-sensitivity to doxorubicin despite almost complete inhibition of P-gp mediated drug efflux, may be due to activation of other resistance mechanisms becoming active after *MDR1* silencing such as enhanced detoxification, decreased activity or expression of topoisomerase II and increased levels of DNA repair.

3.6 Wound Healing Assay: Determination of Cell Migration

Recent studies suggest that soluble factors such as cytokines, hormones, and growth factors (Barut *et al*., 1993; Cotlett-Falcone *et al*., 1999; Lichtenstein *et al*., 1989; Klein *et al*., 1995), as well as interactions between tumor cells and extracellular matrix (ECM) molecules (de la Fuente *et al.,* 1999; O'Brien *et al*., 1996) or adjacent cells (Sutherland and Durand, 1972; Ctroix *et al.*, 1996), may contribute to the survival of cancer cells after initial therapy, allowing resistant cells to proliferate and acquire multidrug resistance phenotype (Shain and Dalton, 2001). Yang and co-workers (Yang et al., 1999) noticed increased motility, invasion, and metastasis of certain P-gp-overexpressing multidrug resistant (MDR) cancer cells. In another study, they (Yang *et al*., 2003) have found out that the activity and expression of distinct matrix metalloproteinases were increased in the MDR cell lines in comparison to the sensitive lines. Further, doxorubicin resistant 8226/Dox cells demonstrated a significant increase in α4ß1 integrin expression and fibronectin adhesion when compared to sensitive 8226 cells, indicating a correlation between drug selection and increased adherent potential (Damiano *et al*., 1999; Shain and Dalton, 2001). Weinstein and co-workers (Weinstein *et al*., 1991) reported an increased potential for metastatic dissemination in P-glycoprotein overexpressing invasive colon cancer cells, implying that P-gp may influence cell behavior. Additionally, Zorzos and co-workers (Zorzos *et al*., 2003) suggested a probable involvement of P-glycoprotein in the processes of local invasion and metastasis in colon cancer cells. Finally, Miletti-Gonza´lez and co-workers (Miletti-Gonza´lez *et al*., 2005) silenced *MDR1* gene with siRNA to display the effect of P-gp on cell migration in MDR MCF-7 cells. They demonstrated reduced cell migration and proposed that the expression of P-glycoprotein alone does not increase migration rate, instead, its interaction with CD44 (a membrane receptor implicated in cell adhesion, motility, and metastases) has a role on cell migration.

MCF-7/Dox cells, used in the present study, were previously shown to overexpress a variety of genes encoding extracellular matrix (ECM) proteins, including integrins, collagens, laminins, fibronectins, claudin, glypican, keratin, syndecan, and microfibrils (Işeri *et al*., 2010). The relationship between tumor cell adhesion to the

ECM and establishment of invasion and metastasis has long been discussed at molecular level (Lester and McCarthy, 1992). For the assessment of the role of P-gp in migration characteristics of MCF-7/Dox cells, wound healing assay was performed after *MDR1* silencing.

The wound-healing assay is one of the earliest developed methods to study directional cell migration and its regulation by cell interaction with ECM and cell–cell interactions in vitro (Todaro *et al.*, 1965). The assay mimics cell migration during wound healing in vivo (Rodriguez *et al.*, 2005). MCF-7/Dox cells were transfected with siRNAs. After 72 hours of transfection, cell confluency reached 100% and a wound was created on cell monolayer. Cells were exposed to doxorubicin; an untreatment control group was also assayed. The images were taken after 24 hours using a phase contrast microscopy with a 4 X objective (overall magnification: 40 X) (Figure 3.18). Image analyses were carried out and wound healing percents of the cells were represented as a bar graph (Figure 3.19). Accordingly, in the absence of doxorubicin, there was no significant difference between the wound healing percents of mock and *MDR1* siRNA transfected cells. As a result, *MDR1* silencing did not have any effect on migration of MCF-7/Dox cells. However, when the cells were subjected to doxorubicin, wound healing percent for *MDR1* siRNA treated cells decreased significantly (approximately 27% reduction) in comparison to mock treated cells. *MDR1* siRNA caused about 70% reversal of cellular resistance to doxorubicin (see *3.5 Cell Proliferation Assay with XTT Reagent: Chemo-sensitivity to Doxorubicin*). Consequently, fewer cells survived in the presence of the drug and the wound was healed slower when compared to mock-treated cells.

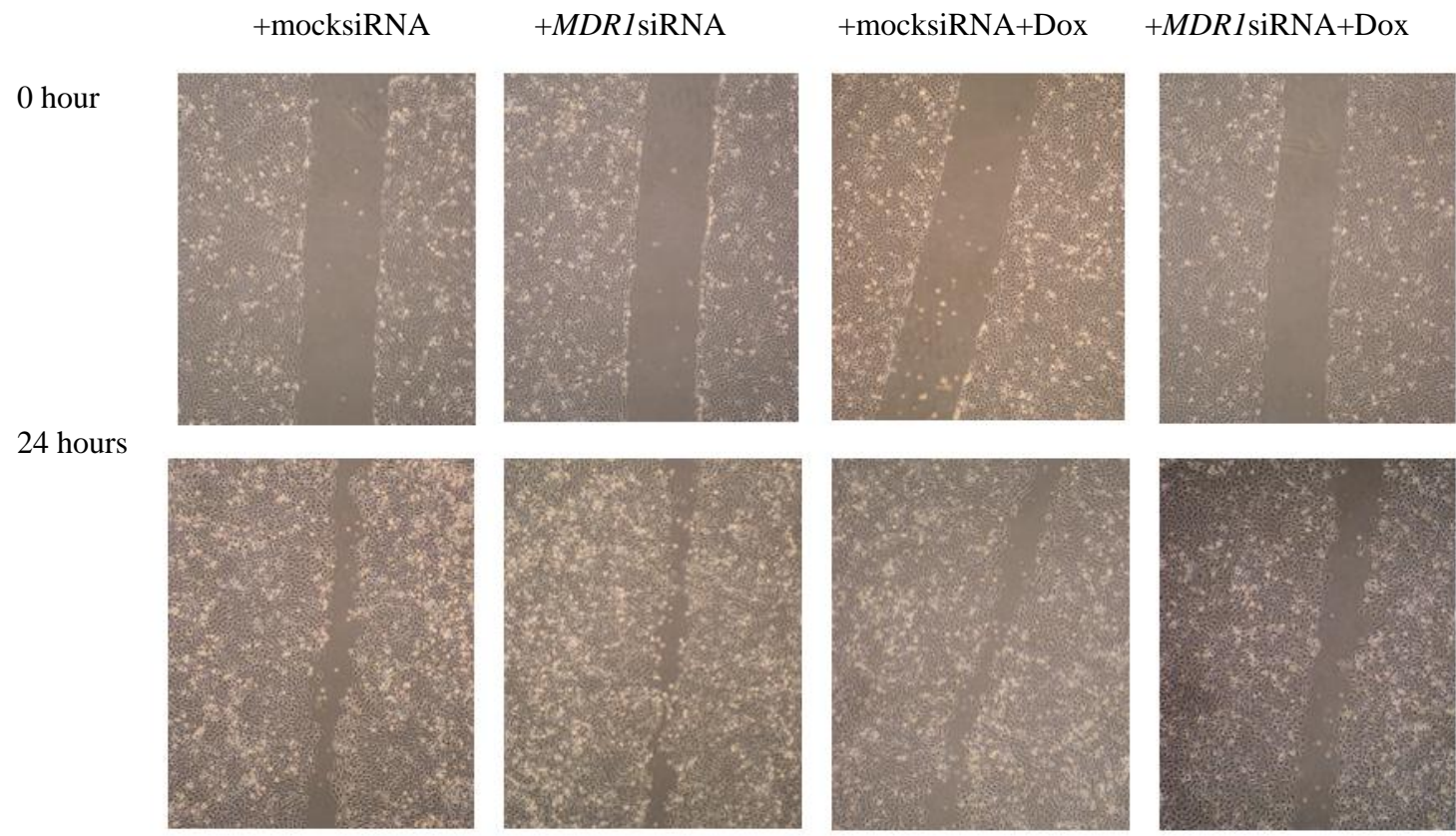|	+mocksiRNA	+*MDR1*siRNA	+mocksiRNA+Dox	+*MDR1*siRNA+Dox
0 hour				
24 hours				

Figure 3. 18 Wound healing images of mock or *MDR1* siRNA treated MCF-7/Dox cells (overall magnification: 40 X).
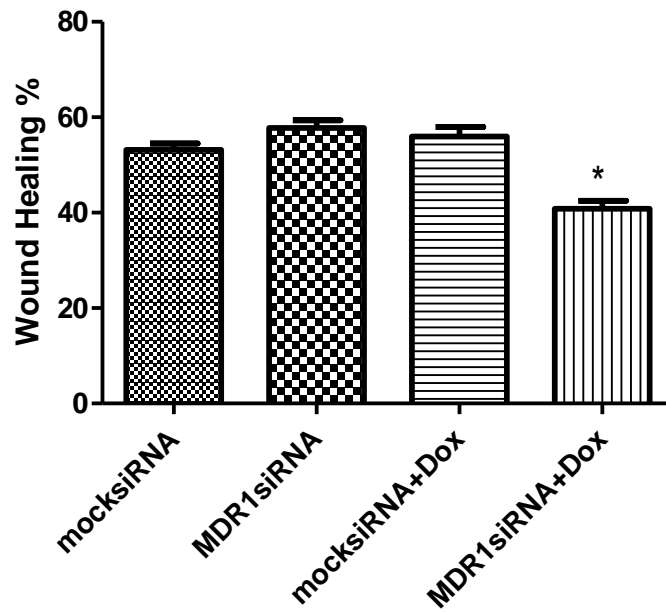
Figure 3. 19 Wound healing percents of mock or *MDR1* siRNA treated MCF-7/Dox cells. *p < 0.001 compared to mocksiRNA treated cells.

CHAPTER 4

CONCLUSION

1. Successful uptake of Alexa Fluor® oligo in to the MCF-7/Dox cells demonstrated that 20 nM siRNA would be efficiently taken by the cells. Therefore, transfection with higher concentrations, which would possibly induce nonspecific responses in the cells, was not required for further experiments.

2. Around 85 - 90% reduction in *MDR1* expression with the selected *MDR1* siRNA duplex in doxorubicin resistant MCF-7 cells demonstrates its high efficiency for *MDR1* inhibition even the concentration of siRNA was low as 20nM.

3. *MDR1* silencing did not have any effect on *MRP1* expression.

4. In MCF-7/S cells, high doxorubicin accumulation was observed with most of the drug concentrated in the cell nucleus. However, in MCF-7/Dox cells, which overexpress P-gp, doxorubicin was concentrated mainly at the cell periphery and it had limited access to the nucleus.

5. *MDR1* siRNA and verapamil treatments enabled doxorubicin to access to the nuclei. However, in promethazine treatment, doxorubicin accumulated at the cell periphery like in the case of untreated MCF-7/Dox cells.

6. Introduction of *MDR1* siRNA increased intracellular doxorubicin accumulation: *MDR1* silencing with siRNA resulted in approximately 2.5 fold increase in fluorescence intensity when compared to untreated MCF-7/Dox cells in response to 1μM doxorubicin. Transfection with *MDR1* siRNA for 48 and 72

hours led to approximately 2.8 and 5.4 fold increase in intracellular doxorubicin accumulation, respectively, in response to 4μM doxorubicin.

7. Silencing of P-gp encoding *MDR1* gene for 72 hours resulted in almost complete restoration of the intracellular doxorubicin accumulation and re-localization of the drug to the nucleus.

8. MDR modulators verapamil and promethazine led to significantly higher doxorubicin accumulation inside the cells in response to 4μM doxorubicin: 3.8 and 1.6 fold increases in fluorescence intensity, respectively, when compared to untreated MCF-7/Dox cells.

9. IC_{50} values of MCF-7/S and MCF-7/Dox cells for doxorubicin were determined as 1.8 μM and 202.5 μM, respectively, with a relative resistance index of nearly 110. *MDR1* siRNA caused a decrease in IC_{50} value to nearly 56.8 μM, and relative resistance index to 31, that is, nearly 70% re-sensitization against doxorubicin was obtained.

10. *MDR1* silencing did not affect migration characteristics of MCF-7/Dox cells, so P-gp expression does not seem to correlate with the motility of the cells. Reduced healing was only obtained in the presence of doxorubicin due to increased chemo-sensitivity of *MDR1* siRNA treated resistant cells to the drug.

Consequently, transient transfection with the selected siRNA duplex may be an efficient tool to reverse MDR phenotype of resistant cells and provide a considerable reduction in dose-dependent cardiac toxicity of doxorubicin in clinics, increasing the success of chemotherapy.

REFERENCES

Ambudkar S, Kimchi-Sarfaty C, Sauna Z, Gottesman M. 2003. P-glycoprotein: from genomics to mechanism. Oncogene 22: 7468–7485.

American Cancer Society. 2007. Cancer Facts & Figures 2007. Atlanta: American Cancer Society; 2007.

American Cancer Society. 2008. Promethazine. <http://www.cancer.org /docroot/CDG/content/CDG_promethazine.asp?internal=1>. Last accessed date: 2009, November 24.

American Cancer Society. 2009. Cancer Facts & Figures 2009. Atlanta: American Cancer Society; 2009.

Baba AI, Cătoi C. 2007. Principles of Anticancer Therapy. in Comparative Oncology. Romania: The Publishing House of the Romanian Academy. Chapter 19.

Bachur NR, Gee MV, Friedman RD. 1982. Nuclear catalyzed antibiotic free radical formation. Cancer Res 42: 1078-1081.

Barut B, Chauhan D, Uchiyama H, Anderson KC. 1993. Interleukin-6 functions as an intracellular growth factor in hairy cell leukemia *in vitro*. J Clin Investig 92: 2346-2352.

Battisti RF. 2007. Modifying the sugar moieties of daunorubicin overcomes P-gp-mediated multidrug resistance. [Senior Honors Thesis] Columbus: The Ohio State University.

Bertram JS. 2001. The molecular biology of cancer. Molecular Aspects of Medicine 21: 167-223

Biological Industries. 2002. Cell Proliferation Assay with XTT Reagent Protocol.<http://www.bioind.com/HTMLs/article.aspx?C2004=12557&BSP=12410 >. Last accessed date: 2009, October, 20.

Borowski E, Bontemps-Gracz MM, Piwkowska A. 2005. Strategies for overcoming ABC-transporters-mediated multidrug resistance (MDR) of tumor cells. Acta Biochim Pol 52(3):609-27.

Borowski E, Bontemps-Gracz MM, Piwkowska A.2005. Strategies for overcoming ABC-transporters-mediated multidrug resistance (MDR) of tumor cells. Acta Biochim Pol 52(3): 609-27.

Borst P, Kool M, Evers R. 1997. Do cMOAT (MRP2), other MRP homologues, and LRP play a role in MDR. Sem Cancer Biol 8: 205-213.

Breastcancer.org. 2008. Symptoms. <http://www.breastcancer.org/symptoms /understand_bc/what_is_bc.jsp>. Last accessed date: 2009, December 7.

Breastcancer.org. 2008. Tratment & side effects. <http://www.breast cancer.org/treatment/surgery/>. Last accessed date: 2009, December 7.

Breastcancer.org. 2008. When is radiation appropriate? <http://www. breastcancer.org/treatment/radiation/when_appropriate.jsp>. Last accessed date: 2009, December 7.

Bridge AJ, Pebernard S, Ducraux A, Nicoulaz AL, Iggo R. 2003. Induction of an interferon response by RNAi vectors in mammalian cells. Nat Genet 34: 263–264.

Burden DA, Osheroff N. 1998. Mechanism of action of eukaryotic topoisomerase II and drugs targeted to the enzyme. Biochim Biophys Acta 1400:139–54.

Catlett-Falcone R, Landowski TH, Oshiro MM, Turkson J, Levitzki A, Savino R, Ciliberto G, Moscinski L, Fernandez-Luna JL, Nunez G, Dalton WS, Jove R. 1999. Constitutive activation of Stat3 signaling confers resistance to apoptosis in human U266 myeloma cells. Immunity 10: 105-115.

Celius T, Garberg P, Lundgren B. 2004. Stable suppression of MDR1 gene expression and function by RNAi in Caco-2 cells. Biochemical and Biophysical Research Communications 324: 365-371.

Chabner A and Longo DL. 2005. Cancer chemotherapy and biotherapy: principles and practice. 4th Ed. Lippincott Williams & Wilkins, p. 416.

Chaudhary PM and Roninson IB. 1992. Activation of MDR1 (Pglycoprotein) gene expression in human cells by protein kinase C agonists. Oncol Res 4: 281-290.

Chu E and DeVita VT. 2009. Physicians' cancer chemotherapy drug manual. 9. Ed. LLC: Jones and Bartlett Publishers. p2.

Cohen D, Yang CP, Horwitz SB. 1990. The products of the *MDR1*a and *MDR1b* genes from multidrug resistant murine cells have similar degradation rates. Life Sci 46:489-95.

Coley HM, Amos WB, Twentyman PR, Workman P. 1993. Examination by laser scanning confocal fluorescence imaging microscopy of the subcellular localisation of anthracyclines in parent and multidrug resistant cell lines. Br J Cancer 67(6): 1316-1323.

Colowick NP, Jakoby WB, Pastan IH, Kaplan NP, Abelson J, Simon IS. 1979. Cell Culture: Volume 58: Cell culture (Methods in Enzymology). 3rd Ed. USA: Academic Press, p. 331.

Consoli U, Van NT, Neamati N, Mahadevia R, Beran M, Zhao S, Andreeff M. 1997. Cellular pharmacology of mitoxantrone in p-glycoprotein-positive and -negative human myeloid leukemic cell lines. Leukemia 11(12): 2066-74.

Cucco C and Calabretta B. 1996. *In Vitro* and *in Vivo* Reversal of Multidrug Resistance in a Human Leukemia-resistant Cell Line by *mdr1* Antisense Oligodeoxynucleotides. Cancer Res 56: 4332-4337.

Cullena KV, Daveyb RA, Daveya MW. 2001. Verapamil-stimulated glutathione transport by the multidrug resistanceassociated protein (MRP1) in leukaemia cells. Biochemical Pharmacology 62: 417-424.

Cummings SR, Eckert S, Krueger KA, Grady D, Powles TJ, Cauley JA, Norton L, Nickelsen T, Bjarnason NH, Morrow M, Lippman ME, Black D, Glusman JE, Costa A, Jordan VC. 1999. The effect of raloxifene on risk of breast cancer in postmenopausal women: results from the more randomized trial. Multiple outcomes of raloxifene evaluation. JAMA 281(23): 2189-2197.

Dalton WS, Durie BG, Alberts DS, Gerlach JH, Cress AE. 1986. Characterization of a new drug-resistant human myeloma cell line that expresses P-Glycoprotein.Cancer Res. 46(10): 5125-30.

Damiano JS, Cress AE, Hazlehurst LA, Shtil AA, Dalton WS. 1999. Cell adhesion mediated drug resistance (CAM-DR): role of integrins and resistance to apoptosis in human myeloma cell lines. Blood 93:1658–1667.

Dano K. 1973. Active outward transport of daunomycin in resistant Ehrlich ascites tumor cells. Biochim Biophys Acta 323: 466-483.

de la Fuente MT, Casanova B, Garcia-Gila M, Silva A, Garcia-Pardo A. Fibronectin interaction with α4ß1 integrin prevents apoptosis in B cell chronic lymphocytic leukemia: correlation with Bcl-2 and Bax. Leukemia (Baltimore) 13: 266-274.

DeVita VT, Hellman S, Rosenberg SA. 2001. Cancer, principles and practice of oncology. Philadelphia: Lippincott Williams & Wilkins. p243.

Dillin A. 2003. The specifics of small interfering RNA specificity. PNAS 100(11): 6289-6291.

Doench JG, Petersen CP, Sharp PA. 2003. siRNAs can function as miRNAs. Genes Dev 17: 438-442.

Duan Z, Brakora KA, Seiden MV. 2004. Inhibition of *ABCB1* (*MDR1*) and *ABCB4* (*MDR3*) expression by small interfering RNA and reversal of paclitaxel resistance in human ovarian cancer cells. Mol Cancer Ther 3: 833–838.

Elbashir SM, Lendeckel W, Tuschl T. 2001. RNA interference is mediated by 21- and 22-nucleotide RNAs. Genes Dev. 15: 188-200.

El-Khoury V, Breuzard G, Fourre N, Dufer J. 2007. The histone deacetylase inhibitor trichostatin A downregulates human *MDR1* (*ABCB1*) gene expression by a transcription-dependent mechanism in a drug-resistant small cell lung carcinoma cell line model. Br J Cancer 97(4): 562-573.

Engi H, Gyèmánt N, Ugocsai K, Pajak B, Kars MD, Molnar J. 2006. Reversal of multidrug resistance of cancer cells by synthetic and plant-derived compounds. European Conf. on the Reversal of MDR: From Bacteria to Cancer Cells and Parasites 29-35.

Faneyte IF, Kristel PM, Maliepaard M, Scheffer GL, Scheper RJ, Schellens JH, van de Vijver MJ. 2002. Expression of the breast cancer resistance protein in breast cancer. Clin Cancer Res 8(4): 1068-74.

Fearon ER. 1999. Cancer progression. Current Biology 9 (23): 873-875.

Ferte J. 2000. Analysis of the tangled relationships between P-glycoprotein-mediated multidrug resistance and the lipid phase of the cell membrane. Eur J Biochem 267, 277-294.

Filipits M, Pohl G, Rudas M, Dietze O, Lax S, Grill R, Pirker R, Zielinski CC, Hausmaninger H, Kubista E, Samonigg H, Jakesz R. 2005. Clinical role of multidrug resistance protein 1 expression in chemotherapy resistance in early- stage breast cancer. Clin Oncol 23: 1161-8.

Fire A, Xu S, Montgomery MK, Kostas SA, Driver SE, Mello CC. 1998. Potent and specific genetic interference by double-stranded RNA in *Caenorhabditis elegans*. Nature 391: 806–811.

Fisher B, Anderson S, Bryant J, Margolese RG, Deutsch M, Fisher ER, Jeong JH, Wolmark N. 2002. Twenty-year follow-up of a randomized trial comparing total mastectomy, lumpectomy, and lumpectomy plus irradiation for the treatment of invasive breast cancer. N Engl J Med 347(16):1233-41.

Freshney, R. 1987. Culture of Animal Cells: A Manual of Basic Technique. 1st Ed. New York: Alan R. Liss, Inc. p.117.

Futscher BW, Foley NE, Gleason-Guzman MC, Meltzer PS, Sullivan DM, Dalton WS. 1996. Verapamil suppresses the emergence of P-glycoprotein-mediated multi-drug resistance. Int. J. Cancer 66: 520-525.

G JL. 2005. Cell Migration. 1st Ed. Totowa: Humana Press. p23.

Gan HZ, Zhang GZ, Zhao JS, Zhang FC, Bu LS, Yang SJ, Piao SL, Du ZW, Gao S, Zheng DM. 2005. Reversal of MDR1 gene-dependent multidrug resistance using short hairpin RNA expression vectors. Chin Med J 118(11): 893-902.

Goldman B. 2003. Multidrug resistance: can new drugs help chemotherapy score against cancer? J Natl Cancer Inst 95:255-7.

Goormaghtigh E, Chatelain P, Caspers J, Ruysschaert JM. 1980. Evidence of a specific complex between adriamycin and negativelycharged phospholipids. Biochim Biophys Acta 597: 1-14.

Gottesman MM, Fojo T, Bates SE. 2002. Multidrug resistance in cancer: role of ATP-dependent transporters. Nat Rev Cancer 2(1):48-58.

Guano F, Pourquier P, Tinelli S, Binaschi M, Bigioni M, Animati F, Manzini S, Zunino F, Kohlhagen G, Pommier Y, Capranico G. 1999. Topoisomerase poisoning activity of novel disaccharide anthracyclines. Mol Pharmacol 56(1): 77-84.

Hanahan D and Weinberg RA. 2000. The Hallmarks of Cancer. Cell 100: 57–70.

Hutvagner G. 2005. Small RNA asymmetry in RNAi: function in RISC assembly and gene regulation. FEBS Lett 579: 5850-5857.

Integrative Medical Arts Group. 2000. Promethazine <http://dailymed. nlm.nih.gov/dailymed/fda/fdaDrugXsl.cfm?id=702&type=display>. Last accessed date: 2009, December 13.

Integrative Medical Arts Group. 2000. Verapamil <http://home.caregroup. org/clinical/altmed/interactions/Images/ Drugs/verapamil.gif>. Last accessed date: 2009, December 13.

Invitrogen. 2006. BLOCK-iT™ Alexa Fluor® Red Fluorescent Oligo. <https://products.invitrogen.com/ivgn/product/14750100>. Last accessed date: 2009, November, 23.

Işeri OD, Kars MD, Arpaci F, Gündüz U. 2010. Gene expression analysis of drug-resistant MCF-7 cells: implications for relation to extracellular matrix proteins. Cancer Chemother Pharmacol 65(3): 447-55.

Işeri ÖD. 2009. Investigation of docetaxel and doxorubicin resistance in MCF-7 breast carcinoma cell line. [PhD Thesis] Ankara: METU.

Jagla B, Aulner N, Kelly PD, Song D, Volchuk A, Zatorski A, Shum D, Mayer T, De Angelis DA, Ouerfelli O, Rutishauser U, Rothman JE. 2005. Sequence characteristics of functional siRNAs. RNA 11: 864-872.

Jin S, Gorfajn B, Faircloth G, and Scotto KW. 2000. Ecteinascidin 743, a transcription-targeted chemotherapeutic that inhibits MDR1 activation. *PNAS* 97 (12): 6775-6779.

Kanzaki A, Toi M, Nakayama K. 2001. Expression of multidrug resistance transporters in human breast carcinoma. JpnJ Cancer Res 92: 452-458.

Karp G. 2002. Cell and Molecular Biology Concepts and Experiments. 3rd Ed. NY: JohnWiley & Sons, Inc. p672.

Kars MD, Iseri OD, Gunduz U, Molnar J. 2008. Reversal of MDR by Synthetic and Natural Compounds in Drug Resistant MCF-7 Cell Lines. Chemotherapy 54: 194-200.

Kars MD, Iseri OD, Gunduz U, Ural AU, Arpaci F, Molnar J. 2006. Development of rational in vitro models for drug resistance in breast cancer and modulation of MDR by selected compounds. Anticancer Res. 26: 4559-68.

Klein B. 1995. Cytokines, cytokine receptors, transduction signals, and oncogenes in human multiple myeloma. Semin Hematol 32: 4-19.

Kobayashi H, Dorai T, Holland JF, Ohnuma T. 1994. Reversal of Drug Sensitivity in Multidrug-Resistant Tumor Cells by an *MDR*1 (*PGY*1) Ribozyme. Cancer Res 54: 1271-1275.

Krishna R and Mayer LD. 2000. Multidrug resistance (MDR) in cancer: mechanisms, reversal using modulators of MDR and the role of MDR modulators in influencing the pharmacokinetics of anticancer drugs. Eur J Pharm Sci 11: 265-283.

Kruh GD and Belinsky MG. 2003. The MRP family of drug efflux pumps. Oncogene 22: 7537-7552.

Kumar C. 2006. Nanometarials for Cancer Therapy.1. Ed. Weinheim: Wiley-VCH. p187-198.

Lage H. 2005. Potential applications of RNA interference technology in the treatment of cancer. Future Oncology 1(1): 103-113.

Leonard GD, Fojo T, Bates SE. 2003. The role of ABC transporters in clinical practice. Oncologist 8(5): 411-424.

Leslie EM, Deeley RG, Cole SP. 2003. Bioflavonoid Stimulation of Glutathione Transport by the 190-kDa Multidrug Resistance Protein 1 (MRP1). Drug Metab Dispos 31: 11-15.

Lester BR and McCarthy JB. 1992. Tumor cell adhesion to the extracellular matrix and signal transduction mechanisms implicated in tumor cell motility, invasion and metastasis. Cancer Metastasis Rev 11(1): 31-44.

Li L, Xu J, Min T, Huang W. 2006. Reversal of MDR1 gene-dependent multidrug resistance using low concentration of endonuclease-prepared small interference RNA. Eur J Pharmacol 536(1-2): 93-7.

Lichtenstein A, Berenson J, Norman D, Chang MP, Carlile A. 1989. Production of cytokines by bone marrow cells obtained from patients with multiple myeloma. Blood 74: 1266-1273.

Lim MN, Lau NS, Chang KM, Leong CF, Zakaria Z. 2007. Modulating multidrug resistance gene in leukaemia cells by short interfering RNA. Singapore Med 48 (10): 932.

Lin JH. 2003. Drug–drug interaction mediated by inhibition and induction of P-glycoprotein. Advanced Drug Delivery Reviews 55: 53-81.

Lin JH. 2003. Drug–drug interaction mediated by inhibition and induction of P-glycoprotein. Advanced Drug Delivery Reviews 55:53–81.

Ling V. 1997. Multidrug resistance: molecular mechanisms and clinical relevance. Cancer Chemother Pharmacol 40: S3–S8.

Livak KJ and Schmittgen TD. 2001. Analysis of relative gene expression data using real-time quantitative PCR and the $2^{-\Delta\Delta C_T}$ method. Methods 25: 402-408.

Loe DW, Deeley RG, Cole SP. 2000. Verapamil stimulates glutathione transport by the 190-kDa multidrug resistance protein 1 (MRP1). J Pharmacol Exp Ther 293(2): 530-8.

Logashenko EB, Vladimirova AV, Repkova MN, Venyaminova AG, Chernolovskaya EL, Vlassov V. 2004. Silencing of MDR 1 Gene in Cancer Cells by siRNA. Nucleosides, Nucleotides and Nucleic Acids 23(6): 861-866.

Longkey DB and Johnston PG. 2005. Molecular mechanisms of drug resistance. J Pathol 205: 275-292.

Ludwig JA, Szakács G, Martin SE, Chu BF, Cardarelli C, Sauna ZE, Caplen NJ, Fales HM, Ambudkar SV, Weinstein JN, Gottesman MM. 2006. Selective toxicity of NSC73306 in *MDR1*-positive cells as a new strategy to circumvent multidrug resistance in cancer. Cancer Res 66(9): 4808-15.

Matsushita H, Kizaki M, Kobayashi H, Ueno H, Muto A, Takayama N, Awaya N, Kinjo K, Hattori Y, Ikeda Y. 1998. Restoration of retinoid sensitivity by MDR1 ribozymes in retinoic acid-resistant myeloid leukemic cells. Blood 91(7): 2452-8.

Miao ZH, Tang T, Zhang YX, Zhang JS, Ding J. 2003. Cytotoxicity, apoptosis induction and downregulation of *MDR-1* expression by the anti-topoisomerase II agent, salvicine, in multidrug-resistant tumor cells. Int J Cancer 106: 108-115.

Michalak K, Hendrich AB, Wesolowska O, Pola A. 2001. Compounds that modulate multidrug resistance in cancer cells. Cell Biol Mol Lett 6(2A): 362-368.

Michalak K, Wesołowska O, Motohashi N, Hendrich AB. 2007. The role of the membrane actions of phenothiazines and flavonoids as functional modulators. Top Heterocycl Chem 8: 223-302.

Miletti-González KE, Chen S, Muthukumaran N, Saglimbeni GN, Wu X, Yang J, Apolito K, Shih WJ, Hait WN, Rodríguez-Rodríguez L. 2005. The CD44 receptor interacts with p-glycoprotein to promote cell migration and invasion in cancer. Cancer Res 65(15): 6660-7.

Mittal V. 2004. Improving the efficiency of RNA interference in mammals. Nature Reviews Genetics 5: 355-365.

Modok S, Mellor HR, Callaghan R. 2006. Modulation of multidrug resistance efflux pump activity to overcome chemoresistance in cancer. Current Opinion in Pharmacology 6:350–354.

Monson K, Schoenstadt A. 2009. Side Effects of Verapamil. <http://heart-disease.emedtv.com/verapamil/side-effects-of-verapamil.html>. Last accessed date: 2009, November 24.

Morrow CS, Cowan KH. 1997. Drug resistance and its clinical circumvention. Cancer Medicine. 4th Ed. Baltimore: Williams &Williams. p 799-815.

Motomura S, Motoji T, Takanashi M, Wang YH, Shiozaki H, Sugawara I, Aikawa E, Tomida A, Tsuruo T, Kanda N, Mizoguchi H. 1998. Inhibition of P-Glycoprotein and Recovery of Drug Sensitivity of Human Acute Leukemic Blast Cells by Multidrug Resistance Gene (*mdr1*) Antisense Oligonucleotides. Blood 91 (9): 3163-3171.

Muller C, Laurent G, Ling V. 1995. P-glycoprotein stability is affected by serum deprivation and high cell density in multidrug-resistant cells. J Cell Physiol 163:538-44.

Nagata J, Kijima H, Hatanaka H, Asai S, Miyachi H, Abe Y, Yamazaki H, Nakamura M, Watanabe N, Mine T, Kondo T, Scanlon KJ, Ueyama Y. 2002. Reversal of drug resistance using hammerhead ribozymes against multidrug resistance-associated protein and multidrug resistance 1 gene. Int J Oncol 21(5): 1021-1026.

National Cancer Institute. 2009. Breast cancer treatment. <http://www.cancer.gov/cancertopics/pdq/treatment/breast/Patient/page5>. Last accessed date: 2009, December 7.

Nicloay K, Sautereau AM, Tocanne JF, Brasseur R, Huart P, Ruysschaert JM, de Kruijff B. 1988. A comparative model membrane study on structural effects of membrane-active positively charged antitumor drugs. Biochim Biophys Acta 940: 197-208.

Nieth C, Priebsch A, Stege A, Lage H. 2003. Modulation of the classical multidrug resistance (MDR) phenotype by RNA interference (RNAi). FEBSLetters 545: 144-150.

Nykanen A, Haley B, Zamore PD. 2001. ATP requirements and small interfering RNA structure in the RNA interference pathway. Cell 107: 309– 321.

O'Brien V, Frisch SM, Juliano RL. 1996. Expression of the integrin α5 subunit in HT29 colon carcinoma cells suppresses apoptosis triggered by serum deprivation. Exp. Cell Res 224: 208-213.

Olofsson MH. 2006. Translational studies of drug-induced tumor cell death. [PhD Thesis] Stockholm: Cancer Center Karolinska.

Ozben T. 2006. Mechanisms and strategies to overcome multiple drug resistance in cancer. FEBS Letters 580: 2903–2909.

Pai SI, Lin YY, Macaes B, Meneshian A, Hung CF, Wu TC. 2006. Prospects of RNA interference therapy for cancer. Gene Ther 13(6): 464-77.

Pajeva I, Todorov DK, Seydel J. 2004. Membrane effects of the antitumor drugs doxorubicin and thaliblastine: comparison to multidrug resistance modulators verapamil and *trans*-flupentixol. Eur J Pharm Sci 21(2-3): 243-50.

Pajeva IK, Wiese M, Cordes HP, Seydel JK. 1996. Membrane interactions of some catamphiphilic drugs and relation to their multidrug-resistance ability. J Cancer Res Clin Oncol 122: 27-40.

Paul D and Cowan KH. 1999. Drug resistance in breast cancer. In: Breast Cancer Molecular Genetics, Pathogenesis and Therapeutics. Ed. Bowcock AM. Totowa: Humana Press. p481-517.

Peng Z, Xiao Z, Wang Y, Liu P, Cai Y, Lu S, Feng W, Han ZC. 2004. Reversal of P-glycoprotein-mediated multidrug resistance with small interference RNA (siRNA) in leukemia cells. Cancer Gene Therapy 11: 707-712.

Perrotton T, Trompier D, Chang XB, Di Pietro A, Baubichon-Cortay H. 2007. (R)- and (S)-verapamil differentially modulate the multidrug-resistant protein MRP1. J Biol Chem 282(43): 31542-8.

Persengiev SP, Zhu X, Green MR. 2004. Nonspecific, concentration-dependent stimulation and repression of mammalian gene expression by small interfering RNAs (siRNAs). RNA 10(1): 12-8.

Ren YY. 2006. Suppression of MDR1 expression and restoration of sensitivity to chemotherapy in multidrug-resistant hepatocellular carcinoma cell line Bel7402/5-Fu by RNA interference. Zhong Nan Da Xue Xue Bao Yi Xue Ban 6:872-6.

Reynolds A, Leake D, Boese Q, Scaringe S, Marshall WS, Khvorova A. 2004. Rational siRNA design for RNA interference. Nat Biotechnol 22(3): 326-30.

Richert ND, Aldwin L, Nitecki D, Gottesman MM, Pastan I. 1988. Stability and covalent modification of P-glycoprotein in multidrug-resistant KB cells. Biochemistry 27:7607-13.

Rieger PT. 2004. The biology of cancer genetics. Seminars in Oncology Nursing 20 (3): 145-154.

Roepe PD. 1992. Analysis of the steady-state and initial rate of doxorubicin efflux from a series of multidrug-resistant cells expressing different levels of P-glycoprotein. Biochemistry 31: 12555–12564.

Roland T. 2007. Handbook of cancer chemotherapy. 7. Ed. Lippincott: Williams & Wilkins. p307-319.

Schneider J, Gonzalez-Roces S, Pollán M, Lucas R, Tejerina A, Martin M, Alba A. 2001. Expression of LRP and MDR1 in locally advanced breast cancer predicts axillary node invasion at the time of rescue mastectomy after induction chemotherapy. Breast Cancer Res 3(3): 183-91.

Seelig A. 1998. A general pattern for substrate recognition by P-glycoprotein. Eur J Biochem 251: 252–261.

Semizarov D, Frost L, Sarthy A, Kroeger P, Halbert DN, Fesik SW. 2003. Specificity of short interfering RNA determined through gene expression signatures. PNAS 100 (11): 6347-6352.

Shain KH and Dalton WS. 2001. Cell adhesion is a key determinant in de novo multidrug resistance (MDR): new targets for the prevention of acquired MDR. Mol Cancer Ther 1(1): 69-78.

Shankar P, Manjunath N, Lieberman J. 2005. The prospect of silencing disease using RNA interference. Jama 293: 1367–1373.

Shapiro AB and Ling V. 1995. Using purified P-glycoprotein to understand multidrug resistance. J Bioenerg Biomembr 27: 7-13.

Sharom FJ. 1997. The P-glycoprotein efflux pump: How does it transport drugs? J Membr Biol 160:161-175.

Shen F, Chu S, Bence AK, Bailey B, Xue X, Erickson PA, Montrose MH, Beck WT, Erickson LC. 2008. Quantitation of Doxorubicin Uptake, Efflux, and Modulation of Multidrug Resistance (MDR) in MDR Human Cancer Cells. J Pharmacol Exp Ther 324 (1):95-102.

Simon SM and Schindler M. 1994. Cell biological mechanisms of multidrug resistance in tumors. Proc Nati Acad Sci 91: 3497-3504.

Sioud M and Leirdal M. 2004. Potential Design Rules and Enzymatic Synthesis of siRNAs. Methods in Molecular Biology, vol. 252: Ribozymes and siRNA Protocols. 2nd Ed. Totowa: Humana Press Inc. p. 457-469.

Sledge GW, Jr. 1996. Adjuvant therapy for early stage breast cancer. Semin Oncol 23: 51-54.

Sledz CA, Holko M, de Veer MJ, Silverman RH, Williams BR. 2003. Activation of the interferon system by short-interfering RNAs. Nature Cell Biol 5: 834-839.

Speelmans G, Staffhorst RWHM, de Kruijff B, de Wolf FA. 1994. Transport studies of doxorubicin in model membranes indicate a difference in passive diffusion across and binding at the outer and inner leaflets of the plasma membrane. Biochemistry 33:13761-13768.

St. Croix B, Florenes VA, Rak JW, Flanagan M, Bhattacharya N, Slingerland JM, Kerbel RS. 1996. Impact of the cyclin-dependent kinase inhibitor p27Kip1 on resistance of tumor cells to anticancer agents. Nat. Med 2: 1204-1210.

Stanford Medicine. 2009. Breast cancer surgery. <http://cancer.stanford.edu/ patient_care/services/surgery/breast.html>. Last accessed date: 2009, December 7.

Stavrovskaya AA. 2000. Cellular Mechanisms of Multidrug Resistance of Tumor Cells. Biochemistry 65(1): 95-106.

Stege A, Priebsch A, Nieth C, Lage H. 2004. Stable and complete overcoming of MDR1/P-glycoprotein-mediated multidrug resistance in human gastric carcinoma cells by RNA interference. Cancer Gene Ther 11(11): 699-706.

Stierle´ V, Laigle A, Jolle`s AB. 2007. Expression in MCF7-R cells when combined with a second siRNA. Biochimie 89: 1033-1036

Stierle´ V, Laigle A, Jolle`s B. 2005. Modulation of MDR1 gene expression in multidrug resistant MCF7 cells by low concentrations of small interfering RNAs. Biochemical Pharmacology 70: 1424-1430.

Sutherland RM and Durand RE. 1972. Cell contact as a possible contribution to radiation resistance of some tumours. Br. J. Radiol 45: 788-789.

Swift LP, Rephaeli A, Nudelman A, Phillips DR, Cutts SM. 2006. Doxorubicin DNA adducts induce a non-topoisomerase II–mediated form of cell death. Cancer Res 66 (9): 4863-71.

Takeshita F and Ochiya T. 2006. Therapeutic potential of RNA interference against Cancer. Cancer Sci 97: 689-696.

Theilen GH, Madewell BR, Carter SK. 1987. Chemotherapy. Ed. Theilen, Madewell. Veterinary Cancer Medicine. Philadelphia: Lea & Febiger. p157–166.

Tiwari AK, Sodani K, Chen ZS. 2009. Current Advances in Modulation of ABC Transporter-mediated Multidrug Resistance in Cancer. International Journal of Toxicological and Pharmacological Research 1(1):1-6.

Todaro GJ, Lazar GK, Green H. 1965. The initiation of cell division in a contact inhibited mammalian cell line. J Cell Physiol 66:325-333.

Triton TR and Yee G. 1982. The anticancer agent adriamycin can be actively cytotoxic without entering cells. Science 217: 248-250.

Tsuruo T, Iida H, Tsukagoshi S, Sakurai Y.1981. Overcoming of vincristine resistance in P388 leukemia *in vivo* and *in vitro* through enhanced cytotoxicity of vincristine and vinblastine by verapamil. Cancer Res 41:1967-1972.

Veronesi U, Cascinelli N, Mariani L, Greco M, Saccozzi R, Luini A, Aguilar M, Marubini E. 2002. Twenty-year follow-up of a randomized study comparing breast-conserving surgery with radical mastectomy for early breast cancer. N Engl J Med 347(16): 1227-32.

Watanabe T, Onuki R, Yamashita S, Taira K, Sugiyama Y. 2005. Construction of a functional transporter analysis system using *MDR1* knockdown Caco-2 Cells. Pharm Res 22 (8): 1287-93.

Weinstein RS, Jakate SM, Dominguez JM, Lebovitz MD, Koukoulis GK, Kuszak JR, Klusens LF, Grogan TM, Saclarides TJ, Roninson IB. 1991. Relationship of the expression of the multidrug resistance gene product (P-glycoprotein) in human colon

carcinoma to local tumor aggressiveness and lymph node metastasis. Cancer Res 51: 2720–6.

Wesołowska O, Mosiadz D, Motohashi N, Kawase M, Michalak K. 2005. Phenothiazine maleates stimulate MRP1 transport activity in human erythrocytes. Biochim Biophys Acta 1720(1-2):52-8.

Williams BR. 1997. Role of double stranded RNA-activated protein kinase (PKR) in cell regulation. Biochem Soc Trans 25: 509-513.

Wodarz D. 2005. Somatic evolution of cancer cells. Seminars in Cancer Biology 15: 421–422.

World Health Organization. 2006. Projections of global mortality and burden of disease from 2002 to 2030. <http://www.who.int/healthinfo/statistics/ bod_projections2030_paper.pdf>. Last accessed date: 2009, December 5.

Wu H, Hait WN, Yang JM. 2003. Small Interfering RNA-induced Suppression of *MDR1* (P-Glycoprotein) Restores Sensitivity to Multidrug-resistant Cancer Cells. Cancer Res 63: 1515–1519.

Yagqe E, Higgins CF, Raguz S. 2004. Complete reversal of multidrug resistance by stable expression of small interfering RNAs targeting *MDR1*. Gene Ther 11: 1170–1174.

Yang JM, Xu Z, Wu H, Wu X, Hait WN. 2003. Overexpression of extracellular matrix metalloproteinase inducer in multidrug resistant cancer cells. Mol Cancer Res 1: 420-7.

Yang JM, Yang GY, Medina DJ, Vassil AD, Liao J, Hait WN. 1999. Treatment of multidrug resistant (MDR1) murine leukemia with P-glycoprotein substrates accelerates the course of the disease. Biochem Biophys Res Commun 266: 167- 173.

Yusa K and Tsuruo T. 1989. Reversal mechanism of multidrug resistance by verapamil: direct binding of verapamil to p-glycoprotein on specific sites and transport of verapamil outward across the plasma membrane of K562/ADM cells. Cancer Res 49: 5002-5006.

Zhang YW, Shi J, Li YJ, Wei L. 2009. Cardiomyocyte death in doxorubicin-induced cardiotoxicity. Arch Immunol Ther Exp 57: 435–445.

Zorzos HS, Lazaris AC, Korkolopoulou PA, Kavantzas NG, Tseleni-Balafouta S, Patsouris ES, Tsavaris NV, Davaris PS. 2003. Multidrug resistance proteins and topoisomerase II a expression in colon cancer: association with metastatic potential. Pathology 35: 315–8.

APPENDIX A

CELL CULTURE MEDIUM

Table A. 1 RPMI 1640 Medium formulation (in mg/L) (Biochrom AG).

NaCl	6000	L-methionine	15
KCl	400	L-phenylalanine	15
Na2HPO4·7H2O	1512	L-proline	20
MgSO4·7H2O	100	L-serine	30
Ca(NO3)2·4H2O	100	L-threonine	20
D-glucose	2000	L-tryptophane	5
Phenol red	5	L-tyrosine	20
NaHCO3	2000	L-valine	20
L-arginine	200	Glutathione	1
L-asparagine	50	Biotine	0.2
L-aspartic acid	20	Vitamin B12	0.005
L-cystine	50	D-Ca-pantothenate	0.25
L-glutamine	300	Choline chloride	3
L-glutamic acid	20	Folic acid	1
Glycine	10	Myo-inositol	35
L-histidine	15	Nictoninamide	1
L-hydroxyproline	20	p-amino-benzoic-acid	1
L-isoleucine	50	Pyridoxin·HCl	1
L-leucine	50	Riboflavin	0.2
L-lysine·HCl	40	Thiamine·HCl	1

APPENDIX B

BUFFERS AND SOLUTIONS

- Diethylpyrocarbonate (DEPC) treated dH_2O (1L):

  1mL DEPC was added to 1 L dH_2O and mixed well. After overnight incubation, autoclavation was performed.

- 50X Tris-acetate-EDTA (TAE) buffer (1L):

Tris base (MW: 121.14)	242 g
Acetic Acid	57.1 mL
0.5 M EDTA disodium dihydrate (MW: 372.24)	100mL

  Volume was completed to 1 L with dH_2O and pH was adjusted to 8.5. After autoclavation, solution was diluted to 1X with dH_2O.

- Ethidium bromide (EtBr) solution:

  10 mg EtBr was dissolved in 1 mL dH_2O and stored in dark.

- 2 % (w/v) paraformaldehyde

  2 g paraformaldehyde was added to 10 mL phosphate buffered saline (PBS) and heated at 70 ºC until the color turns to transplant.

- 6X DNA Loading Dye (Fermentas)

10 mM Tris-HCl (pH 7.6)	0.03% bromophenol blue
0.03% xylene cyanol FF	60% glycerol
60mM EDTA	

TRESHOLD CYCLE VALUES

Table C. 1 Treshold cycle values (C_T) of qPCR

	MDR1	MRP1	β-actin
No Treatment	13.81	16.6	7.22
	13.91	15.92	6.77
	13.76	15.70	6.57
Mock siRNA/48h	14.14	16.01	6.22
	13.7	15.60	6.33
	14.07	15.76	6.58
*MDR1*siRNA/48h	16.23	15.72	6.57
	15.86	16.13	6.78
	16.32	15.61	6.66
Mock siRNA/72h	14.09	15.44	6.60
	14.05	16.43	6.58
	13.86	16.08	6.76
MDR1 **siRNA/72h**	17.01	16.89	6,96
	17.05	15.64	6,78
	16.94	15.82	7.09
	MDR1	**MRP1**	**β-actin**
No Treatment	16.25	14.40	6.04
	15.57	14.61	6.69
	16.17	14.79	6.73
Mock siRNA/48h	16.05	14.28	6.13
	16.18	14.64	6.54
	15.84	14.27	5.78
*MDR1*siRNA/48h	19.19	14.07	6.17
	18.17	14.56	6.15
	18.18	14.14	6.02
Mock siRNA/72h	16.44	14.14	6.32
	16.28	14.48	6.41
	15.71	14.50	6.15
MDR1 **siRNA/72h**	19.50	13.98	6.28
	20.31	15.23	6.38
	19.89	14.11	6.10
	MDR1	**MRP1**	**β-actin**
No Treatment	12.49	12.32	4.85
	11.94	11.14	4.75
	11.93	10.55	4.08
Mock siRNA/48h	11.96	10.96	4.84
	11.43	11.05	4.06
	12.38	11.27	4.64
*MDR1*siRNA/48h	16.02	10.71	4.73
	15.01	11.57	4.72
	15.06	11.35	4.62
Mock siRNA/72h	12.52	11.76	5.21
	12.14	11.09	4.86
	11.92	11.10	4.83
MDR1 **siRNA/72h**	15.59	11.19	4.93
	15.61	11.67	4.79
	15.83	11.75	4.69

CELL PROLIFERATION GRAPHS AND LOGARITHMIC EQUATIONS

All experiments were performed in triplicates. IC_{50} values are calculated from the logarithmic trend line of the %cell proliferation versus concentration plots for each plate and expressed as mean ± SEM.
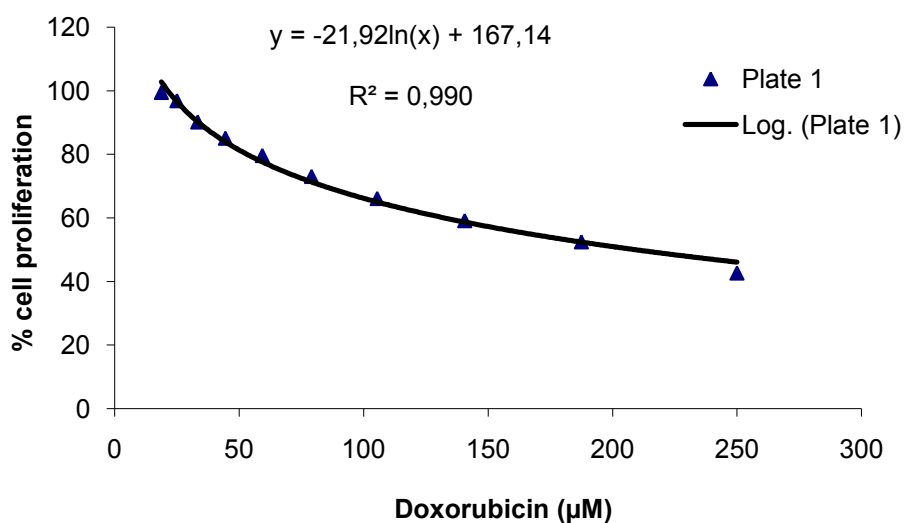

Figure C. 1 Cell Proliferation of MCF-7/Dox after exposure to increasing concentrations of doxorubicin (Plate 1).
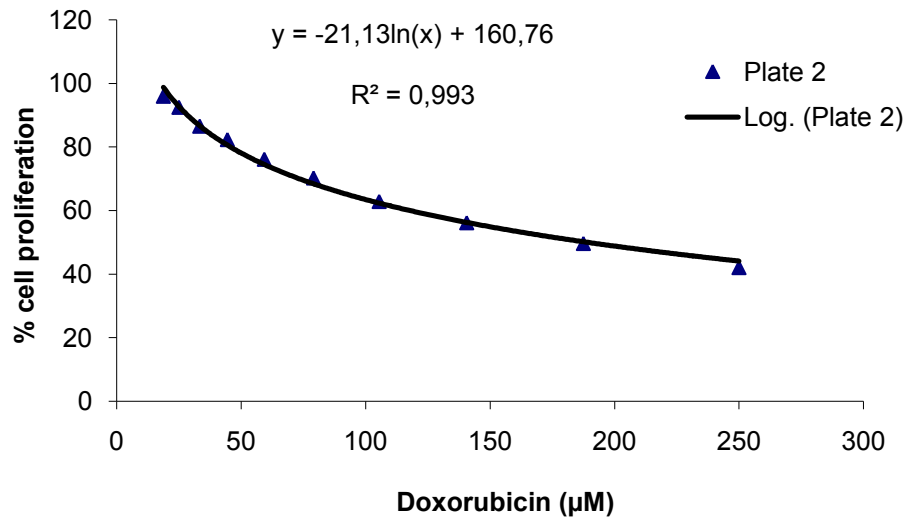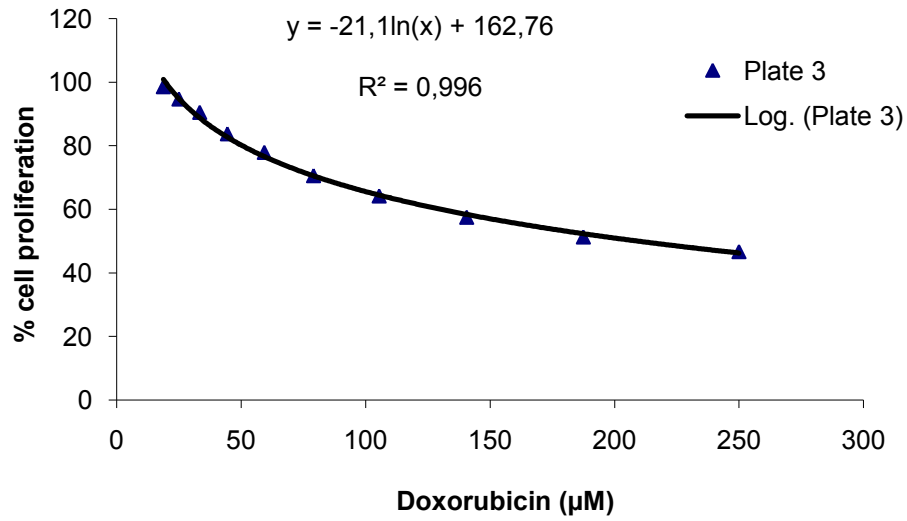
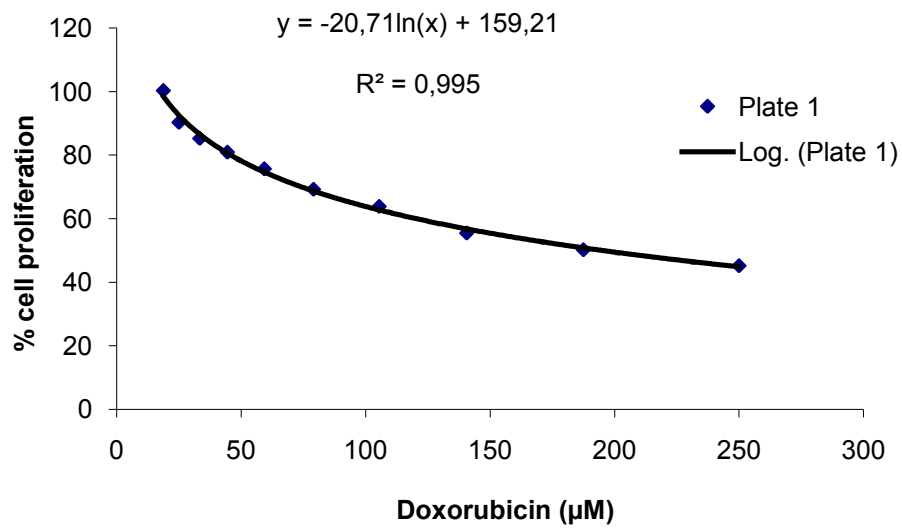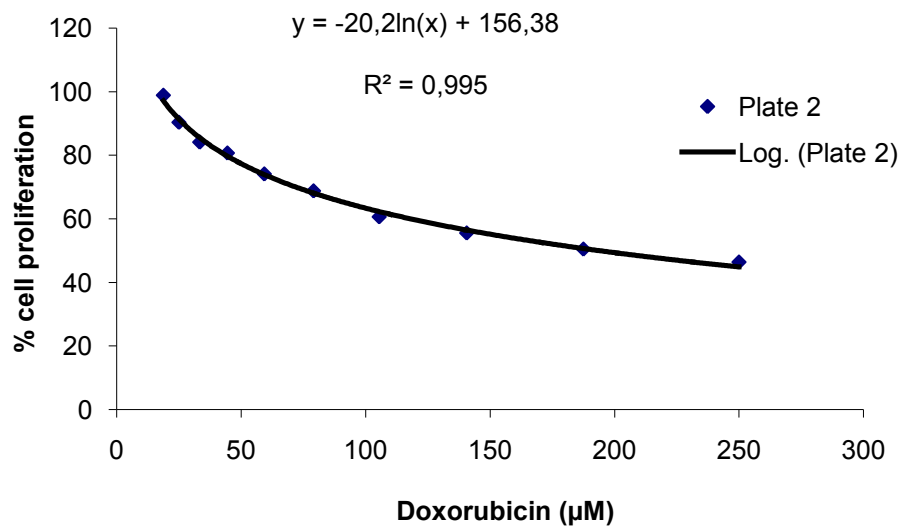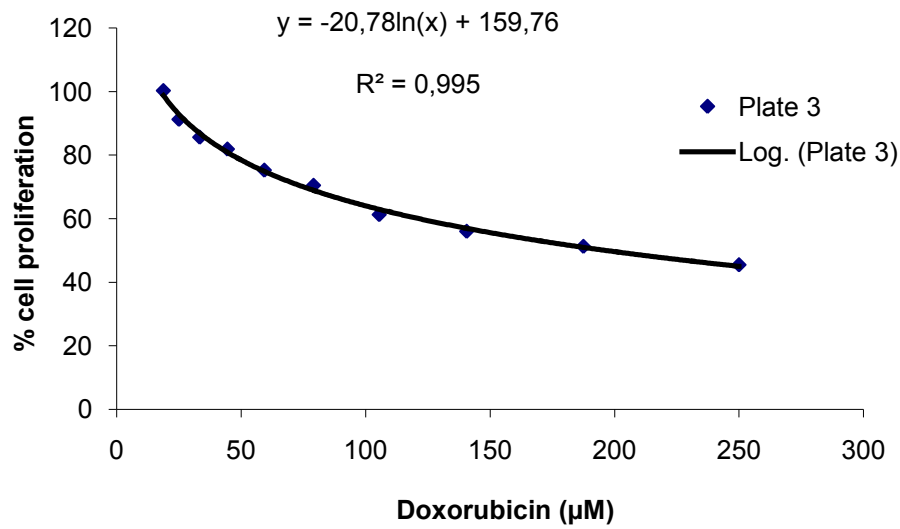Figure C. 2 Cell Proliferation of MCF-7/Dox after exposure to increasing concentrations of doxorubicin (Plate 2).

Figure C. 3 Cell Proliferation of MCF-7/Dox after exposure to increasing concentrations of doxorubicin (Plate 3).

Figure C. 4 Cell Proliferation of mocksiRNA treated MCF-7/Dox after exposure to increasing concentrations of doxorubicin (Plate 1).
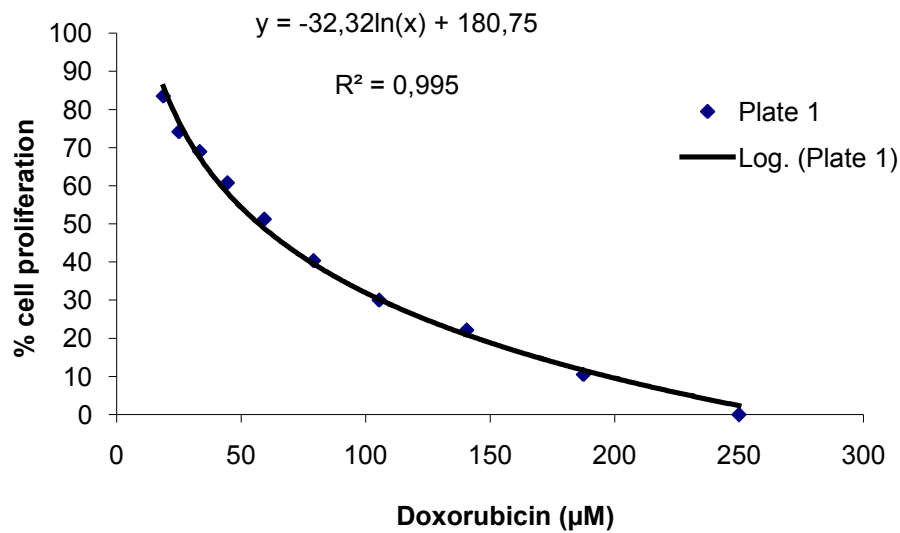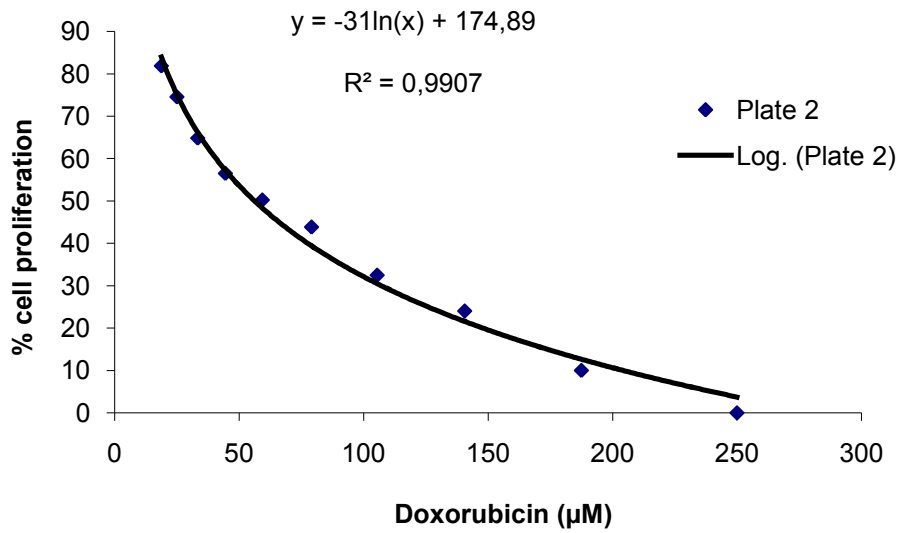

Figure C. 5 Cell Proliferation of mocksiRNA treated MCF-7/Dox after exposure to increasing concentrations of doxorubicin (Plate 2).

Figure C. 6 Cell Proliferation of mocksiRNA treated MCF-7/Dox after exposure to increasing concentrations of doxorubicin (Plate 3).

Figure C. 7 Cell Proliferation of *MDR1* siRNA treated MCF-7/Dox after exposure to increasing concentrations of doxorubicin (Plate 1).

Figure C. 8 Cell Proliferation of *MDR1* siRNA treated MCF-7/Dox after exposure to increasing concentrations of doxorubicin (Plate 2).
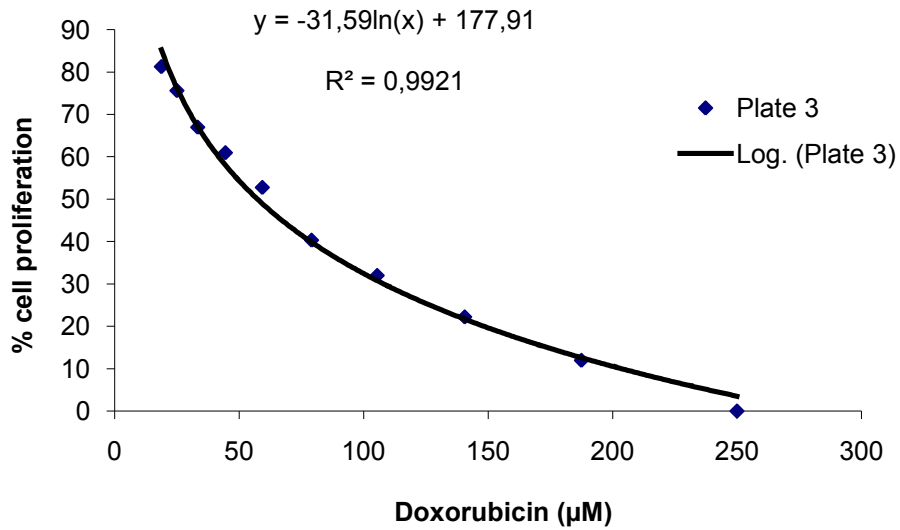

Figure C. 9 Cell Proliferation of *MDR1* siRNA treated MCF-7/Dox after exposure to increasing concentrations of doxorubicin (Plate 3).
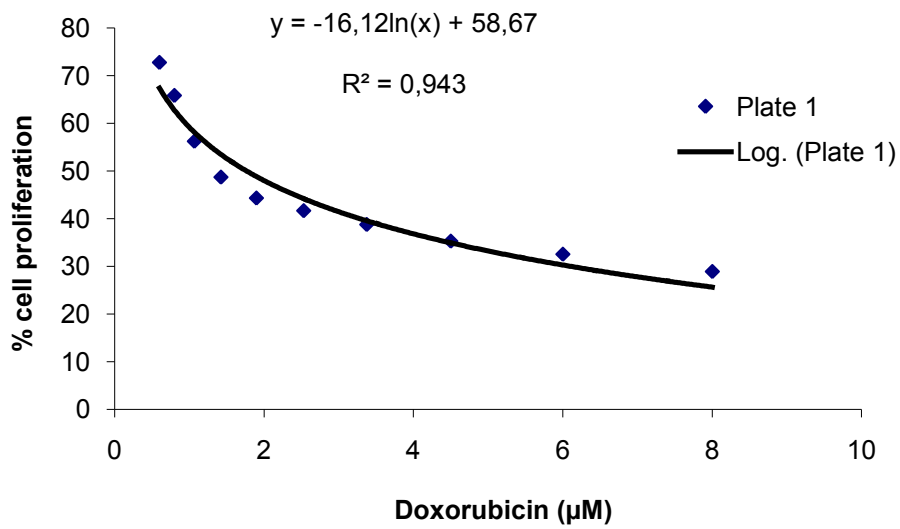
Figure C. 10 Cell Proliferation of MCF-7/S after exposure to increasing concentrations of doxorubicin (Plate 1).
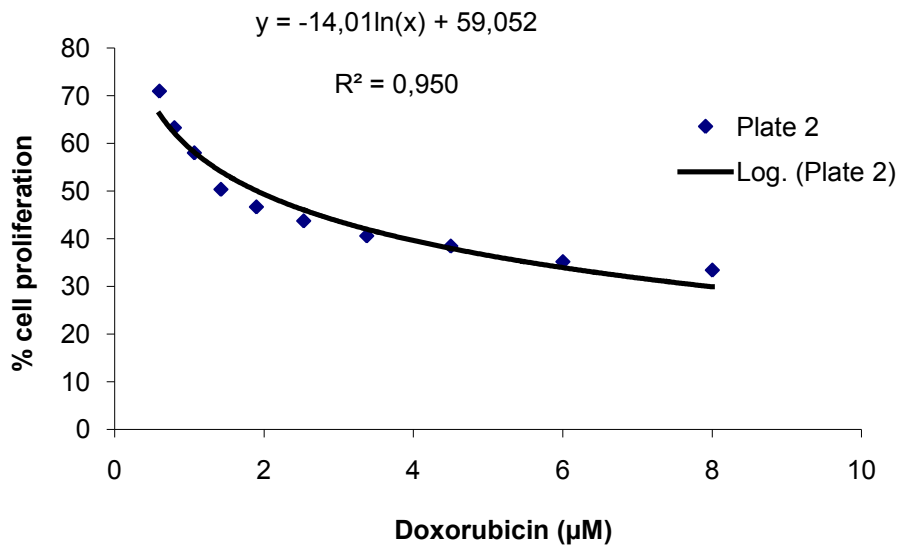

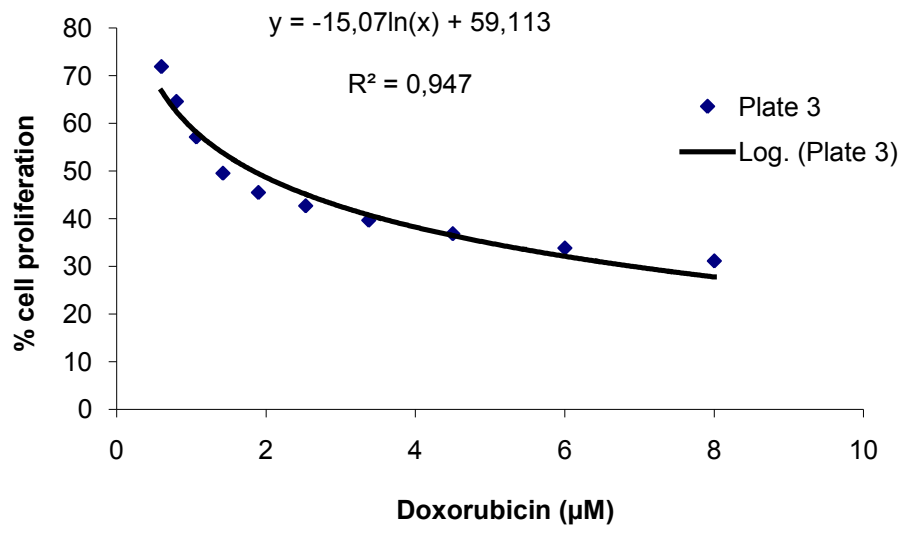Figure C. 11 Cell Proliferation of MCF-7/S after exposure to increasing concentrations of doxorubicin (Plate 2).

Figure C. 12 Cell Proliferation of MCF-7/S after exposure to increasing concentrations of doxorubicin (Plate 3).